Behaviour of over reinforced HSC helically confined beams

Nuri Mohamed Elbasha
University of Wollongong

BEHAVIOUR OF OVER REINFORCED HSC HELICALLY CONFINED BEAMS

A thesis submitted in fulfilment of the requirements for the award of the degree

DOCTOR OF PHILOSOPHY

from

SCHOOL OF CIVIL, MINING AND ENVIRONMENTAL ENGENEERING

THE UNIVERSITY OF WOLLONGONG

BY

NURI MOHAMED ELBASHA, B.E., M.ENG (First class)

2005

DECLARATION

I hereby declare that the research work described in this thesis is my own work and the experimental program was carried out by the candidate in the laboratories of Civil, Mining and Environmental Engineering, University of Wollongong, NSW, Australia. This is to certify that this work has not been submitted for a degree to any university or institute except where specifically indicated.

Nuri Mohamad Elbasha

December 2005

ACKNOWLEDGEMENTS

I wish to express my profound gratitude to my supervisor, Associate Professor Muhammad N.S. Hadi, for his invaluable advice and academic guidance during the completion of this thesis. His invaluable suggestions, excellent guidance constant support and encouragement for the past three years are gratefully acknowledged.

My apology in advance is to those who have been left off the acknowledgement list. Their contribution to this work is greatly appreciated.

Many thanks go to Dr. Troy Coyle for her encouragement and interest throughout this project. I would like also to thank Dr. Chandra Gulati for the statistical advice.

I would like also to thank the School of Civil, Mining and Environmental Engineering, University of Wollongong, for providing all necessary facilities and good conditions for my research and for awarding me the Peter Schmidt award for best performance-postgraduate research. I thank the Research office for awarding the highly commended student prize for recognition of the commercial potential

I would like also to thank the Ministry of Culture and Higher Education of Libya for providing my Ph.D scholarship.

I would like to thank friends, colleagues, Bachelor students, Joshua Overell, Chris Foye and Mark Barwell and the technical staff, Mr Ian Bridge, Mr Alan Grant, Mr Bob Rowlan. Mr Ken Malcolm and Mr Steve Selby for their invaluable assistance and co-operation in conducting the experimental work. Naturally, this work could not have been completed without their support.

Finally, I would like to express my deepest gratitude to my parents, brothers, wife, and my children for their understanding and patience with my long hours away from home, during my study at the University of Wollongong.

LIST OF PUBLICATIONS

List of relevant journal and conference papers published during Ph.D candidature.

Elbasha, N. M. and Hadi, M. N. S. (2005). "Experimental testing of helically confined HSC beams." Structural Concrete Journal (Thomas Telford and *fib*), 6(2), 43-48.

Hadi, M. N. S. and Elbasha, N. M. (2005). **"**Effect of Tensile Reinforcement Ratio and Compressive Strength on the Behaviour of Over Reinforced HSC Helically Confined." Construction and Building Materials Journal, (In Press). Letter of acceptance 2 Sept 2005

Elbasha, N. M. and Hadi, M. N. S. (2004). "Investigating the Strength of Helically Confined HSC Beams." Int. Conf. Of Structural & Geotechnical Engineering, and Construction Technology, IC-SGECT'04, Mansoura, Egypt, 23-25 March 2004, pp. 817-828.

Elbasha, N. M. and Hadi, M. N. S. (2004). "Effects of the Neutral Axis Depth on Strength Gain Factor for Helically Confined HSC Beam." Int. Conf. on Bridge Engineering & Hydraulic Structures, BHS2004. Kuala Lumpur, Malaysia. ISBN 983-2871-62-X. 26-27 July 2004, pp. 213-217.

Hadi, M. N. S. and Elbasha, N. M. (2004). "A New Model for Helically Confined High Strength Concrete Beams." 7th International Conference on Concrete Technology in Developing Countries. Modelling and Numerical Methods for Concrete Materials. 5-8 October 2004. Kuala Lumpur, Malaysia. University of Technology MARA. pp. 29-40.

Hadi, M. N. S. and Elbasha, N. M (2005). "The Effect of Helical Pitch on the Behaviour of Helically Confined HSC Beams." Australian Structural Engineering Conference, ASEC 2005. Newcastle. Editors: MG Stewart and B Dockrill. 11-14 September. Paper 54. 10 pages.

Elbasha, N. M. and Hadi, M. N. S. (2005). "Flexural Ductility of Helically Confined HSC Beams." ConMat'05 Third International Conference on Construction Materials: Performance, Innovations and Structural Implications Vancouver, Canada, August 22-24, 2005. Paper number 50. 10 pages.

ABSTRACT

The technology of high strength concrete and high strength steel have improved over the last decade although high strength concrete is still more brittle than normal strength concrete. As this brittleness increases, particularly with the use of over-reinforced sections, they may, suddenly fail without any warning.

The research reported in this thesis deals with the installation of helical confinement in the compression zone of over-reinforced high strength concrete beams. This study is divided into three parts as follows:

1) State of the Art & Literature Review

This part deals with state of the art and literature review. Helical confinement is more effective than rectangular ties, compression longitudinal reinforcement and steel fibres in increasing the strength and ductility of confined concrete. Helical reinforcement upon loading increases the ductility and compressive strength of axially loaded concrete due to resistance to lateral expansion caused by Poisson's effect. Based on this concept helical reinforcement could be used in the compression zone of over-reinforced high strength concrete beams. The effectiveness of helical confinement depends on different important variables such as helical pitch and diameter. Thus there is a need for an experimental programme

to prove that installing helical confinement in the compression zone of an over-reinforced concrete beam enhances its strength and ductility and to study the behaviour of over-reinforced high strength concrete beams subjected to different variables.

2) The Experimental Programme & Test Analysis

This part deals with an experimental programme and analysis of test results. Extensive experimental work was done because the beams should be full size in order to accurately represent real beams. Twenty reinforced concrete beams, 4 m long × 200 mm wide × 300 mm deep were helically confined in the compression zone and then tested in the civil engineering laboratory at the University of Wollongong. In this programme the following areas were studied: the effect of helical pitch, helical diameter, concrete compressive strength and longitudinal reinforcement ratio, on the behaviour of over-reinforced HSC helically confined beams.

3) Analytical Models to Predict the Strength & Ductility

This part deals with the analytical models used to predict the strength and ductility of over-reinforced high strength concrete beams based on the findings of this study. A comparison between the experimental and predicted results shows an acceptable agreement.

This study concludes that helical reinforcement is an effective method for increasing the strength and ductility of over-reinforced high strength concrete beams.

TABLE OF CONTENTS

LIST OF FIGURES

PAGE

LIST OF TABLES

NOTATION LIST

A_c	cross-section area of the concrete core, in mm^2
A_g	gross area of the section, in mm^2
A_h	cross-section area of helix bar, in mm^2
A_{sh}	total cross-section area of rectangular ties, in mm^2
A_s	area of longitudinal tensile reinforcing steel, in mm^2
b	width of the cross-section of the beam, mm
C	compressive force, N or kN
d	effective depth of the cross-section, mm
d_{co}	effective depth of the section excluded the concrete cover, mm
d_h	helix bar diameter, in mm
d	effective depth of a cross-section, mm
D	the concrete core diameter, in mm
E_c	modulus of elasticity of concrete, in MPa
E_s	modulus of elasticity of reinforcement steel, in MPa
f_c'	concrete compressive strength, in MPa
f_{cc}'	axial compressive strength of confined concrete, in MPa
f_R	modulus of rupture, in MPa
f_t	tensile splitting strength, in MPa

f_{sy}	yield strength of tension reinforcement, MPa
f_{yh}	yield strength of helical reinforcement, in MPa.
h_c	maximum unsupported length of rectangular hoop, mm
K_s	ratio of the confined strength of concrete to the unconfined compressive strength of concrete
K_u	neutral axis parameter
M_u	ultimate moment capacity of a beam, in kN.m
M_{ud}	calculated moment by assuming the concrete strain at the extreme compression fibre is 0.003 of an over-reinforced concrete beam, in kN.m
P	lateral pressure on the confined concrete in MPa.
T	tensile force in longitudinal steel, N or kN
W_c	unit weight of concrete, kg/m^3
μ_d	displacement ductility factor
μ_e	strain ductility factor
μ_ϕ	curvature ductility factor
ρ_h	total volumetric ratio of helices
ρ	longitudinal reinforcement ratio
ρ_c	compression steel ratio
ρ_b	balanced reinforcement ratio
ρ_{max}	maximum reinforcement ratio

Δ_u	midspan deflection at ultimate load, in mm
Δ_y	midspan deflection at first yield of tensile steel, in mm
β	ratio depth of the rectangular stress block to the neutral axis
α	factors for intensity of stress in a rectangular stress block
φ	capacity reduction factors
ϕ_u	ultimate curvature
ϕ_y	yield curvature
ε_u	sustainable strain in concrete
ε_y	yield strain in concrete
ε_{con}	ultimate confined compressive strain
ε_{cu}	compressive strain at extreme compression fibre of confined concrete at ultimate load
ε_o	strain at top surface of the beam
ε_{st}	average steel strain

CHAPTER 1

INTRODUCTION

1.1 GENERAL

In recent years, there have been significant improvements in the properties of concrete and steel reinforcing bars. Although high strength concrete and high strength steel have only recently begun to be used in Australia, researchers and construction companies have been encouraged to utilise them, because they are cost effective and have other advantages.

Primarily, high strength steel is extremely reliable, and grade 500 reinforcing bars provide high design strength. Being stronger, high strength steel is economical because it reduces the size and weight of the concrete member. Moreover, high strength steel can be welded by conventional processes, less weight and has an increased resistance to corrosion.

The primary long and short term advantages of high strength concrete are, low creep and shrinkage, higher stiffness, higher elastic modulus, higher tensile strength, higher durability (resistance to chemical attacks) and higher shear

resistance. In addition, high strength concrete reduces the size of the member, which in turn reduces the form size, concrete volume, construction time, labour costs and dead load. Reducing the dead load reduces the number and size of the beams, columns and foundations. Thus there is a positive impact on reduction of maintenance and repair costs and an increase in rentable space. Other, yet to be discovered advantages may also exist. High strength concrete has definite advantages over normal strength concrete.

It is generally accepted that helical confinement increases the strength and ductility of confined concrete better than rectangular ties. Helical reinforcement increases the ductility and compressive strength of concrete under compression by resisting lateral expansion due to Poisson's effect. In this study helical reinforcement is used in the compression zone of over-reinforced high strength concrete beams. The effectiveness of helical confinement depends on variables such as helical pitch and diameter.

1.2 RESEARCH SIGNIFICANCE

HSC has been used extensively in civil construction projects world wide because it reduces the cross section and the weight of long construction members. In recent years a marked increase in the use of High Strength Concrete (HSC) has been evident in Australian building construction despite the fact that the current

Australian design standard, AS3600 (2001) provides no design rules for such a material. Very limited information on the properties of HSC and its design and construction processes are available in Australia, although in recent times many studies have been undertaken to produce material and, more importantly, to determine its characteristic properties and behaviour.

The lack of ductility of HSC is a definite concern. Plain HSC is less ductile than normal strength concrete. It is important that reinforced concrete members are able to withstand large deformations whilst maintaining strength capacity in situations where there is a need to withstand significant overloads. Here is where HSC comes into its own. If adequately confined, a greater load carrying capacity can be achieved, and along with properties such as higher elastic modulus, higher resistance to physical and chemical deteriorations and the early stripping of formwork all make this material's use very advantageous (Webb, 1993).

Avoiding brittle compression failure by using proper confinement, which restrains lateral expansion, enhances concrete' strength and ductility. Base and Read (1965) showed through experimental testing that helical confinement enhances the strength and ductility of a beam containing high tensile longitudinal steel percentage.

For an over-reinforced concrete beam, proper confinement enhances ductility and increases the compressive strength in the confined region. It has been observed that

all research concerning confinement of the compression zone in beams is based on the results of research on columns, because this idea has only recently been developed. Based on these results, more study and data on the behaviour of confined HSC beams is needed. This study presents the experimental results of testing 20 full-scale beams 4000 mm long by 200 mm wide by 300 mm deep.

1.3 OBJECTIVE

High strength concrete and high strength steel are used together to increase a beams' load capacity and reduce its cross section. Using these two materials to design over-reinforced beams will reduces costs, which is a desirable result, but because they lack ductility, the current codes of practice disallow their use. This study shows that ductility can be significantly improved by installing helical confinement in the compression zone.

There is limited data regarding the strength, concrete cover spalling off, confined concrete strain and ductility for over-reinforced HSC helically confined beams. This study provides experimental evidence that installing helical confinement in the compression zone of over-reinforced high strength concrete beams enhances their strength and ductility. This study also examines the effect of variables such as helical pitch, the tensile reinforcement ratio and compressive strength on the

strength, concrete cover spalling off, confined concrete strain and ductility for an over-reinforced HSC helically confined beam.

The current design provisions of AS 3600 (2001) do not allow for over-reinforced concrete beams because they lack ductility, but this study provides experimental proof that installing a helix with a suitable pitch and diameter in the compression zone of beams significantly enhances their ductility. Therefore designers could confidently use high-strength concrete and high-strength steel to design over-reinforced beams to fully realise their full potential.

The main objective of this research is to utilise the advantages of high strength concrete and high strength steel and to improve our understanding of how over-reinforced HSC helically confined beams behave. It is therefore necessary to provide experimental data to facilitate the study of the effect of different variables such as helical pitch, the tensile reinforcement ratio and compressive strength on the behaviour of over-reinforced HSC helically confined beams.

1.4 SCOPE OF THE PRESENT RESEARCH

The current investigation is limited to high strength concrete with concrete compressive strength from 72 to 105 MPa. The general focus is only on the enhanced strength and displacement ductility as a result of installing helical

confinement in the compression zone of the over-reinforced beams. An experimental study, included testing 20 beams, with a cross section of 200×300 mm, and with a length of 4 m and a clear span of 3.6 m. These beams were tested, on the strong floor of the civil engineering laboratory at the University of Wollongong, under a four-point loading regime with an emphasis on the midspan deflection. The following variables were investigated:

1- Helical pitch
2- Helical diameter
3- Helical yield strength
4- Longitudinal reinforcement ratio and
5- Concrete compressive strength

1.5 OUTLINE OF THE THESIS

This thesis contains nine Chapters set out as follows:

Chapter 1 introduces the advantages of high strength concrete and high strength steel, discusses the enhanced strength and ductility that results from installing helical confinement in the compression zone, and presents the significance, objectives and organisation of this thesis.

Chapter 2 describes high strength steel and high strength concrete and briefly discusses the mechanical properties and advantages of high strength steel reinforcing bars. It also presents a definition of high strength concrete and some information about materials that constitute high strength concrete, such as cement, silica fume and superplastisizers with an emphasis on the advantages of high strength concrete and the main factors affecting its cost.

Chapter 3 discusses the concept of confinement, presents an up to date description of concrete confinement including a comparison between helix and tie confinement. It further summarises the requirements of the codes for lateral reinforcement, discusses the compressive strength of confined concrete including a description of the theoretical basis of the ductility of confined concrete beams.

Chapter 4 presents an extensive literature review of research carried out on the behaviour of confined concrete. A detailed discussion of the literature review is included.

Chapter 5 describes an experimental study of 20 helically confined beams. It describes the details of the helical confinement used in this research, test set-up, test procedure and then presents the results illustrated by figures and photographs.

Chapter 6 presents the experimental results of the tested 20 over-reinforced HSC helically confined beams, including the effects of helical pitch, helical yield strength, helical diameter, tensile reinforcement ratio and compressive strength, and the resulting analysis and discussion.

Chapter 7 describes the model proposed to predict the strength gain factor for over-reinforced helically confined HSC beams, and presents a new model for predicting the ultimate confined strain. The stress block parameters were chosen to predict the flexure strength of over-reinforced helically confined HSC beams. There is a good agreement between the predicted moment capacities and the experimental moment capacities.

Chapter 8 presents three non-dimensional ratios used to propose an analytical model to predict the displacement ductility index of over-reinforced helically confined HSC beams. The proposed model is reasonable at estimating experimental data.

Chapter 9 outlines the main conclusions reached, based on the investigation reported here and recommendations for future research.

A number of appendices are enclosed in the thesis. Appendix A contains the stress-strain diagrams of longitudinal, helical confinement and shear reinforcing steel

bars. Appendix B contains load versus midspan deflection of the 20 beams tested. Appendix C contains strains at 0, 20 and 40 mm depth from top surface of the beams. Appendix D contains a prototype example to predict the moment capacity of an over-reinforced section. Finally, Appendix E contains statistical modelling output.

CHAPTER 2

HIGH STRENGTH STEEL AND HIGH STRENGTH CONCRETE

2.1 GENERAL

Reinforcing steel and concrete are the two main materials that constitute reinforced concrete, which is then used in different construction members such as footings, columns, slabs and beams. More research has been carried out on concrete than reinforcing steel because its behaviour is more complicated. Concrete depends on its constituent materials such as cement, aggregates, and chemical admixtures such as fly ash and polymers. This chapter presents the properties of steel reinforcing bars and concrete with a particular focus on high strength steel and concrete.

The introduction of high strength concrete and steel reduces the size of structural members whilst having the same load carrying capacity and a resultant saving on construction time, material, labour and space. Therefore, using both high strength steel and high strength concrete in construction is very important.

2.2 HIGH STRENGTH STEEL

Steel is a general term for iron that contains small amounts of carbon, manganese, and other elements. Steel reinforcing bar is a composite material that uses its ability to yield to ensure a ductile mode of failure, and is therefore an important component in concrete design. Reinforcing bars are used with concrete members to resist tensile stresses and come in three different styles, deformed (having lugs or deformation), plain, welded wire fabric, or wires. Wires are either individual or groups (Warner et al. 1999). According to AS 3600 (2001) the modulus of elasticity of high strength steel may be taken as 200,000 MPa. Also the Australian/ New Zealand Standard AS/NZS 4671:2001 (2001) defines the high strength steel reinforcing bars as the steel with a minimum yield stress of 500 MPa.

2.2.1 Reinforcing steel bars

A reinforcing steel bar has a circular cross section that resists stresses in the concrete. They are either deformed (with deformation transverse ribs on the surface) or plain (without ribs). In practice, deformed bars are used for longitudinal reinforcement, plain bars for stirrups to resist shear forces, or as confining bars to restrain expansion. Nevertheless there are different standards in various countries designed to prevent the steel industry from using a higher content of alloying elements to achieve high strength steel. These standards specify a name and the percentage of chemical composition required to improve important properties such

as strength, ductility, and weldability. The Australian/ New Zealand Standard AS/NZS 4671:2001 (2001) designates the shape, ductility, and the tensile strength as follows:

1- Shape

Plain Round bars are designated by the letter R, deformed ribbed bars by the letter D, and deformed Indented bars by the letter I.

2- Ductility

Ductility is designated by the letters L, N or E, which mean Low, Normal, or Earthquake, respectively.

3- Strength

Strength is designated by the numerical value in mega Pascals of the lower characteristic yield stress 250 MPa or 500MPa. For example, D250N32 is a description of a deformed ribbed bar, grade 250 MPa, normal ductility steel with a nominal diameter of 32 mm.

2.2.2 Types of reinforcing steel bars

In the construction material market, two types of reinforcing bars are widely used. They are classified based on minimum yield strength as follows:

a) High strength steel

High strength steel is a deformed reinforcing bar with 500 MPa minimum yield strength.

b) Low strength steel

Low strength steel is a plain reinforcing bar (undeformed) with 250 MPa minimum yield strength and less than 500 MPa. Plain bars are restricted for use as stirrups in beams, or rectangular and circular ties for columns.

2.2.3 Mechanical properties

1- Tensile properties

The yield stress, maximum tensile strength and the extension shall be determined according to reinforcing steel test standard. Australian/ New Zealand Standard AS/NZS 4671:2001, (2001) states that the 0.2% proof stress shall be determined if an observed yield phenomenon is not present.

2- Bending and re-bending

A bending and re-bending test usually applies to deformed reinforcing bars and is determined by bending around mandrel diameters and angles as specified by the Australian/ New Zealand Standard AS/NZS 4671:2001 (2001). There should be no evidence of surface cracking after bending or re-bending.

3- Geometric properties

Geometric properties of reinforcing steels such as diameter, cross-sectional areas, and masses are specified in the Australian/ New Zealand Standard AS/NZS 4671:2001 (2001).

4- Geometric Surface

A deformed bar has deformations on its surrounding surface which enhances the bond between the steel and concrete. Al-Jahdali et al. (1994) tested 36 pullout specimens with different concrete compressive strengths and found that the compressive strength significantly influences the bond characteristics due to the mechanical interaction between deformation on the bars and the concrete.

2.2.4 Advantages of high strength steel

The construction industry's desire for lower costs is driving manufacturers to develop better and stronger materials to facilitate more efficient designs. In recent years a significant improvement in the properties of reinforcing bars has been achieved and advances in Australian technology has made the use of 500 N grades common. High strength 500 N steel contains a high percentage of carbon and has a yield strength greater than 500 MPa. High strength steel reduces the main reinforcement ratio required for designing reinforced concrete and also reduces steel congestion in beams, columns, slabs, and beam to column connections. As a result, the volume of steel is reduced compared to normal strength steel which is a significant cost saving.

High strength steel has a number of advantages, including strength, reliability, ductility, bending strength, durability, economy, weldability, lighter in weight, corrosion resistant, and radiation free (AS/NZS 4671:2001, 2001). The strength of

material and its ductility are often inversely related, that is, by increasing strength, ductility is reduced. However, new advances in material science could produce reinforcing bars that have higher strength and higher ductility. It will be great innovation if material science can produce high strength steel without compromising ductility.

2.3 HIGH STRENGTH CONCRETE

2.3.1 Definition

High strength concrete is defined as n having a greater compressive strength than normal strength concrete. However, this definition is changing from country to country and from time to time. For example "high strength concrete is defined by FIP/CEB as concrete with a cylinder strength above 60 MPa" Helland (1995), but the ACI318-002 (2002) definition of HSC is a concrete with a cylinder strength above 42 MPa. The Australian standard AS3600 (2001) classifies high strength concrete as having a cylinder strength above 65 MPa. There is a belief that taking the strength as an indicator of high strength concrete is more reliable than its performance (high performance concrete) because measuring performance is very difficult compared to measuring strength. However, the title high strength concrete is not an indicator of its strength only but also of its high quality and durability. Therefore this thesis uses the term high strength rather than high performance concrete. Aggregate, cement, and water are the main materials of normal strength

and high strength concrete. However, the difference between these materials for normal and high strength concrete is adding water reduction admixture and their quality and ratio. The material characteristics of high strength concrete are as follows.

a) Cement

Cement has cohesive and adhesive properties that set and harden in the presence of water to form a bond between it and any steel reinforcement. Reinforced concrete usually consists of Portland cement whose primary components are lime, silica, alumina, and secondary components are iron oxide, magnesia and alkalis. Adding pozzolan to the concrete could prevent internal disintegration but then a calcium silicate hydrate is produced as a result of the reaction between lime and pozzolan (Nawy, 2001).

b) Aggregate

Aggregate, of which there are fine and coarse, is about 80% of the volume of a mixture of concrete. Aggregate greater than 6 mm is classified as coarse. It is preferable to use fine aggregate with round particles for high strength concrete because it requires less water during mixing. The compressive strength and disintegration are affected by the properties of coarse aggregate. Blick (1973) showed that the maximum size of coarse aggregate should be 10 mm to gain optimum compressive strength. Natural crushed stone, natural gravel, artificial

coarse aggregate, and heavy weight are four types of coarse aggregate. Fine aggregate is sand which fills the spaces between the coarse aggregate. According to the American Society of Testing and Material (ASTM, 1994), fine aggregate should have a well graded combination, free of organic impurities and clay.

c) Water

The water used in mixing concrete should be clean and free from injurious amounts of oils, acids, alkalis, salts, and organic materials, that is, water suitable for drinking.

d) Chemical and mineral admixtures

Chemical and mineral admixtures are materials that may be added before or while mixing the cement, aggregate, and water. Chemical and mineral admixtures are widely used in the production of high strength concrete. Concrete with a compressive strength of 102 MPa was the first high strength concrete produced in Japan without using any chemical and mineral admixture. The only other way to produce high strength concrete was by vibration and compaction (Nagataki, 1995). Selection of the quantity and quality of the admixtures is based on the performance of the main material used to produce the concrete mix. Chemical and mineral admixtures are materials which are added to improve its properties. They include, accelerating admixtures, admixtures, air entraining admixtures, water reducing and set controlling admixtures and a high range water reducing agent (Super-

plasticisers). In recent years, other materials have been used to increase the strength and improve the properties of concrete. They are generally finer than cement and include fly ash and silica fume. Below is a brief description of these materials.

Fly ash:

Fly ash is produced from the exhaust fumes of coal fired power stations, contains complex chemicals and minerals and is widely used to improve g strength and durability and produce high strength concrete. There are two types, one has pozzolanic properties produced from burning anthracite or bituminous coal, while the other has pozzolanic and autogenous cementitious properties produced from burning lignite or sub-bituminous coal (ACI 363R-92, 1992). The experimental programme conducted by Malhotra et al. (2000) was to study the relative performance of concrete after 8 years of exposure to 4% calcium chloride solution, with or without fly ash. Their test results showed that concrete containing fly ash protected the reinforcing steel from corrosion.

Silica fume:

Silica fume is very fine, has a high silica content and is a competent material for producing high strength concrete. It comes as an ultra fine powder, as loose bulk, compacted, slurry, or in the form of blended silica fume Portland cement (Nawy, 2001). Silica fume increases the strength of the paste and the bond between paste and aggregate due to the effect of Pozzolanic and fine particle size. The first

country to produce, utilise, and conduct research on silica fume is Norway. Depending on the compressive strength of concrete required, the silica fume range is from 5 to 30 percent of the weight of the cement. The curing method affects the ratio of silica fume required to gain maximum strength. For example, the water curing method requires silica fume at 15% of the weight of cement weight to gain maximum strength, but high temperature curing requires silica fume at 30% of the weight of cement. On the other hand, Bhanja and Sengupta (2003) stated that the optimum silica fume replacement percentage is not constant but is function of the ratio of water to cement. Thus there is no unique, accepted method. Companies in different countries have their own optimum content of silica fume.

2.3.2 Properties of high strength concrete

High strength concrete has characteristics that cannot be found in normal concrete. A huge volume of concrete is produced in the world every year to construct bridges, high rise structures, and waste water treatment plants. However, the costs of rehabilitation and replacing are very high, for example in the United States about $500 billion is re needed just to replace existing bridges and highways (Nawy, 2001). There is a need to reduce construction or rehabilitation costs through utilising the new technology of high strength concrete. The following are the main characteristics of high strength concrete.

a) Compressive strength

Compressive strength is the most important engineering property. The proportion of cement, coarse and fine aggregates, water, and a range of chemical and mineral admixtures such as silica fume and fly ash affect its strength. The early hydration of Portland cement is affected by silica fume. Montes et al. (2005) conducted an extensive experimental programme to study the effect of fly ash, silica fume, and the calcium nitrite based corrosion inhibitor (CNI) on compressive strength. The calcium nitrite based corrosion inhibitor (CNI) protects reinforcement from corrosion. The main finding of Montes et al. (2005) study was that when fly ash was used to replace Portland cement in a mixture containing silica fume, the 28-day compressive strength decreased. This effect is more pronounced as the w/c decreases from 0.45 to 0.29. Also Montes et al. (2005) noted that increasing CNI to a mixture increases the 28-day compressive strength by approximately 15%. However, adding CNI to a mixture with or without fly ash does not adversely affect the compressive strength.

The presence of silica fume and super-plasticiser in the concrete affects its compressive strength. Bartlett and Macgregor (1995) found that the compressive strength after 28 days for concrete containing fly ash is roughly equal to the cylinder compressive strength at 28 days. The compressive strength of all types of concrete generally increases at a slow rate over time. However, its strength at 28 days with silica fume added increases slower than concrete without silica fume.

However Schmidt and Hoffman (1975) stated that the compressive strength for HSC at 56 and 90 days needs to be specified, unlike that at 28 days.

It is well known that HSC has higher strength but lower ductility. Building codes such as AS 3600 (2001) and ACI 318R-02 (2002) generally apply maximum compressive strain in concrete designed as 0.003. Walraven (1995) tested 81 prisms under compressive load with different strain rates and found that the ultimate stress for high strength concrete depends on the loading rate, which affect the ultimate stress of normal strength concrete.

b) Poisson's ratio

Poisson's ratio of high strength and normal strength concrete is similar in the elastic range although it contains limited experimental data for high strength concrete. However Chan et al. (2000) conducted an extensive experimental programme on high strength concrete. The experimental results of specimens with a compressive strength between 70 and 100 MPa showed that the Poisson's ratio of high strength concrete was in the range of 0.17 to 0.2. Chan et al. (2000) found that the Poisson's ratio of high strength concrete was slightly affected by the curing conditions that affect its density. AS 3600 (2001) recommended using a Poisson's ratio of 0.2 for concrete with a compression strength equal to or less than 65 MPa.

c) Modulus of Elasticity

The static modulus of elasticity is defined as the ratio of normal stress to corresponding strain for compressive stress-strain. The modulus of elasticity is affected by age, loading rate, and properties of the concrete material. “usually the secant modulus at from 25 to 50% of the compressive strength is considered to be the modulus of elasticity” (Wang and Salmon, 1985). There are different empirical formulas to predict the static modulus of elasticity and these models are proposed through a relationship between the compressive strength and modulus of elasticity. For a compressive strength up to 83 MPa, the modulus of elasticity could be calculated using Equation 2.2 (Nawy, 2001). The predicted values are dependent on the properties of the coarse aggregate. However, when the compressive strength is between 83 and 140 MPa, the modulus of elasticity could be calculated using the stress strain diagram.

$$E_c = \left(3.32\sqrt{f_c'} + 6895\right)\left(\frac{W_c}{2320}\right)^{1.5} \qquad (2.2)$$

where E_c is modulus of elasticity in MPa; f_c' is the concrete compressive strength in MPa and W_c is the unit weight of concrete, kg/m^3

d) Tensile splitting strength

The size of cracking in a reinforced concrete structure is greatly affected by its tensile strength. A split cylinder test is used to measure the tensile splitting strength. This test is conducted on the same cylinder size used for the compression test. Equation 2.3 is recommended by Carrasquillo et al. (1981) for predicting the tensile splitting strength of concrete with a compressive strength between 21 to 83 MPa. Mokhtarzadeh and French (2000) found that the tensile splitting strength for high strength concrete was between 5 and 8 percent of the compressive strength.

$$f_t = 0.59\sqrt{f_c'} \qquad (2.3)$$

where f_t is the tensile splitting strength and f_c' is the compressive strength in MPa.

e) Modulus of rupture

The modulus of rupture is tensile strength in flexure. Legeron and Paultre (2000) stated that for durability reasons tensile strength in flexure is desirable to prevent concrete structures from cracking under permanent loading. Equation 2.4 (Legeron and Paultre, 2000) is used for predicting the modulus of rupture.

$$f_R = 0.94\sqrt{f_c'} \qquad (2.4)$$

where f_R is the modulus of rupture in MPa. and f_c' is the compressive strength in MPa.

f) Workability

Reducing the water content is essential for gaining high strength concrete but reducing the water content reduces its ability to work. On the other hand increasing the super-plasticiser content improves its ability to work. Thus reducing the water content and increasing the super-plasticiser content is an efficient way of producing high strength concrete while reducing voids and improving the bond between steel reinforcement and concrete.

g) Permeability

Permeability is the degree of penetration of solutions through the concrete (Nawy, 2001). Permeability depends on the pore and void characteristics of the concrete and is therefore inversely proportional to resistance to chemical attack. However, high strength concrete has low permeability due to low voids, high compaction, and low fineness of added material such as slag and fly ash.

h) Creep

Creep is plastic flow of the material under sustained load and is a very important factor in the long term deformation performance of structures. High strength

concrete has a smaller coefficient value of creep compared to normal strength concrete (Nawy, 2001). Huo et al. (2001) found experimentally that a smaller coefficient value of creep was obtained from specimens with a higher compressive strength. It was also noticed that the coefficient of creep tended to develop rapidly during the early age of concrete.

2.3.3 Economics of HSC

High strength concrete with a compressive strength of 100 MPa is used widely in high rise buildings and bridges. In France concrete with a strength up to 800 MPa is produced for special applications (Nawy 2001). In the last 20 years there has been extensive research to economically utilise new components to improve the quality of HSC. HSC produces smaller but stronger structural elements with large spaces available. There are several publications to study the cost of using HSC instead of NSC in different types of constructions. For example Schmidt and Hoffman (1975) found that the cost of elements made from 41 MPa compressive strength concrete is reduced when 62 MPa compressive strength concrete was used. This proved that structures constructed with HSC are more economical than those constructed with NSC.

In the long term durability significantly affects project costs. In other words after several years a concrete structure needs rehabilitation or in critical cases must be demolished, therefore the price of a project consists of initial costs plus those

covering any rehabilitation. A huge amount of money could be saved by utilising the durability characteristics of high strength concrete. Haug (1994) stated that most platforms have been designed with a service life of approximately 30 years but projects constructed with high strength concrete have a service life of approximately 70 years. Thornton et al. (1994) stated that using high strength concrete of 80 MPa reduces the size of the elements, saves rentable space, which makes the project economical.

2.3.4 Main factors affecting the cost of HSC

a) Research and development

Research on high strength concrete has been under way for many years in many countries. However, HSC is the most prestigious subject for research at the international level. Researchers aim to find ways of maximising performance over the long term while minimising the cost. Continuous funding for research is important to gain new information and develop new technology to produce the best quality HSC and reduce the cost. The characteristics of HSC differ from normal strength concrete because of the different materials used to make them. Thus the stress-strain diagram for normal strength is parabolic but linear for HSC, up to failure. This difference may cause differences in design parameters especially those related to the stress-strain relationship. However estimating the cost is affected by the differences in the design methods of HSC and NSC although there is no evidence so far which suggests there is a major difference in design factors between

them. Nawy (2001) stated that "No conclusive evidence exists at this time on the need for major changes in the provisions of the ACI 318 code parameters for design of very high strength concrete structures, that is concrete with compressive strength exceeding 83 MPa". However there is a strong need for research to study the properties of high strength concrete structure. The use of HSC with longitudinal and lateral reinforcement improves mechanical qualities, fire resistance, the ductility of reinforced concrete components, flexibility and cracking, the dynamic behaviour of structures, and shock resistance (Malier and Richard, 1995). However ongoing research into the design structure of HSC may reduce the cost of the raw materials through more efficient design methods.

b) Type and location of the structure

The cost is affected by its location, and whether the concrete is required to resist temperature changes and the deleterious effect of chemicals and acid rain. The cost is also affected by the type of structure, eg, nuclear, and its location, eg, under water. Thus the type of concrete depends on the cost of its placement and finishing and any other special requirements.

c) Design Mixture

HSC quality depends on the quality and percentage of materials used. Quality could be controlled through a quality control programme by testing samples in lab and

field. The cost of material is affected by demands for the material and the cost of transportation.

d) Quality Control

HSC is a material whose properties such as compressive strength and tensile strength are difficult to predict. The mix must be designed to have an average compressive strength greater than the required value of its compressive strength. HSC needs a large number of control tests compared to NSC which should be done by professional teams with experience, which will eventually increase the cost. Full scale laboratory and training for HSC has not reached the required level which can cause an unacceptable number of problems in handling delicate qualities of HSC to the market (Helland, 1995). On the other hand the number of clients and competition between suppliers reduces the cost.

2.3.5 Advantages of using HSC

It has been proven that HSC can carry a compressive load at a lower cost than NSC (Schmidt and Hoffman, 1975). However, the advantages of HSC more than compensate for the increased costs of raw materials and quality control. The following are the main advantages of high strength concrete (Schmidt and Hoffman, 1975), (Nawy, 2001) and (Chan and Anson, 1994).

1- It satisfies the need for a high modulus of elasticity.

2- It reduces member size which leads to:

a) increasing rentable space
b) reducing the formwork
c) reducing the volume of concrete
d) reducing construction time
e) reducing labour
f) reducing the dead load reduces the size of the foundation plus gaining the previous benefits from b to e.

3- Saving in high rise building; by saving in one storey multiplied by the number of stories.

4- Using HSC reduces the number of beams which increases their span.

5- Using HSC reduces the number of columns and foundations

6- Higher resistance to freezing, thawing, and chemical attack.

7- Reduced maintenance and repair costs

8- Early removal of formwork and an avoidance of re-shoring

2.4 SUMMARY

In this chapter, the most important information about high strength steel and high strength concrete was presented. Firstly, information about high strength steel reinforcing bars was discussed and the mechanical properties and advantages of high strength steel were presented. Secondly, the definition of high strength

concrete and information about cement, aggregate, water, and chemical and mineral admixtures such as fly ash, silica fume and super-plasticisers were summarised. Also the main factors affecting the cost of high strength concrete and the advantages of high strength concrete were discussed.

The next chapter (Chapter 3) is titled Concrete Confinement-state of the art. Chapter 3 presents the mechanism of confinement, a comparison between helix and tie confinement, confinement efficiency, code provisions for confinement, factors affecting confinement, confined concrete compressive strength, ductility, beam ductility factors and prediction of its ductility.

CHAPTER 3

CONCRETE CONFINEMENT- STATE OF THE ART

3.1 GENERAL

The confinement of concrete in compression is a complicated phenomenon, but there is a continuing effort to understand its behaviour through extensive international experimental programmes. Confinement is either, active or passive confinement. Active confinement occurs when concrete is subjected to pressure such as a confining fluid, while passive confinement occurs when lateral reinforcement applies a confining reaction towards the concrete. As a result of this compressive load, confined concrete will expand but the confinement resists expansion due to passive confining pressure, thus lateral reinforcement is called passive confinement. The confining pressure is affected by several factors such as the spacing and yield strength of the confining reinforcement.

This thesis focuses only on passive confinement where concrete is confined by transverse reinforcement via a rectangular tie or helix. Concrete expands laterally under a compressive load but the confinement will resist concrete expansion and then reduce the tendency for internal cracking, which significantly enhances it

strength and ductility. Brittle compression failure can be avoided by using proper confinement, which restrains lateral expansion and increases ductility and strength of concrete. Most of the studies about confinement of concrete in the compression zone in beams is based on the results of research on columns, as the idea of a confined compression zone in beams has only been developed recently. Based on this, more study and data on the behaviour of confined HSC beams is needed. Base and Read (1965) showed through experimental testing that helical confinement enhances the strength and ductility of beams with high tensile longitudinal steel percentage.

3.2 CONFINEMENT MECHANISM

As mentioned above, the confining reinforcement increases ductility and compressive strength of concrete under compression by resisting lateral expansion due to Poisson's effect upon loading. The behaviour of confined concrete depends on the effectiveness of the confinement, which in turn is affected by several important variables such as helical pitch, helix yield strength and helix bar diameter. There is no confining effect after loading, until a particular lateral stress due to Poisson's effect is reached and then the confinement commences. Confinement does not increase strength or ductility initially, but when the axial stress is about 60% of the maximum cylinder strength, the concrete is effectively

confined (Sargin, 1971). However, there is no additional confinement effect if the confining steel reaches its yield strength.

The concrete cover spalling off phenomenon becomes visible when the concrete is confined. This is caused by the closely spaced reinforcement of confinement physically separating the concrete cover from the core, causing an early failure of the cover (Foster and Sheikh, 1998), (Ziara, 1993), (Ziara et al., 2000). This statement has an emphasis on closely spaced reinforcement of confinement and does not consider the helix diameter or variables such as confining steel yield strength, concrete compressive strength and longitudinal reinforcement ratio, which may affect the concrete cover spalling off phenomenon. Solving the concrete cover spalling off phenomenon is complex and further research to find out why this occurs is justified.

3.3 COMPARISON BETWEEN HELIX AND TIE CONFINEMENT

Helical reinforcement can be used to achieve the required ductility. It is generally accepted that helical confinement is more effective than rectangular ties in increasing the strength and ductility of confined concrete.

Hatanaka and Tanigawa (1992) stated that the lateral pressure produced by a rectangular tie is about 30 to 50 percent of the pressure introduced by a helix. This is in agreement with the experimental research conducted by Chan (1955), who showed that the efficiency of tie confinement is 50% of the helical confinement for the same lateral reinforcement ratio. The effectiveness of helix applies to concrete in compression for both beams and columns. The reason why helix is more effective than tie is because it applies a uniform radial stress along the concrete member, whereas a rectangle tends to confine the concrete, mainly at the corners. Thus the effective area of concrete at the cross section is reduced because the pressure will tend to bend the sides of the tie outwards due to their low stiffness compared with the four corners, as shown in Figure 3.1. As a result, a significant portion of concrete in the cross section will be effectively unconfined. On the other hand the arching of concrete between the ties reduces the effective confined concrete at the level of the concrete member length, as shown in Figure 3.2. Thus using helical confinement in the compression zone of rectangular beams is more effective than rectangular and square ties even though there is a very small portion of unconfined concrete in compression. This area is at the corner, as shown in Figure 3.3. However, to prove experimentally that a helix is more effective, there is a need to compare helically confined beams with beams confined by rectangular ties. An experimental study recently conducted by Whitehead and Ibell (2004) proved in beams that helical confinement is more effective than a rectangular tie.

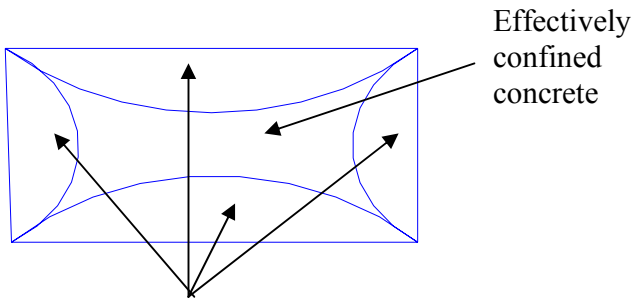

Unconfined concrete at the rectangular tie confinement

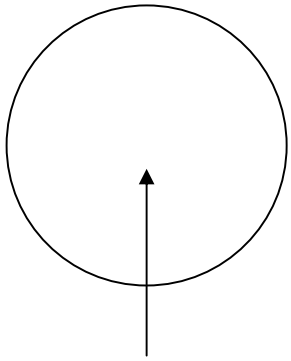

Effectively confined concrete for helix confinement

Figure 3.1. Effectively confined concrete for helix and rectangular tie

3.4 EFFICIENT CONFINEMENT

Brittle failures (compression failures) could be prevented when the beam is designed as an under-reinforced section, as recommended by design codes such as AS3600 (2001). However, providing a longitudinal reinforcement ratio more than the maximum longitudinal reinforcement ratio enhances the flexural capacity of the beam but creates brittle failure (non-ductile failure), which is not allowed by the design standards because ductility is an important factor related to human safety. Kwan et al. (2004) found that using a higher yield strength steel as longitudinal reinforcement enhances the flexural strength but reduces the flexural ductility of a beams' section. On the other hand using a higher yield strength steel to reinforce compression zone might not benefit the flexural strength of the beam section, but it does increase the flexural ductility. However, the most important issue is enhancing the concrete strength as well as the ductility.

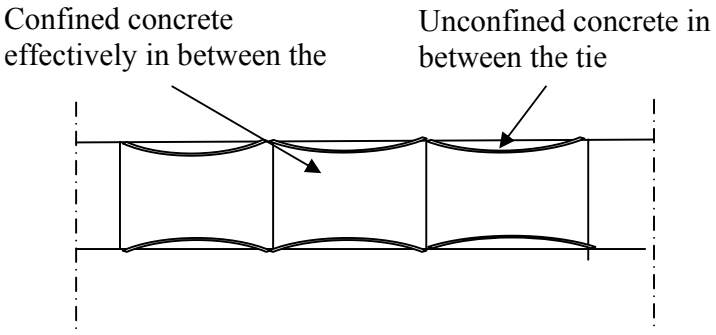

Figure 3.2 Effective confined concrete for rectangular tie

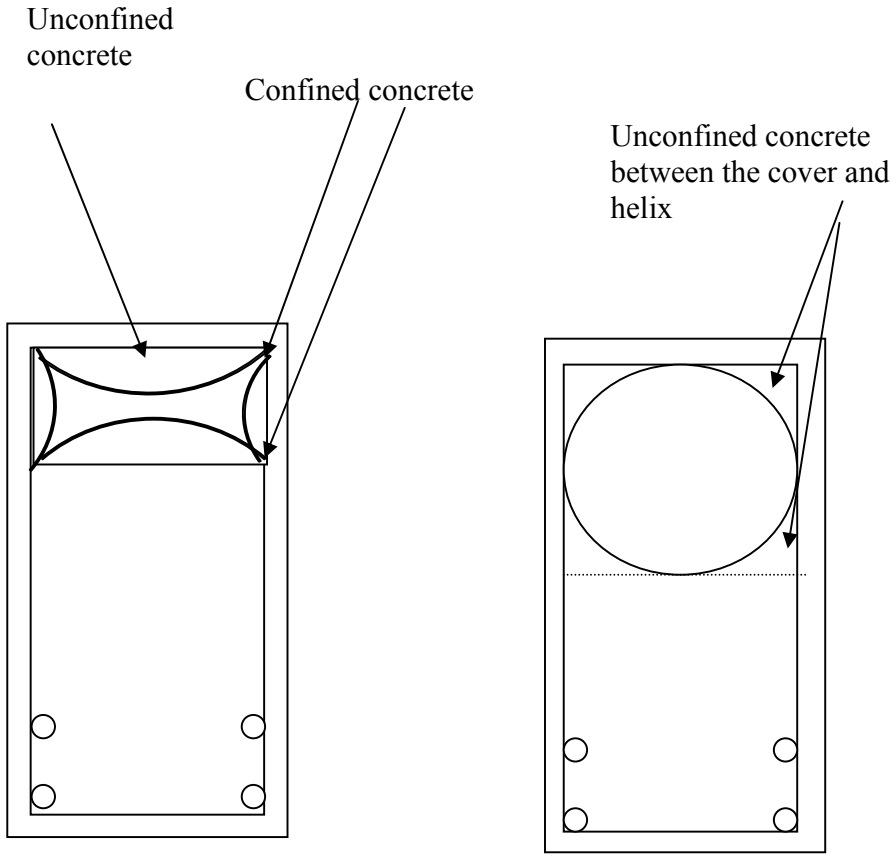

Figure 3.3. Confined and unconfined compression concrete in beams

There are a few ways of improving the ductility of concrete in compression, providing longitudinal compression reinforcement, using randomly oriented steel fibre, or installing a helical or tie confinement in the compression zone. A comparison between them to find the most effective way is presented below.

Shah and Rangan (1970) tested 24 groups of beams to compare their ductility. The tests were designed to be under four point loading to ensure failure in the central zone of constant moment. This zone contained various volumes of closed stirrups, different amounts of steel fibres or different volumes of compression longitudinal reinforcement. The test results showed that the ductility of a beam confined with stirrups has 10 times the ductility of the control beams (without any ductility reinforcement), while the fibres increased the ductility 4.5 times and the compression longitudinal reinforcement increased the ductility by twice that of the control beam. These results show that confinement with stirrups enhances ductility more than both the compression longitudinal reinforcement and the steel fibres. Also the beams, which had longitudinal compression reinforcement failed earlier because this type of reinforcing tends to buckle prematurely. Based on the experimental programme conducted by Shah and Rangan (1970), confinement in the compression zone of a beam is more efficient than steel fibres or longitudinal compression reinforcement.

Also, most of the literature, such as Park and Paulay (1975), Sheikh and Uzumeri (1980), Sheikh and Yeh (1986), Hatanaka and Tanigawa (1992) and Cusson and Paultre (1994) prove that helical confinement is more effective than rectangular tie confinement. Figure 3.4 shows the capacity for plastic deformation of a column confined by spiral reinforcement, and the brittle failure of a column confined by rectangular tie (Park and Paulay, 1975). In addition, the efficiency of helical confinement was recognised by several building codes such as ACI-318 (2002). However, since 1971 the ACI-318 Code uses an equation based on the concept that the efficiency of rectangular confinement is 50% of the helical confinement for calculating the rectangular confinement required.

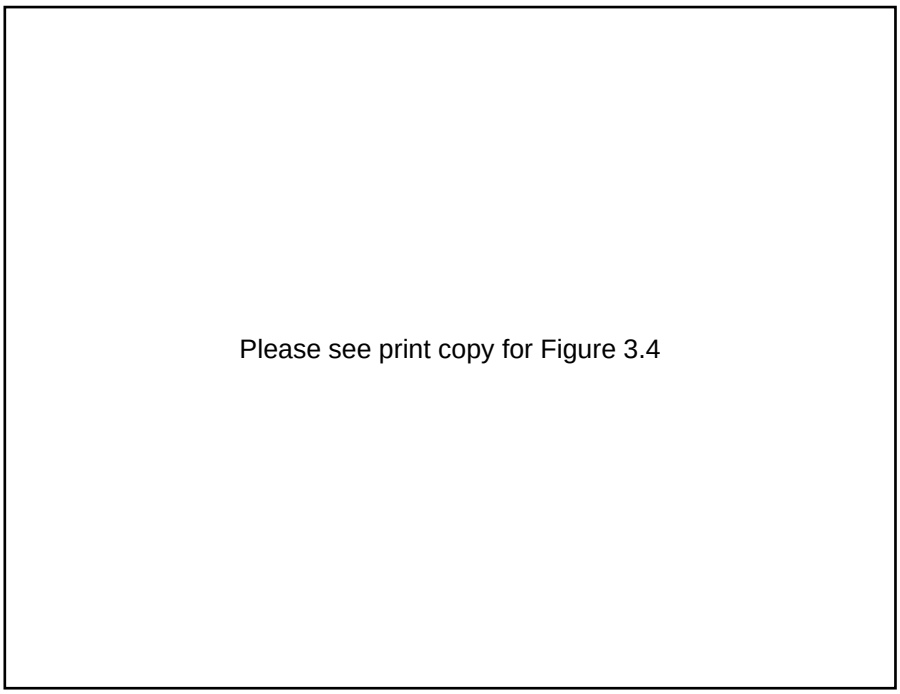

Figure 3.4 Comparison of total axial load strain curves of tied and spiral columns (Park and Paulay, 1975).

3.5 CODE PROVISIONS FOR CONFINEMENT

Design standards such as ACI 318R-02 (2002) encourage the use of the helix confinement rather than tie. However, these design standards provide design equations for volumetric reinforcement ratio for rectangular tie and helical confinement. The following equation was suggested to calculate the volumetric ratio of tie reinforcement in rectangular columns by ACI-318-95 (1995).

$$A_{sh} = 0.3 s h_c \left(\frac{A_g}{A_c} - 1 \right) \frac{f_c'}{f_{yh}} \tag{3.1}$$

but not less than

$$A_{sh} = 0.09 s h_c \left(\frac{f_c'}{f_{yh}} \right) \tag{3.2}$$

where A_{sh} is the total cross section area of rectangular ties; s is the spacing of the hoops; h_c is the maximum unsupported length of rectangular hoop measured between perpendicular legs of the hoop; A_g is the gross area of the section; A_c is the area of the core; f_c' is the concrete compressive strength and f_{yh} is the yield stress of helical reinforcement.

The total volumetric ratio of helices required by ACI-318-95 (1995) and the codes after 1995 are shown in Equations 3.3 and 3.4. After 1995 however, the codes ACI-

318 express the volumetric ratio of the helices reinforcement required for confining circular columns in terms of the volumetric ratio of the helices steel to the confined concrete core (excluding concrete cover). Nevertheless the ACI-318 codes before 1995 express the volumetric ratio of helices required for confinement reinforcement in circular columns in terms of the volumetric ratio of helices steel, to the total concrete cross sectional area (including concrete cover).

$$\rho_h = 0.45\left(\frac{A_g}{A_c} - 1\right)\frac{f_c'}{f_{yh}} \tag{3.3}$$

but not less than

$$\rho_h = 0.12\frac{f_c'}{f_{yh}} \tag{3.4}$$

where ρ_h is the total volumetric ratio of helices; A_g is the gross area of the section; A_c is the area of the core; f_c' is the concrete compressive strength and f_{yh} is the yield stress of helical reinforcement.

The Australian design standard AS3600 (2001) does not provide an equation for calculating the required volumetric reinforcement ratio for rectangular tie and helical confinement. Also the Australian design standard AS3600 (2001) does not consider the effectiveness of helices. The following are the specifications of the diameter and spacing of ties and helices in the Australian design standard AS3600 (2001):

a) The bar diameter of the tie or helix shall not be less than that given in Table 3.1.

b) The spacing of ties, or the pitch of a helix, shall not exceed the smaller of D_c or $15d_b$, where D_c is the smaller column dimension if rectangular or the column diameter if circular and d_b is the diameter of the smallest bar in the column.

Table 3.1. Bar dimension for ties and helices (AS3600, 2001)

Please see print copy for Table 3.1

Equation 3.3 was derived to compensate the strength lost by spalling off the concrete cover. There is a need for an equation to compensate for strength and ductility, and consider the helical pitch.

Helical pitch is an important parameter in enhancing the strength and ductility of beams. However, building codes such as ACI 318R-02 (2002) and AS3600 (2001) do not take helical pitch or tie spacing as an explicit design parameter. For example, Equation 3.3 of ACI 318R-02 (2002) for the design of helical reinforcement of columns does not directly include the helical pitch. The design is only for the quantity of lateral steel (volumetric ratio) without specifying the pitch.

3.6 FACTORS AFFECTING CONFINEMENT

The behaviour of confined concrete at maximum strain depends on the confining pressure, which in turn is affected by several factors. These factors could be determined through the mechanism of concrete confined by helix. Referring to Figure 3.5, the lateral pressure on the confined concrete P can be derived as follows:

$$2 f_y A_h = D s P \tag{3.5}$$

$$P = \frac{\pi f_y d_h^{\,2}}{2 D s} \tag{3.6}$$

where the core diameter is D, the helical pitch is s, the helix bar area is A_h, the helix bar diameter is d_h , f_y is the yield strength of helix bar

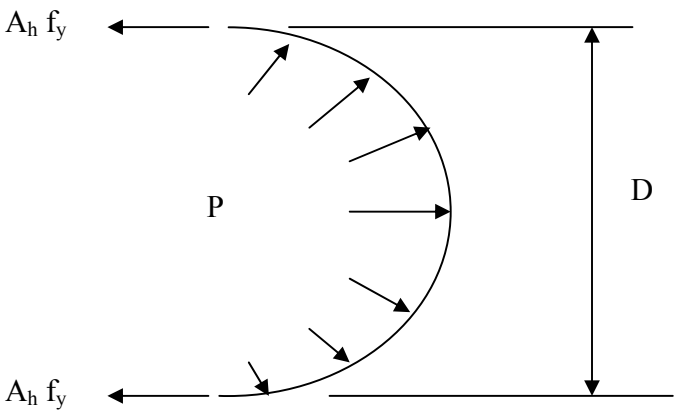

Figure 3.5 Confining pressure by helix confinement

The following are the main factors that affect the confinement of concrete under compression:

1- Lateral reinforcement ratio

Lateral reinforcement ratio is the ratio of the volume of lateral reinforcement to the volume of core concrete. Increasing the lateral reinforcement ratio increases confining pressure which then enhances confined concrete strength and ductility. Thus the lateral reinforcement ratio required for high strength concrete is higher than the lateral reinforcement ratio required for normal strength concrete.

2- Characteristics of lateral steel

The stress-strain relationship of lateral reinforcement and its yield strength affects the confining pressure. The concrete will expand without restraint and cracks will appear at the yield stress of the lateral reinforcement. However, lateral reinforcement with a strain-hardening stress-strain relationship restrains expansion until either the internal cracking gradually progresses up to the stage where the concrete cannot carry any further load, or up to the tension failure of the confining steel (Sheikh, 1978). However, Muguruma et al. (1979) stated that high tensile steel stirrups provide a higher degree of confinement if yielding of the confining reinforcement causes the confined concrete to fail.

3- Lateral reinforcement spacing

Effective reinforcement spacing increases the strength and ductility of compressive concrete members. Razvi and Saaticioglu (1994) stated that tie spacing is more effective in columns with a relatively high volumetric ratio of confinement steel. Affectively confined concrete tends to arch between ties, as shown in Figure 3.2. Thus confined concrete is significantly reduced if the spacing is large. In the other words, the effective confined concrete is decreased as the tie spacing increases, up to the stage where lateral confinement becomes negligible. However, helical confinement could be represented by the ratio of the helical pitch to the diameter of the concrete core. For example Martinez et al. (1984) stated that the confinement is negligible when the spacing is equal to its diameter and Ahmad and Shah (1982) observed that it was negligible when the spiral pitch exceeded 1.25 times the diameter of the confined core.

4- The diameter of lateral reinforcement

The diameter of lateral reinforcement may have a negligible effect on strength and ductility when the compressed concrete member is well confined but it will affect spalling off the concrete cover because the size of the steel confinement will separate the confined concrete from the concrete cover. Thus as the confinement bar size increases the concrete cover spalls off earlier. In some cases however, when the tie spacing is high an increase in the diameter of the lateral steel may not affect the concrete at all. In these cases the spacing

between the transverse ties is reduced in order to improve the performance of the concrete section (Bayrak, 1998).

3.7 CONFINED CONCRETE COMPRESSIVE STRENGTH

The strength of concrete increases significantly under triaxial compression but lateral pressure counteracts its tendency to expand laterally, which increases its strength. The confined concrete compressive strength can be predicted by using the simple Equation 3.7 which was proposed by Richart et al. (1929)

$$f_{cc}' = f_c' + 4.1\,P \qquad (3.7)$$

where f_{cc}' is the axial compressive strength of confined concrete in MPa; f_c' is uniaxial compressive strength of unconfined concrete and P is the lateral pressure on confined concrete in MPa.

By substituting the value of lateral pressure on the confined concrete (P) from Equation 3.5 into Equation 3.7, the axial compressive strength of concrete confined by helices could be predicted using Equation 3.8.

$$f_{cc}' = f_c' + 8.2\frac{f_y A_h}{D\,s} \qquad (3.8)$$

Over the years different models have been proposed by researchers to predict confined concrete compressive strength. Some of these models basically try to improve the equation proposed by Richart et al. (1929). For example the model proposed by Martinez et al. (1984) added the confinement effectiveness (the ratio of helical pitch to the core diameter) $\left(1-\frac{s}{D}\right)$ to equation 3.7. The confinement effectiveness proposed was based on an experimental observation that the effect of confinement is negligible when the spacing is equal to the confinement diameter. From Equation 3.9 the confined concrete compressive strength increases when the helical pitch decrease. Also the confined concrete compressive strength is equal to the unconfined concrete compressive strength when the helical pitch is equal to the concrete core diameter. Martinez et al. (1984) model is shown in Equation 3.9.

$$f_{cc}' = f_c' + 4P\left(1-\frac{s}{D}\right) \qquad (3.9)$$

Where P is the confinement pressure, $P=\frac{2 f_y A_h}{D s}$; f_{cc}' is the confined compressive strength of a confined column; f_c' is the compressive strength of unconfined concrete; D is the concrete core diameter; s is the helical pitch; f_y is the yield stress of the helix and A_h is the cross section area of helix steel bar diameter.

Small specimens generally don't represent the correct effect of different variables on how confined concrete behaves. Thus, realistic models for predicting the compressive strength of confined concrete are those, based on testing full size specimens with variables such as the longitudinal and lateral reinforcement ratios and helical spacing. This fact was proved experimentally by King (1946), where he stated that "The behaviour of large size columns was different from that of the small sized columns".

The concept of beam confinement is not fully understood because of limited research on this topic, although interest is gradually increasing. The availability of high strength materials such as high strength steel and high strength concrete enhances the strength of reinforced concrete columns as well as beams, but increasing strength decreases beam ductility. Installing confining reinforcement in the compression zone of a reinforced concrete beam enhances it's ductility and compressive strength. This confined concrete compressive strength cannot be predicted using models for columns such as Equation 3.9, because columns behave differently. The position of helices in beams affects confinement, the spalling off phenomena, and the confined strain developed from resisting the concrete expansion. Figure 3.6 (a) shows that the lateral forces are restrained by helix confinement in the compression zone of a reinforced concrete beam. Figure 3.6 (b) displays the nearly intact compression core after the concrete cover has spalled off due to excessive compressive forces. Extensive experimental data and worthy

observation are required to understand and develop a model to predict the behaviour of over-reinforced high strength concrete beams.

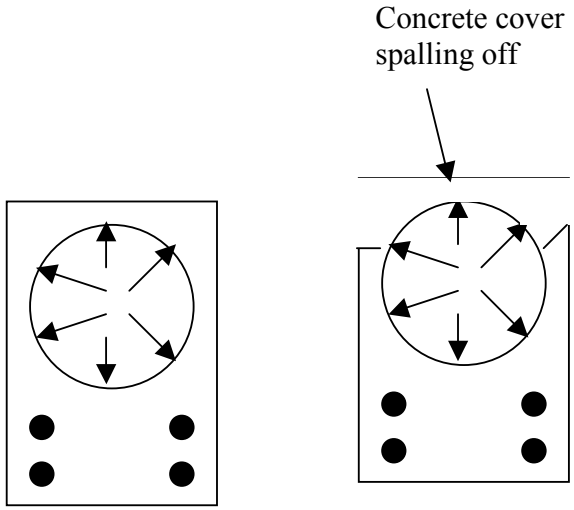

(a) Resisting the concrete expansion before the concrete cover spalls off

(b) Resisting the concrete expansion after the concrete cover spalls off

Figure 3.6 Effect of helical confinement on beams before and after the concrete cover spalling off

3.8 DUCTILITY

3.8.1 Definition

Ductility ensures that large deflections will occur under overload conditions before a structure fails. This large deflection warns of impending failure. Ductility is an important requirement when designing structures subjected to earthquake loading. "Use of confining steel in the critical regions of columns designed for earthquake resistance is a common way of achieving ductile structural behaviour" (Sheikh and Yeh, 1990). Ductility could be estimated through the displacement ductility factor, which is defined as the ratio of deflection at ultimate load to the deflection when the tensile steel yields. As stated above, design standards such as ACI 318R-02 (2002) and AS3600 (2001) do not allow design of over-reinforced sections and balanced beams because they are both brittle at overload. However, recent earthquakes have provide encouragement for more research into improving structural ductility.

3.8.2 Beam Ductility Factors

Beams are expected to yield before columns, and therefore the flexure ductility required for beams is higher (Paulay and Priestly, 1990). Under-reinforced beams fail in a ductile manner, where the steel reinforcing bars yield before brittle failure

in the concrete. However, over-reinforced beams and columns fail in a brittle way if there is no lateral confinement. Nilson (1985) stated that high strength concrete is a brittle material and consequently structures constructed using it fail in a brittle manner. This failure is a major concern when using high strength concrete.

There are different ways to describe beam ductility. This thesis focuses on the main ductility measures. The first, and most common one, is the displacement ductility factor, which expresses overall structural ductility. The second is the curvature ductility factor, which describes local ductility in the hinging zone, and the final one is the strain ductility factor.

1- Displacement ductility

Displacement ductility factor is defined as the ratio of maximum displacement to yield displacement, as expressed in the following equation.

$$\mu_d = \frac{\Delta_u}{\Delta_y} \qquad (3.10)$$

Where μ_d is the displacement ductility factor; Δ_u is the ultimate deflection and Δ_y is the yield deflection.

Idealising the relationship between the real load and displacement, Priestly and Park (1987) suggest that the yield displacement is defined as the intersection between the extension of elastic behaviour and the maximum load capacity where

the ultimate displacement corresponds to either the hoop fracture in a confined concrete, or 80% of the maximum load, whichever is smaller, as shown in Figure 3.7. The displacement ductility factor applies to a beam as a structural unit, whereas the curvature ductility factor applies to a particular beam cross-section. The Structural Engineers Association of California, (SEAOC, 1973) recommended that the displacement ductility factor for suitable dissipation of energy in the event of seismic activity should be from 3 to 5.

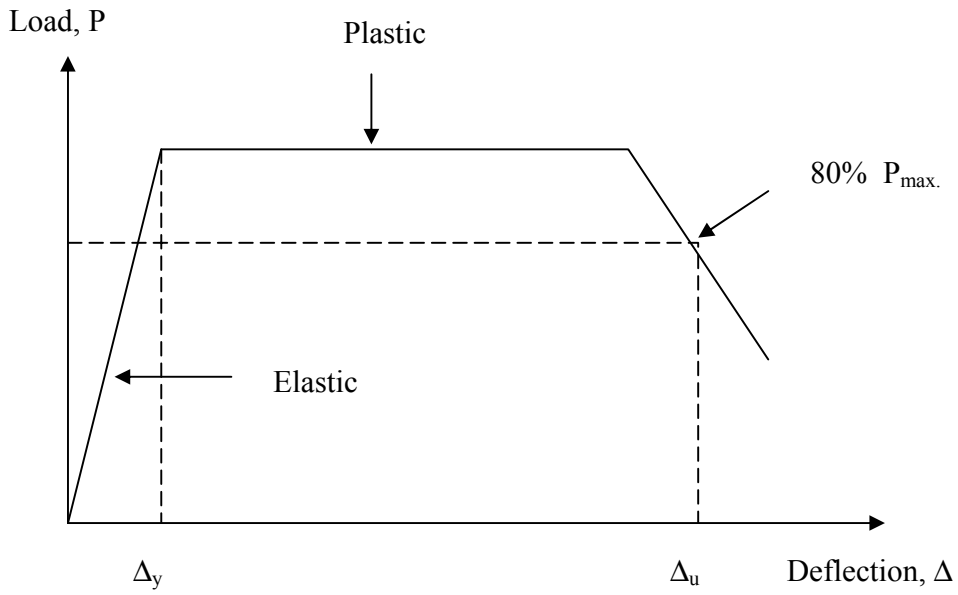

Figure 3.7 Idealised load mid-span deflection for displacement ductility factor

2- Curvature ductility

Curvature ductility factor is one way for presenting the elastic-plastic behaviour of a reinforced concrete section. Elastic, plastic and softening are the three phases of the moment curvature diagram (Pendyala et al., 1996). Firstly, a reinforced concrete beam behaves elastically as the moment increases which uniformly distributes curvature along the entire length of the beam. Secondly, the range of plasticity occurs when deformation increases at a constant bending moment, but at this stage, curvature is not distributed uniformly along the length of the beam. The final stage is softening, where the moment decreases with an increase in curvature. Figure 3.8 shows the moment curvature relation for a reinforced concrete section where the yield curvature could be defined as curvature at the intersection of the extension of elastic behaviour with the maximum moment capacity. Maximum curvature, as suggested by Priestly and Park (1987) and Shin et al. (1989), is defined as the value corresponding to 80% to 90% of the maximum moment capacity.

$$\mu_{\phi} = \frac{\phi_u}{\phi_y} \tag{3.11}$$

Where μ_{ϕ} is the curvature ductility factor; ϕ_u is the ultimate curvature and ϕ_y is the yield curvature.

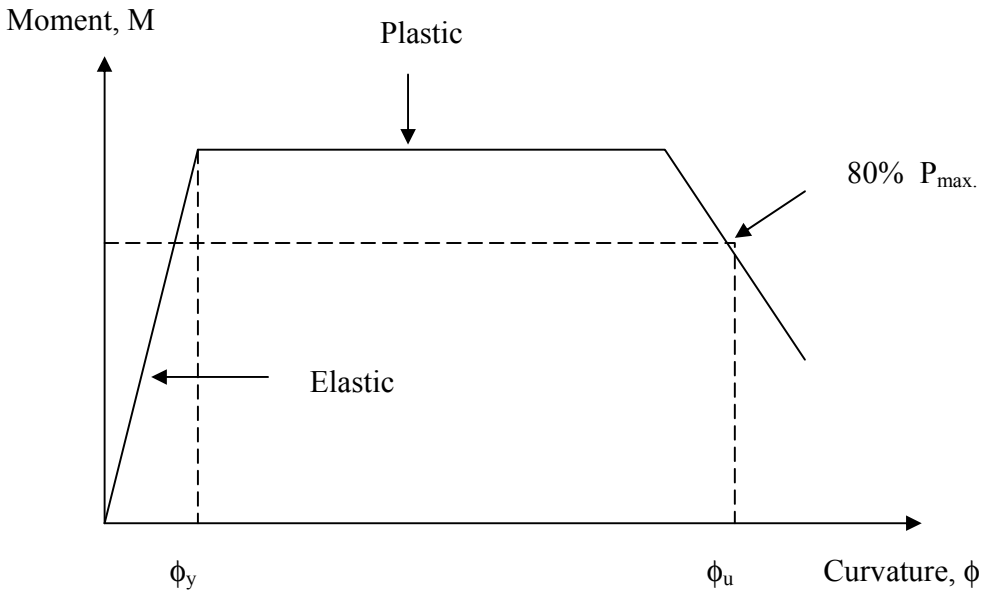

Figure 3.8 Idealised moment curvature for curvature ductility factor

3- Strain ductility factor

This is not as common as the curvature ductility factor or displacement ductility factor. Figure 3.9 shows an idealised load concrete compressive strain for strain ductility factor, where the ultimate strain corresponds to 80% of the maximum load. However the strain ductility factor is defined by the following equation.

$$\mu_e = \frac{\varepsilon_u}{\varepsilon_y} \qquad (3.12)$$

where μ_e is the strain ductility factor; ε_u is the sustainable strain and ε_y the yield strain.

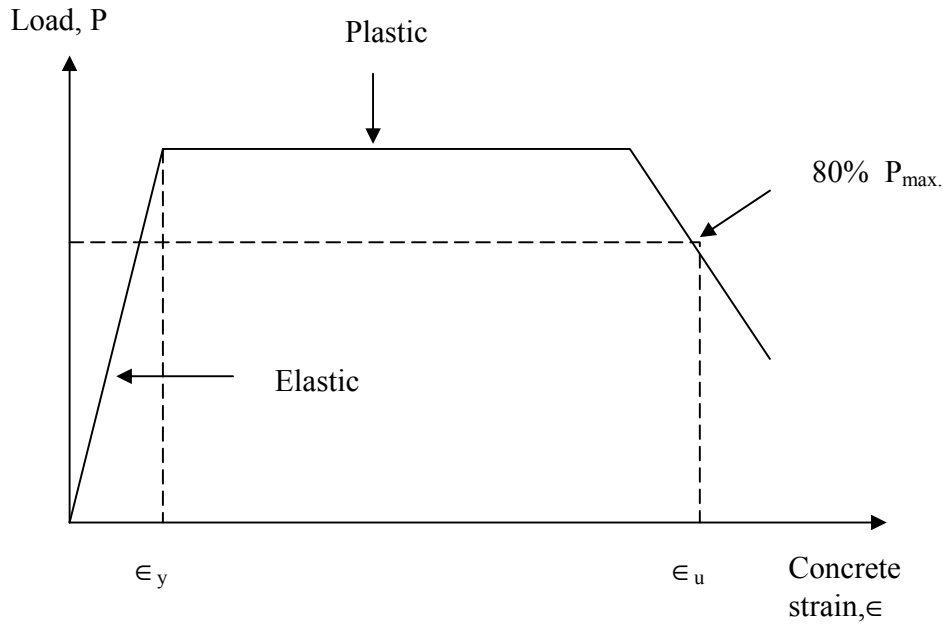

Figure 3.9 Idealised load concrete compressive strain for strain ductility factor

3.8.3 Predicting beams ductility

There are a limited number of proposed models for predicting the curvature ductility factor, displacement ductility factor and the strain ductility factor. Following below is a short review of the available models for predicting the ductility factor of reinforced concrete beams. It is not known why there is a limited

number of proposed models, but they do not reflect what was mentioned earlier about the importance of ductility. This area needs more research. However Pastor et al. (1984) have derived an analytical formula to predict the curvature ductility factor, and it is given as follows:

$$\mu_{\phi} = \frac{(1-k)\alpha f_c^{'} E_s \varepsilon_{cu}}{f_y(\rho f_{sy} - \rho_c f_{su})} \tag{3.14}$$

where, μ_{ϕ} is the curvature ductility factor; k is the ratio of depth to neutral axis at first yield of tension reinforcement, to effective beam depth; α is the rectangular stress block parameter; E_s is the modulus of elasticity of reinforcement; ε_{cu} is the compressive strain at extreme compression fibre of confined concrete at ultimate load; f_{su} is the stress in compression reinforcement; f_{sy} is the stress in tension reinforcement; ρ is the tensile steel ratio; ρ_c is the compression steel ratio

Suzuki et al. (1996) proposed an equation to predict the displacement ductility as follows:

$$\mu_d = \frac{1.68\rho_b}{\rho^{-0.68}} \tag{3.15}$$

where, ρ is the longitudinal reinforcement ratio provided and ρ_b is the balanced reinforcement ratio.

In order to predict the strain ductility factor for confined beams the confined compressive strain (ε_{con}) needs to be predicted. However the expressions proposed by Corley (1966) are those most commonly used to predict the confined compressive strain (ε_{con}), which depends only on the volumetric lateral reinforcement ratio and the yield strength of reinforcement ratio. Corley (1966) proposed a model to predict the confined compressive strain (ε_{con}) as shown in Equation 3.16.

$$\varepsilon_{con} = 0.003 + 0.02\frac{b}{z} + \left(\frac{\rho_t f_{yt}}{20}\right)^2 \qquad (3.16)$$

Where b is the width of the compression face of the flexural member; z is the distance between points of zero and maximum moments; ρ_t is the volumetric compressive and lateral tie steel ratio and f_{yt} is the tie steel yield stress. For pure bending Equation 3.17 is used.

$$\varepsilon_{con} = 0.003 + \left(\frac{\rho_t f_{yt}}{20}\right)^2 \qquad (3.17)$$

Kaar et al. (1977) modified Equation 3.17 to become as follows

$$\varepsilon_{con} = 0.003 + \left(\frac{\rho_t f_{yt}}{15} \right)^2 \quad (3.18)$$

Mattock (1964) expressed confined compressive strain using only the lateral reinforcement ratio as follows:

$$\varepsilon_{con} = 0.003 + 0.2\rho_t \quad (3.19)$$

Thus one could predict the strain ductility factor for confined beam using Equation 3.20 through predicting the yield and ultimate confined compressive strains. The ultimate confined compressive strain could be predicted using one of the models mentioned above, in Equations 3.16, 3.17, 3.18 or 3.19. However to the best knowledge of the Author, there is no expression to predict the yield confined compressive strain. Thus in order to determine the strain ductility factor for confined beams, there is a need to predict the yield confined compressive strain.

$$\mu_e = \frac{\varepsilon_{con}}{\varepsilon_{y,con}} \quad (3.20)$$

where μ_e is the strain ductility factor; ε_{con} is the ultimate confined compressive strain and $\varepsilon_{y,con}$ is the yield confined compressive strain.

In Chapter 8, Equation 3.18 will be modified to predict the confined concrete compressive strain (ε_{con}) of over-reinforced helically confined HSC beams.

3.9 SUMMARY

The behaviour of confined concrete is discussed in this Chapter. Confinement mechanisms are presented with the factors affecting confinement. A comparison between helix and tie confinement and confinement efficiency are highlighted. The lateral reinforcement ratio required by the code provisions are briefly summarised. Confined concrete compressive strength is discussed. Ductility definition and models for predicting the confined concrete beams' ductility are included in this Chapter.

Chapter 3 provides information about concrete confinement and ductility necessary to facilitate understanding the literature. Chapter 4 presents a literature review.

CHAPTER 4

LITERATURE REVIEW

4.1 GENERAL

The technology of high strength concrete has improved over the last decade. High strength concrete is more brittle than normal strength concrete. This brittleness increases as the reinforcement ratio increases more than the maximum reinforcement ratio recommended by codes of practice of concrete design. Avoiding brittle compression failures by using proper confinement which restrains lateral expansion will increase the strength and ductility of compression concrete. ACI committee 363-High-Strength concrete (1992), has identified the ductility of HSC members as a priority research need. The spacing, amount, and configuration of lateral reinforcement influences the confinement quality provided to the HSC. For the design of HSC members, safety is maintained by providing additional confining reinforcement to achieve a similar ductility level as normal strength concrete, or by modifying the design capacities. The concept of using helical reinforcement in the concrete columns was first introduced by Considere in 1899 (Pessiki and Pieroni, 1997), and perhaps the first use of helical confinement of beams was by Base and Read in 1965.

It has been observed that most research concerning confinement of the compression zone in beams is based on the results of research on columns, because the idea of a confined compression zone in beams has only been developed recently. Based on this, the literature and data available regarding confinement of columns is significantly more than for beam confinement. The following sections present an extensive review of the literature about column and beam confinement.

4.2 PREVIOUS INVESTIGATION ON CONFINED COLUMNS AND BEAMS

4.2.1 Base and Read (1965)

Base and Read (1965) tested 13 reinforced and three pre-stressed beams. The cross section of the beams was 152 × 280 mm × 3050 mm long. The beams were tested using single point loading at mid-span. The beams were designed as under reinforced, balanced and over-reinforced sections. The compression zone of some beams was confined by rectangular stirrups only and the other beams were confined by rectangular stirrups and helical reinforcement. The tie stirrups spacing were 50 and 203 mm. The helical reinforcement diameters were 6.35 and 4.76 mm, the helical pitch was 50 and 25 mm, and the confined concrete core was 82 mm. The main conclusions of Base and Read (1965) are:

1-The ductility of under-reinforced beams is not affected by lateral reinforcement provided in plastic hinges.

2-The type of failure of balanced, reinforced beams was sudden (compression failure) unless the compression zone was confined by tie stirrups or helix.

3- The rotation of beams helically confined was 2.5 times more than the rotation of beams confined using tie stirrups, even though the weight of the helices was 50% of the tie stirrups. Thus this study proved that helical confinement is more economical than close rectangular stirrups in terms of reinforced steel used against the amount of the enhancement of moment rotation characteristics.

4- Helical confinement increases the ductility of rectangular pre-stressed concrete beams. Experimental results show that the rotation from using tie stirrups confinement increased from 0.038 to 0.078 radians at a moment equal to 90% of the ultimate moment, and the helical confinement increased rotation at a moment equal to 90% of the ultimate moment, from 0.038 to 0.135 radians, even though the tie stirrups reinforcement ratio was twice the helical reinforcement ratio. Thus the helical confinement was found to be more economical and effective than the tie stirrups confinement for rectangular concrete beams.

4.2.2 Shah and Rangan (1970)

Shah and Rangan (1970) tested twenty-four groups of beams with two identical beams in each group. Their cross section was 50.8 × 76.2 mm and the length was 914.4 mm. The test was designed to be under four point loading to ensure failure in the central constant moment zone. The finding of Shah and Rangan (1970) was reviewed in Chapter 3, in Section 3.4.

4.2.3 Ahmad and Shah (1982)

Ahmad and Shah (1982) have tested 96 specimens, 75 mm diameter by 300 mm high. All the specimens were without cover. In order to study high strength spiral steel in confined concrete, two-spiral yield strengths were used, 413 MPa and 1433 MPa. Ahmad and Shah (1982) observed that the confinement was negligible when the spiral pitch exceeded 1.25 times the diameter of the confined core. For confined circular columns, the strength of concrete is given by Ahmad and Shah (1982) as follows:

$$f_{cc} = f_c^{'} + K_1 f_r \tag{4.1}$$

$$f_r = \frac{q_s f_y}{2}\left(1 - \sqrt{\frac{S_{sp}}{1.25 d_c}}\right) \tag{4.2}$$

$$q_s = \frac{\pi d^2}{d_c S_{sp}} \tag{4.3}$$

$$K_1 = \frac{6.61}{\sqrt{f_c'}}(f_r)^{0.04} \tag{4.4}$$

Where f_r is the average confining pressure; f_{cc} is the confined concrete compressive strength; f_c' is the unconfined concrete compressive strength; q_s is the ratio of volume of spiral reinforcement to the volume of the confined core; d_c is the diameter of the confined core; and S_{sp}, d and f_y are the pitch, diameter and yield strength of the spiral respectively. K_1 is effectiveness of confinement. Note that the stresses are expressed in ksi.

4.2.4 Martinez et al. (1984)

Martinez et al. (1984) investigated spirally confined normal strength concrete (NSC) and high strength concrete (HSC) by testing 94 small diameter columns. The columns were in four groups, the first were 102 mm diameter by 203 mm high, the second were 102 mm diameter by 406 mm high, the third were 127 mm diameter by 610 mm high, and the last were 152 mm diameter by 610 mm high. 78 columns had no protective concrete cover over the spiral steel but sixteen columns did. The compressive strength varied between 21 to 69 MPa and no longitudinal reinforcement was included. The total axial deformation and strains in the lateral steel were measured. The main objective was to establish any difference in behaviour between the HSC and NSC columns. Based on the experimental results,

Martinez et al. (1984) proposed the following equation to predict the confined strength of HSC and NSC.

$$f_c = f_c'' + 4f_2\left(1 - \frac{s}{d_c}\right) \qquad (4.5)$$

Where f_2 is the confinement stress, $f_2 = 2A_{sp}f_{sy}/d_c s$; f_c is the compressive strength of spiral column; f_c'' is the compressive strength of unconfined column; d_c is outside to outside spiral diameter; s is the spiral pitch; f_{sy} is the yield stress of the spiral steel and A_{sp} is the area of spiral steel.

From this study, the following conclusions are drawn:

1- The modulus of elasticity of columns spirally confined is essentially the same as unconfined concrete.

2- Use of helical steel with a yield stress over 414 MPa may result in unconservative designs if the steel is assumed to be at yield at the computed failure load of the column.

3- The effect of confinement is negligible when the helical pitch is equal to the confinement diameter.

4.2.5 Issa and Tobaa (1994)

Twenty five prismatic specimens (125 × 125 × 400 mm) were confined by continuous circular and square spirals and then tested to obtain the stress-strain characteristics of confined concrete under concentric axial compression.

From this study, the following conclusions are drawn:

1- For plain concrete specimens, a wide vertical crack propagated and led to sudden splitting before they reached maximum load.

2- A ductile failure was observed in the unconfined specimens with the crack spreading before they reached maximum load, which led to the concrete cover spalling off.

3- The load carrying capacity of the confined specimens was influenced by the detailing of the transverse reinforcement.

4- The close spacing and large diameter of the spiral weakened the surface between the concrete cover and the core, which led to the cover spalling early.

5- Issa and Tobaa (1994) proposed a model to predict the confined compressive strength as follows:

$$f_{cc} = f_{co} + K_1 f_r \tag{4.6}$$

$$f_r = \frac{1}{2}\rho_s f_y\left(1-\frac{s}{d_c}\right) \tag{4.7}$$

$$K_1 = \frac{1}{0.0908+0.453\sqrt{\left(\frac{f_r}{f_{co}}\right)}} \tag{4.8}$$

where f_{cc} is confined concrete strength; f_{co} is the unconfined concrete strength; f_r is the effective lateral confining pressure in the concrete; s is the spiral pitch; d_c is the concrete core diameter measured to outside of spiral; ρ_s is volumetric ratio of the transverse reinforcement in the confined core; f_y is the steel yield strength; K_1 is confinement coefficient for strength.

6- An increase in the steel yield strength increases the strength and ductility of the confined concrete.

7- A minimum volumetric ratio ρ_s required by the ACI 318R-89 (1989) code as

$$(\rho_s)_{\min} = 0.45\left(\frac{A_g}{A_c}-1\right)\frac{f_c'}{f_y} \tag{4.9}$$

to satisfy this condition, the strength enhancement should be $\frac{f_{cc}}{f_{co}} \geq \frac{A_g}{A_c}$. The experimental results show that this condition is satisfied by the results of specimens with a lower volumetric ratio than that required by the ACI 318R-89 (1989). HSC with strength up to 82.7 MPa confined by spiral reinforcement according to ACI code requirements shows a gain in strength sufficient to compensate for the concrete cover spalling

4.2.6 Cusson and Paultre (1994)

38 pairs of various column specimens with four types of tie configuration were tested. Their cross section was 235 × 235 mm and their length was 900 mm. The objective was to study seven key variables with respect to gains in strength and ductility. They were compressive strength, tie yield strength, tie configuration, lateral reinforcement ratio, tie spacing, longitudinal reinforcement ratio, and concrete cover.

From this study, the following conclusions are drawn:

1- The test results indicate that a significant increase in strength and ductility can be achieved when lateral reinforcement is provided.

2- Increasing the tie yield strength would only increase the strength and toughness for well confined specimens with large ratios of lateral reinforcement.

3- The axial strain at concrete cover spalling off ranges from 0.0022 to 0.0034.

4- The test results prove that the square tie configuration does not confine the concrete core and should not be used when ductility is required.

5- Increasing the lateral reinforcement ratio increases the strength and ductility of confined columns.

6- Reducing the tie spacing increases the strength and ductility of confined columns.

7- An increase in the longitudinal reinforcement ratio increases the strength and ductility of well confined specimens with large ratios of lateral reinforcement.

8- The early spalling of the concrete cover reduces the axial capacity. At this load level, stress in the transverse reinforcement is generally lower than 50% of the yield stress but after that the axial strength loses 10-15% of its maximum value due to sudden spalling. After the concrete cover has completely spalled off, important gains in strength and ductility have been recorded for the concrete core of well-confined specimens.

Cusson and Paultre (1994) suggest that:

a) Only the concrete core should be considered in calculation unless separation of the concrete cover is restricted.

b) The dense lateral reinforcement steel creates planes of longitudinal weakness between the core and the concrete cover. This phenomenon is more evident when using HSC.

c) The concrete cover significantly affects HSC columns. It should be as thin as possible to lower the loss of axial load capacity after spalling and only be considered as a protection against corrosion and fire for the steel reinforcement.

4.2.7 Ziara et al. (1995)

Ziara et al (1995) tested four beams without confinement and eight beams with tie confinement in the compression zone. The main aim is to study the flexural behaviour of beams with confinement.

Findings which transpired from these tests are as follows:

1- Concrete cover spalling off occurred after the beams reached their maximum load capacity. The confining stirrups delayed failure beyond the point at which the cover first began spalling off, because the pitch was reduced by 50%.

2- All the tested beams reached their full flexural capacity.

3- The test results have shown that confining the compression regions with closed stirrups did not significantly increase their flexural capacity but their ductility increased when the compression zone was confined at the mid-span region.

4- Variation in compressive strength does not significantly influence flexural capacity.

5- Brittle failure of over-reinforced beams can be prevented by using confinement in the compression zone.

6- The proposed flexural capacity for over-reinforced beams was based on ignoring the cover and using the maximum compression strain as 0.005.

7- The strain measured in confined beams 20 mm below the upper surface of the beam just before the cover cracked was 0.0054.

8- It was difficult to define the point of failure during testing because they continued to carry the maximum applied loads until the test was stopped.

9- The strains measured in the stirrups were very high and exceeded the operating range of the electrical resistance strain gauges. For that reason it could be assumed that the stress under ultimate loading would reach yield.

10- ACI 318R-89 (1989) limits the value of $\rho_{max} = 0.75\rho_b$ is too restrictive, when it is possible to increase ductility by confining the compression zone.

4.2.8 Mansur et al. (1997)

Eleven reinforced HSC beams were tested. The overall length was 3.30 m and the cross section was 250 mm deep by 170 mm wide. The main objective was to study the flexural response of mainly over reinforced HSC beams with and without confinement in the compression zone.

From this study, the following conclusions were drawn:

1- Volume fraction of confining ties increases the ductility, but up to a certain limit. In this study a volume fraction of ties in excess of 2.6% showed negligible gain in ductility.

2- An increase in the strength of concrete increases the ultimate strength of the beams but results in more brittle failure. However, for unconfined beams a sudden drop in the applied load occurred immediately after crushing the concrete and the beams with confinement, this sudden drop was arrested by the confined concrete core.

3- Stress strain curves obtained from uni-axial tests can be applied to the flexural analysis of HSC beam. The stress-strain relationship obtained from uni-axially loaded specimens can be applied to predict the ultimate strength and deformation behaviour of HSC flexural members.

4- The maximum design strain of 3000 micro strains for concrete in compression, as used in the ACI-318 code (1995) may be extended to HSC beams.

Equation 4.10 is the simplified design equation to HSC beams without compression reinforcement by ACI 318R-95 (1995):

$$\frac{M}{bd^2 f_c'} = q\left(1 - \frac{K_2}{K_1 K_3} q\right) \tag{4.10}$$

where the tensile reinforcement index q, is

$$q = \rho \frac{f_s}{f_c'}$$

$$K_1 K_3 = 0.85\beta_1$$

$$K_2 = \frac{\beta_1}{2}$$

Where:

M is the maximum moment capacity ; K_1, K_2, K_3 is the flexural constants; f_c' is the compressive cylinder strength, d is the effective depth of beam; b is the breadth of

beam and $\beta_1 = 0.85$ for $f_c \leq 27.6$ MPa, and reduced continuously at a rate of 0.45 for each 6.9 MPa of strength in excess 27.6 MPa. However β_1 is not less than 0.65.

Mansur et al. (1997) data and data from literature were used to determine the values of K_1, K_2, K_3 and β_1. Mansur et al. (1997) found good agreement between the ultimate moments calculated using the proposed values with the experimental results.

4.2.9 Foster and Attard (1997)

Sixty eight columns with cross section 150×150 mm^2 by 1050 mm high were tested under compression. The main objective was to determine the strength and ductility of conventional and HSC columns under a static, eccentric, axial load. The range of compression strength was 40 to 90 MPa.

The conclusions from the study are:

1- For some of the 75 MPa columns their ultimate strengths were lower than predicted. The results for the 90 MPa columns agree with the predictions made using the rectangular stress block model. However the 75 MPa columns had significantly high cover, contained a high percentage of longitudinal reinforcement, and had close tie spacing.

2- There is some doubt that increasing the yield strength will increase the level of confinement and ductility because strain in the ties has not reached yield at peak load. Maximum strain in the ties at peak was between 100 $\mu\varepsilon$ and 1000 $\mu\varepsilon$. Foster and Attard (1997) recommended that further tests are needed.

3- The experimental results prove that the confinement parameter ($\frac{\rho_s f_{yt}}{f'_c}$) reflects the level of affective confinement. However the ductility level is not a function of the confinement parameter alone, it is affected by the tie spacing and configuration, the cover and volume, and the arrangement of longitudinal reinforcement.

4- Steel is needed in an HSC column to obtain a ductility similar to an NSC column. This is accepted if the ties are at yield but further evidence suggests that the ties may not be at yield at the peak load.

5- In this study there was no answer to why the concrete cover spalled.

6- No significant differences can be seen between data for the 10 mm and 20 mm concrete cover, but data for the 0 mm cover gave a consistently higher strength. Further studies are required to prove that the cover should be excluded when calculating the maximum load of an HSC column.

4.2.10 Pessiki and Pieroni (1997)

Eight specimens 559 mm diameter by 2235 mm high were tested. The objective was to study the behaviour of large-scale, spirally reinforced HSC columns subjected to concentric axial load. This research studies the effect of compressive strength, the ratio of longitudinal steel, and pitch of spiral steel on the strength and ductility of a column

From this study, the following conclusions are drawn:

1- The higher strength concrete columns displayed less ductility than the lower strength concrete. This suggests that more than the minimum amount of spiral reinforcement currently prescribed by the ACI 318 code (1989) is needed for HSC columns to achieve the same ductility as those from low strength concrete.

2- A decrease in the pitch of the spiral reinforcement led to an increase in ductility.

3- Higher strength concrete columns experienced first cracking of the concrete cover at a lower load relative to peak load. It may be that the larger volume of spiral reinforcement creates a plane of separation between the cover and core concrete.

4.2.11 Bing et al. (2001)

Bing et al. (2001) tested 40 reinforced concrete columns 720 mm high. 23 columns had a square cross sectional area of (240 × 240 mm^2), and 17 columns with a 240 mm diameter cross section. The range of compressive strength was between 35 and 82 MPa to cover normal and high strength concretes. In order to study the yield strength of lateral steel on confining concrete, two grades with yield strengths of 445 and 1318 MPa were used, which are very similar to the yield strengths used by Ahmad and Shah (1982).

Equation (4.11) is Mander et al. (1984) model, which covers normal and high strength confined concrete. It was later modified by Bing et al. (2001) taking into account the regression analysis for test results to modify the ($f_l^{'} / f_c^{'}$). Where the effective lateral confining pressure ($f_l^{'}$) is calculated for different types of confinement configurations using different equations.

$$f_{cc} = f_c^{'}\left(-1.254 + 2.254\sqrt{1 + 7.94\frac{f_l^{'}}{f_c^{'}}} - 2\frac{f_l^{'}}{f_c^{'}}\right) \qquad (4.11)$$

$f_l^{'} = 0.5K_e\rho_s f_{yh}$ (for circular hoops and spirals)

For circular hoop, $K_e = \dfrac{(1-0.5S/d_s)^2}{1-\rho_{cc}}$

For spirals, $K_e = \dfrac{(1-0.5S/d_s)}{1-\rho_{cc}}$

Where K_e is the confinement effectiveness coefficient; ρ_{cc} is the volumetric ratio of longitudinal reinforcement in confined concrete core; ρ_x and ρ_y are volumetric ratios for lateral confining steel parallel to x and y axes, respectively; and f_{yh} is the yield strength of transverse reinforcing steel; and d_s is the effective core diameter between circular hoop or spiral bar centres.

Equation (4.12) is the modified equation by Bing et al. (2001).

$$f_{cc} = f_c' \left(-1.254 + 2.254\sqrt{1 + 7.94\alpha_s \frac{f_l'}{f_c'}} - 2\alpha_s \frac{f_l'}{f_c'} \right) \qquad (4.12)$$

where $\alpha_s = \left(21.2 - 0.35 f_c'\right)\dfrac{f_l'}{f_c'}$ when $f_c' \leq 52$ MPa

$$\alpha_s = 3.1\frac{f_l'}{f_c'} \quad \text{when } f_c' > 52 \quad \text{MPa}$$

4.2.12 Hadi and Schmidt (2002)

Seven beams with a cross section of 200 × 300 mm^2 by 4060 mm long with a clear span of 3700 mm were tested. The concrete cover was 20 mm. The main objective was to investigate their ductility when helical reinforcement in the compression region was applied.

From their study, Hadi and Schmidt (2002) concluded that the beam was very brittle in its failure without helix, and the helical reinforced concrete beams are important because of their load carrying capacity coupled with small size, and the long term cost saving for high rise structures.

4.3 DISCUSSION OF PAST RESEARCH

The most relevant experimental literature was evaluated in this chapter and the main observations are discussed in the following sections.

1- High strength concrete is more brittle than normal strength concrete; brittleness increases with the use of over-reinforced sections, which suddenly fail without

warning. Avoiding brittle compression failure by using proper confinement which restrains lateral expansion and increases strength and ductility. However, there is very little experimental data on confined beams using high strength concrete and a longitudinal reinforcement ratio more than 1.5 times the maximum reinforcement ratio allowed by codes such as ACI 318R-02 (2002) and AS3600 (2001).

2- It has been observed that almost all the research concerning confinement of the compression zone in beams is based on the results of research on columns, because the idea of a confined compression zone in beams has only recently been developed. Based on this, more study and data on the behaviour of confined HSC beams is needed.

3- There is a general agreement about the variables that affect the strength of confined concrete but a division about its magnitude. The strength gain factor (K_s) has different magnitudes when using different models. It may be because the strength gain factor model first proposed using spiral confinement data only, is different from the model developed for spiral and rectangular ties, and is different from the model proposed using tie confinement data. Secondly different observations during analysis of the experimental data, for example Martinez et al. (1984) model was based on their observations, where the effect of confinement is negligible when the spacing between the spirals is equal to the diameter of confinement. This finding is different from Ahmad and Shah's (1982) observations,

which neglects confinement when the spiral pitch exceeded 1.25 times the diameter of the confined core. Thirdly, the size of the specimen is an important factor, King (1946). In some cases, results from small specimens have been used to predict the behaviour of full size columns. Such predictions should be further investigated to take their size into account. In general, the model proposed using full size specimens is more rational than that proposing smaller ones. Also some studies do not use longitudinal reinforcement and others use samples without cover, avoiding the concrete cover spalling off.

4- There is a general agreement that when an over-reinforced concrete beam is properly confined, the ductility and compressive strength in the region where this confinement is placed, is increased. The effective place of confinement is the upper part of the beam (compression zone). Mansur et al. (1997) stated “short ties perform better ductility than full depth because one side of the link is at the tension side of the beam, reducing the effectiveness of the confinement”. This statement confirms that helical confinement could be effectively and economically used in the compression zone. Base and Read (1965) showed through experimental testing that helical confinement increases the strength and ductility of a beam of high tensile, longitudinal steel.

5- There are a few ways for improving the ductility of concrete in compression such as providing longitudinal compression reinforcement, by using randomly oriented steel fibres, or by installing helical or tie confinement in the compression zone. Experimental comparisons to find the most effective way is presented by Shah et al. (1970). The test results show that the ductility of beams confined using tie confinement was 10 times the ductility of the control beams (without any ductility reinforcement), while the fibres increased ductility 4.5 times and compression steel increases ductility by twice that of the control beams. This result shows that the tie confinement is better than compression longitudinal reinforcement and steel fibres for increasing ductility. Also, beams which have longitudinal compression reinforcement fail early because of the buckling problem with compression reinforcement. However, it is well known that confinement by helices is generally much more effective than rectangular or square ties. Hatanaka and Tanigawa (1992) stated that the lateral pressure produced by a rectangular tie is about 30 to 50 percent of the pressure introduced by a helix. This is the case for compression concrete in columns and beams. However, helices confine the concrete more effectively than rectangular ties because they apply a uniform radial stress along the member, whereas rectangular ties tend to confine the concrete mainly at the corners. Also the effective area between the ties is reduced, thus using helical confinement in the compression zone of rectangular beams is more effective than rectangular ties. There is a need for extensive experimental research to

understand and provide experimental evidence about the effectiveness of providing helix confinement in over-reinforced HSC beams.

4.4 SUMMARY

In this chapter, literature on confined concrete is reviewed and the experimental results and observation discussed. It can be concluded that there is experimental and analytical evidence that helical confinement is more effective than rectangular ties. In addition full-scale beams are preferable to study the effect of different variables on the behaviour of over-reinforced helically confined HSC beams.

Chapter 5 discusses the properties of the materials used in the experimental work and the procedure for constructing and testing the 20 full-scale beams.

CHAPTER 5

EXPERIMENTAL PROGRAMME

5.1 GENERAL

Many researchers have developed theories and models based on experimental results to study the behaviour of confined columns, but only limited theories and models have been developed to study confined beams. It is not possible to predict the behaviour of confined beams using the confined column models because the loading conditions are different and the column confinement reinforcement is usually placed throughout the column, whereas in beams, this is not likely to be the case. A great deal of experimental work to is needed before developing any model to predict the behaviour of a helically confined beam. Based on the literature review there is a concern about different issues which may be important and are therefore considered in the experimental programme. Firstly, the beams should be full size to represent real beams more accurately. Secondly, isolating the confined beams is a more effective way to study (i.e., fixing all variables except the one which is under investigation). Thirdly, focusing on the main variables because of time and fund limitations. Finally, this research focuses on using high strength

concrete and high strength steel in helically confined over-reinforced concrete beams.

Extensive investigation was carried out at the University of Wollongong on full scale beams to study how different variables affected the behaviour of over-reinforced HSC helically confined beams. Twenty beams 4000 mm long by 200 mm wide by 300 mm deep, with 3600 mm clear span were subjected to four point loading, with an emphasis placed on midspan deflection. A helix confinement was installed at the compression zone, where the outside diameter of confined core was kept consistent at 160 mm for all beams. The concrete cover was kept consistent at 20 mm for all beams.

5.2 MATERIALS

5.2.1 High Strength Concrete

All beams were constructed using ready-mix concrete. The maximum size of coarse aggregate used was 10 mm and the concrete slump test was between 120-140 mm. A high concrete slump was necessary to ensure that the concrete was able to pass between the helical pitch and two layers of steel layed longitudinally.

The concrete cylinders were 100 mm in diameter by 200 mm high. The concrete compressive strength was taken as an average of at least three test results. A high

strength concrete between 72 MPa and 105 MPa was used to construct the 20 beams. The concrete cylinders were tested on the same day as the beam test to determine the actual strength of concrete.

5.2.2 Reinforcement

5.2.2.1 Longitudinal reinforcement

Deformed high strength steel bars with different diameters were used to provide a longitudinal reinforcement ratio for beams over the maximum longitudinal reinforcement ratio ($\rho > \rho_{max}$). ρ_{max} is calculated according to the Australian code AS3600 (2001). Tension tests were run on randomly selected samples on an Instron testing machine with 500 kN capacity. Table 5.1 summarises the mechanical properties of longitudinal steel for the elastic and strain hardening regions. Figures A.1-A.3 in Appendix A show the stress-strain curves of the longitudinal bars with different diameters.

Table 5.1 Mechanical properties of longitudinal reinforcement

Grade of steel	500N	500N	500N
Diameter (mm)	32	28	24
Yield strength (MPa)	500	570	530
Yield strain (mm/mm)	0.0026	0.0025	0.0025
Modulus of elasticity (GPa)	220	230	210
Ultimate stress (MPa)	595	680	635
Ultimate strain (mm/mm)	0.211	0.19	0.20

5.2.2.2 Helical reinforcement

Helical reinforcement with different diameters and tensile strengths has been choosen. Tension tests were run on at least three randomly selected samples. Table 5.2 summarises the mechanical properties of the lateral steel used as helical confinement for both elastic and strain hardening regions. Figures A.4-A.8 in Appendix A show the stress-strain curves of helical bars with different diameters.

Table 5.2 Mechanical properties of helical reinforcement

Grade of steel	N12	R12	R10	N8	R8
Diameter (mm)	12	12	10	8	8
Yield strength (MPa)	500	310	300	500	410
Yield strain (mm/mm)	0.0023	0.0017	0.0017	0.0024	0.0021
Modulus of elasticity (GPa)	217	190	180	205	200
Ultimate stress (MPa)	590	470	400	580	520
Ultimate strain (mm/mm)	0.151	0.310	0.246	0.22	0.36

5.3 BEAMS

Twenty beams were cast in four sets of five each, with similar dimensions. Their cross section was 200×300 mm, they were 4000 mm long and had a clear span of 3600 mm. Their generic details are shown in Figure 5.1. They were constructed with different longitudinal reinforcement ratios, which may be described as follows, A is 4N32, B is 5N28, C is 4N28, D is 6N28 and E is 4N24. Tables 5.3 and 5.4 show the beams' details.

The alphanumeric characters (e.g. R12P25-A100) means the following:

1) R- the type of helical steel
2) 12- the helical diameter

3) P25- a helical pitch of 25 mm

4) A- the longitudinal reinforcement ratio

5) 100- the concrete compressive strength

The reinforced concrete helically confined beams were designed to be over-reinforced, where ρ is higher than the ρ_{max}. ρ_{max} is the maximum allowable tensile reinforcement and has been defined by AS 3600 (2001) as Equation 5.1 and ρ is the longitudinal reinforcement ratio as shown in Equation 5.2.

$$\rho_{\max} = \frac{0.34\gamma f_c'}{f_{sy}} \tag{5.1}$$

$$\rho = \frac{A_s}{b\,d} \tag{5.2}$$

where

γ = ratio of the depth of the assumed rectangular compressive stress block to $K_u d$.

K_u = Ratio of depth to neutral axis to the effective depth.

d = Effective depth.

f_c' = Characteristic concrete compressive strength at 28 days, MPa.

f_{sy} = Yield strength of reinforcing steel, MPa.

b = Beam width

A_s = Longitudinal reinforcement ratio

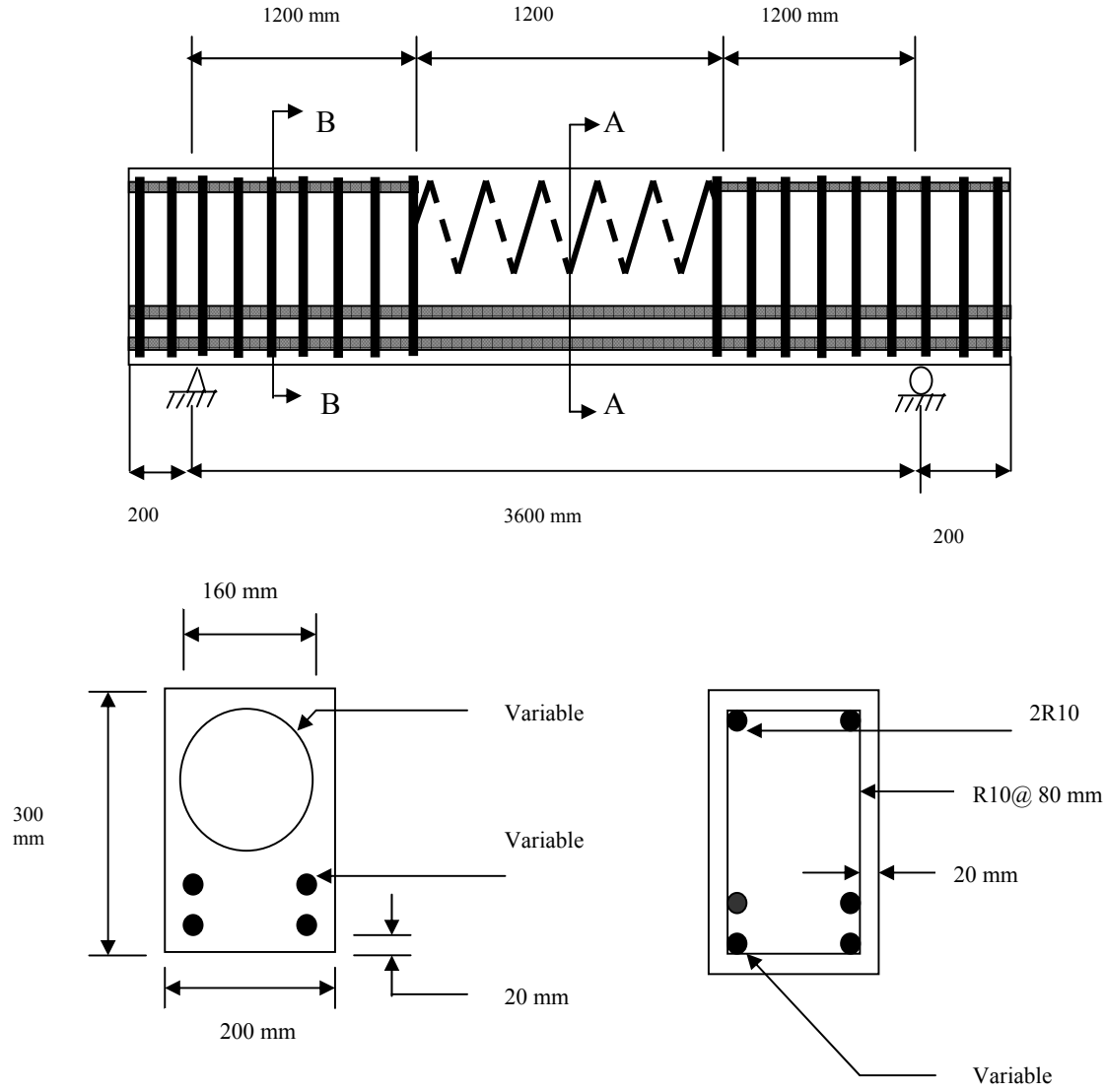

Figure 5.1 Loading configuration and specimen details.

Table 5.3 Concrete compressive strength and helical details of the tested beam

Specimen	Concrete compressive strength, MPa	Helical yield strength, MPa	Helical diameter, mm	Helical pitch, mm	Helical reinforce-ment ratio
R12P25-A105	105	310	12	25	0.120
R12P50-A105	105	310	12	50	0.060
R12P75-A105	105	310	12	75	0.040
R12P100-A105	105	310	12	100	0.030
R12P150-A105	105	310	12	150	0.020
N8P25-A80	80	500	8	25	0.054
N8P50-A80	80	500	8	50	0.0268
N8P75-A80	80	500	8	75	0.018
N8P100-A80	80	500	8	100	0.013
N8P150-A80	80	500	8	150	0.009
R10P35-B72	72	300	10	35	0.060
R10P35-B83	83	300	10	35	0.060
R10P35-B95	95	300	10	35	0.060
R10P35-C95	95	300	10	35	0.060
R10P35-D95	95	300	10	35	0.060
N12P35-D85	85	500	12	35	0.086
R12P35-D85	85	310	12	35	0.086
R10P35-D85	85	300	10	35	0.060
R8P35-D85	85	410	8	35	0.038
0P0-E85	85	0.0	0.0	0.0	0.0

Helical reinforcement ratio = $\rho_h = \frac{\pi d_h^{\,2}}{DS}$

Where

ρ_h = volumetric helical reinforcement ratio

d_h = helix diameter

D = confined concrete core diameter

S = helical pitch

Table 5.4 Longitudinal reinforcement details of tested beam

Please see print copy for Table 5.4

*ρ_{max} = Maximum allowable tensile reinforcement as defined by AS 3600 (2001)

5.3.1 Formwork

Strongly constructed wooden formwork was used for casting the full-scale beams with 4000 mm length and a cross section of 200 mm in width and 300 mm in depth. The formwork was constructed in such a way to be very stiff to prevent any movement during concrete casting. The formwork could be used for casting up to five beams a time. Figure 5.2 shows the forms just before the casting. Before placing the reinforcing cages inside the formwork the inner surfaces of the forms were coated with oil to avoid bond between the concrete and the wooden forms.

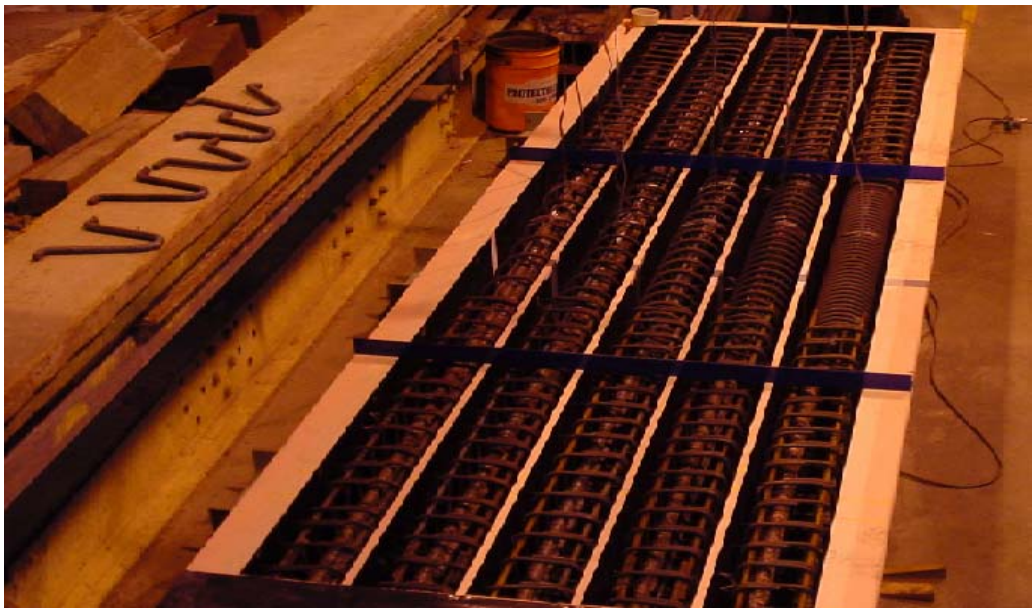

Figure 5.2 Five beams with different helical pitch in wooden formwork

5.3.2 Beam Cages

All the beams have 10 mm diameter shear stirrups (250 MPa tensile strength) 80 mm apart, at either third end of the beams. Figure 5.3 (a) and (b) shows measuring the spacing and connecting the stirrups with longitudinal reinforcement. Figure 5.4 (a) and (b) show fixing the helical confinement and lifting the beam to put it in the formwork. Two 10 mm bars were installed at the top of the beams at either third in order to keep the shear stirrups in-place as shown in Figure 5.5. For all of the beams the size of the shear stirrups from centre to centre was the same 250 × 150 mm. All the longitudinal reinforcement bars are 3960 mm long. For helical confinement, the total length was 1300 mm and the outside diameter was 160 mm but it was 1200 mm for the middle third of the beam. Both ends of the helical confinement fit inside the shear stirrups by about 50 mm which will keep the helical confinement fixed at both ends and prevent it from moving. Also, one 12 mm diameter bar was placed inside the helix and tied to the helical reinforcing to keep the helical confinement and helical pitch from moving. Furthermore the helical cage was tied with thin and strong wire while the other end was joined with a piece of fixed rod to restrain the helical confinement. Figure 5.6 shows the helical confinement configuration.

Figure 5.3(a) Measuring the spacing for stirrups and longitudinal reinforcement

Figure 5.3(b) Fixing the stirrups and longitudinal reinforcement

Figure 5.4(a) Fixing the helical reinforcement

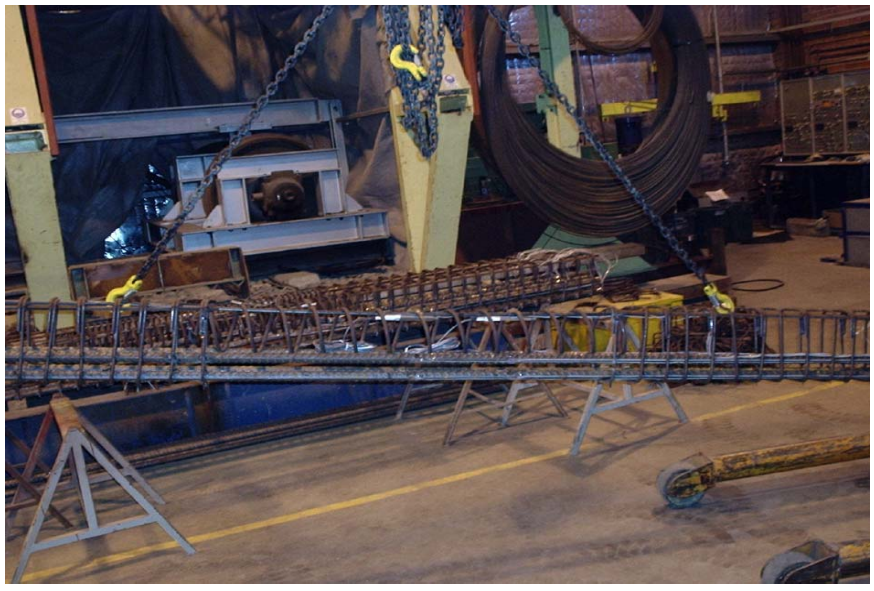

Figure 5.4(b) Handling the cages using lift

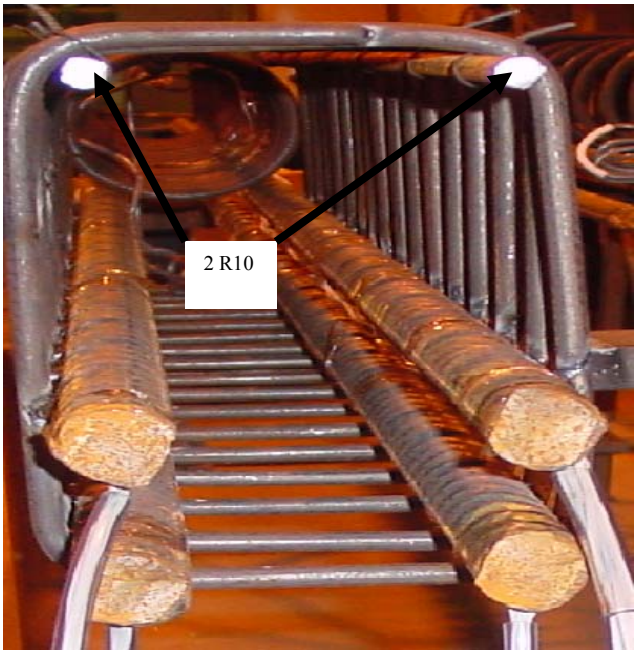

Figure 5.5 Beam Cage cross section

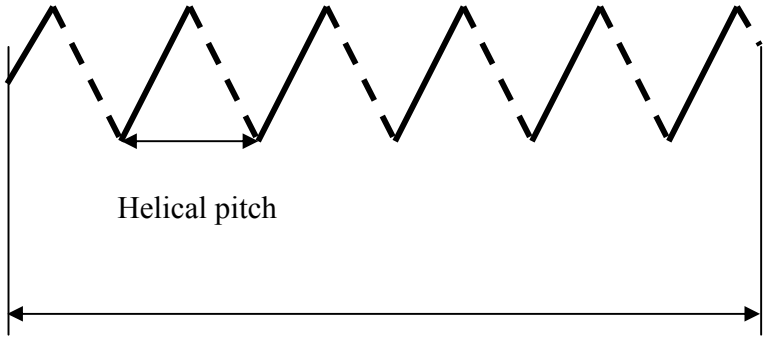

Helical Confinement Length is 1300 mm

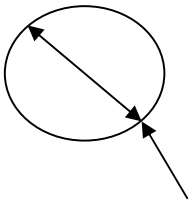

Helical Confinement cross-section diameter is 160 mm

Figure 5.6 Configuration of Helical Reinforcement

5.3.3 Casting and Curing

The cages were placed inside the formwork with a 20 mm gap between it and the longitudinal bars to maintain 20 mm cover of concrete. Adjusting the cages is important to maintain 20 mm of concrete cover around the cages. About seven layers of concrete were placed in each beam, with each vibrated before adding the next layer. Much care was taken to avoid direct application of the vibrator near the centre of the beams where embedment strain gauges are located. Figure 5.7 shows the last stage of casting the concrete. A number of cylinders were cast and compacted using the vibrator. The beams and cylinders were covered with wet Hessian bags and plastic sheets to prevent evaporation while curing. Figure 5.8 shows the beams covered by wet Hessian bags.

Figure 5.7 Beams casting

Figure 5.8 Beams curing

5.3.4 Variables examined

Different variables were studied during this investigation but the focus was on those variables, which affect the behaviour of over-reinforced HSC helically confined beams. These variables are: helical pitch, the helical reinforcement ratio, helical yield strength, longitudinal reinforcement ratio and concrete compressive strength. These variables were studied through the 20 beams divided into four groups of five.

5.3.4.1 First group

The first group was designed to study helical pitch. In this group, the helical diameter was R12, the concrete compressive strength was 105 MPa and the longitudinal reinforcement was 4N32. The only variable in this group is the helical pitch. Five helical pitches 25, 50, 75, 100, 150 mm were chosen to study the effect of helical pitch on the behaviour of over-reinforced HSC helically confined beams. Tables 5.5 (a) and 5.5 (b) show the details.

5.3.4.2 Second group

Based on the effect of helical pitch on the strength and ductility of over-reinforced HSC helically confined beams, it was decided to study this effect again on beams in the second group. However, the concrete compressive strength and helical diameter is not the same as the first group, they were designed to have a helical diameter of N8, a concrete compressive strength of 80 MPa, and longitudinal reinforcement of 4N32. The only variable in this group is the helical pitch, 25, 50, 75, 100, 150 mm. Tables 5.6 (a) and 5.6 (b) show the beam's details.

Table 5.5 (a). Concrete compressive strength and helical details of the tested beams in the first group

Specimen	Concrete compressive strength, MPa	Helical yield strength, MPa	Helical diameter, mm	Helical pitch, mm	Helical reinforcement ratio
R12P25-A105	105	310	12	25	0.120
R12P50-A105	105	310	12	50	0.060
R12P75-A105	105	310	12	75	0.040
R12P100-A105	105	310	12	100	0.030
R12P150-A105	105	310	12	150	0.020

Table 5.5 (b). Longitudinal reinforcement details of the tested beams in the first group

Specimen	Tensile reinforcement	Cross-section area of reinforcement steel, A_s ,(mm)	Yield strength, f_y (MPa)	Effective depth, d (mm)	Actual reinforcement ratio, ρ	ρ_{max}*	ρ/ρ_{max}*
R12P25-A105	4N32	3217	500	235	0.068	0.046	1.47
R12P50-A105	4N32	3217	500	235	0.068	0.046	1.47
R12P75-A105	4N32	3217	500	235	0.068	0.046	1.47
R12P100-A105	4N32	3217	500	235	0.068	0.046	1.47
R12P150-A105	4N32	3217	500	235	0.068	0.046	1.47

*ρ_{max} = Maximum allowable tensile reinforcement as defined by AS 3600 (2001)

Table 5.6 (a). Concrete compressive strength and helical details of the tested beams in the second group

Specimen	Concrete compressive strength, MPa	Helical yield strength, MPa	Helical diameter, mm	Helical pitch, mm	Helical reinforcement ratio
N8P25-A80	80	500	8	25	0.054
N8P50-A80	80	500	8	50	0.0268
N8P75-A80	80	500	8	75	0.018
N8P100-A80	80	500	8	100	0.013
N8P150-A80	80	500	8	150	0.009

Table 5.6 (b). Longitudinal reinforcement details of the tested beams in the second group

Please see print copy for Table 5.6 (b)

*ρ_{max} = Maximum allowable tensile reinforcement as defined by AS 3600 (2001)

5.3.4.3 Third group

The third group was designed to study the effect of concrete compressive strength and longitudinal reinforcement ratio. In this group, all the beams have an R10 helical diameter and a 35 mm helical pitch, but three beams have a 5N28 longitudinal reinforcement while the other two beams are, 4N28 and 6N28. To determine the effect of the compressive strength, the three beams with a 5N28 longitudinal reinforcement were tested on different days. The first of the three beams was tested on the 16^{th} day after casting, where the concrete compressive strength was 72MPa (the average test result of three cylinders). The second beam was tested on the 23^{rd} day, where the concrete compressive strength was 83 MPa. The third beam was tested after 28 days where the concrete compressive strength was 95 MPa. These three beams were used to study the effect of concrete compressive strength that was the only variable. The other two beams with 4N28 and 6N28 longitudinal reinforcement were tested after 28 days after casting, where the concrete compressive strength of 95 MPa. These two beams and the beam, with 5N28 longitudinal reinforcement were used to determine the effect of longitudinal reinforcement ratio. These three beams have the concrete compressive strength as 95 MPa and the only variable considered was the longitudinal reinforcement ratio. Tables 5.7 (a) and 5.7 (b) show the beams' details.

Table 5.7 (a). Concrete compressive strength and helical details of the tested beams in the third group

Specimen	Concrete compressive strength, MPa	Helical yield strength, MPa	Helical diameter, mm	Helical pitch, mm	Helical reinforcement ratio
R10P35-B72	72	300	10	35	0.060
R10P35-B83	83	300	10	35	0.060
R10P35-B95	95	300	10	35	0.060
R10P35-C95	95	300	10	35	0.060
R10P35-D95	95	300	10	35	0.060

Table 5.7 (b). Longitudinal reinforcement details of the tested beams in the third group

Please see print copy for Table 5.7 (b)

*ρ_{max} = Maximum allowable tensile reinforcement as defined by AS 3600 (2001)

5.3.4.4 Fourth group

The fourth group was designed to study helical yield strength and helical diameter. This group was planned to determine the increased strength and ductility through a comparison between the over-reinforced concrete helically confined beams and the balanced reinforced concrete beam (without helix). All the beams in this group have a concrete compressive strength of 85 MPa. The four over-reinforced concrete helically confined beams have 6N28 longitudinal reinforcement and a 35 mm helical pitch. The fifth beam is a balanced reinforced concrete beam without helical confinement and has a 4N24 longitudinal reinforcement. Tables 5.8 (a) and 5.8 (b) show the details of the fourth group.

In order to determine the effect of helical yield strength the two Beams N12P35-D85 and R12P35-D85 only were used for a comparison. These beams have the same 12 mm helical diameter but one has 500 MPa yield strength and the other 310 MPa yield strength.

Three beams R8P35-D85, R10P35-D85 and R12P35-D85 were used to determine the effect of helical diameter. These beams have 8, 10 and 12 mm helical diameters, respectively but they have 410, 300 and 310 MPa yield strength, respectively. Thus the only variable between beams R10P35-D85 and R12P35-D85 is the helical diameter, which facilitates determining the effect of helical diameter on the behaviour of over-reinforced high strength concrete beams. However, it

could be added to the Beam R8P35-D85 which has a yield strength of 410 MPa to determine the effect of helical diameter, because the yield strength is lower than 500 MPa and higher than the lower limit, which was given as 250 MPa. The three helical yield strengths, 410, 300 and 310 MPa are classified under the category of low strength steel. Australian/New Zealand Standard AS/NZS 4671:2001 (2001) stated that low strength steel is a reinforcing bar with 250 MPa minimum yield strength and less than 500 MPa.

In the fourth group, the beam 0P0-E85 was designed to be a balanced-reinforced concrete beam without helical confinement. The concrete compressive strength for this Beam 0P0-E85 was 85 MPa and the steel reinforcement was 4N24. This beam is a balanced-reinforced concrete section because the longitudinal reinforcement ratio (ρ) is approximately equal to the maximum longitudinal reinforcement ratio (ρ_{max}).

An experimental comparison between the balanced high strength reinforced concrete beam (without helical confinement) and the over-reinforced high strength concrete helically confined beam is essential. This comparison will measure the quantity of the increased strength and ductility, when the helical confinement is installed in the compression zone.

Table 5.8 (a). Concrete compressive strength and helical details of the tested beams in the fourth group

Specimen	Concrete compressive strength, MPa	Helical yield strength, MPa	Helical diameter, mm	Helical pitch, mm	Helical reinforcement ratio
N12P35-D85	85	500	12	35	0.086
R12P35-D85	85	310	12	35	0.086
R10P35-D85	85	300	10	35	0.060
R8P35-D85	85	410	8	35	0.038
0P0-E85	85	0.0	0.0	0.0	0.0

Table 5.8 (b). Concrete compressive strength and helical details of the tested beams in the fourth group

Please see print copy for Table 5.8 (b)

*ρ_{max} = Maximum allowable tensile reinforcement as defined by AS 3600 (2001)

5.4 INSTRUMENTATION

The beams were heavily instrumented. Deformation of the steel reinforcement was measured using electrical – resistance strain gauges (10 mm long) glued on both sides of the steel bar in the middle and 300 mm away from mid-span. The helical reinforcement strains were measured using resistance strain gauges (5 mm long) glued in the middle and 300 mm away, at the top, bottom and sides of the helical reinforcement. The strain on the compression zone was measured using two resistance strain gauges (60 mm long) glued in the middle, on the top surface of the concrete beam. The foil strain gauges are products of Showa Measuring Instruments Co., Ltd Company. The specification of the foil strain gauges is as follows. Type is N11-FA-60-120-11, gauge length is 60 mm, resistance is 120.0 ± 0.3%, gauge factor is 2.16 ± 1% and thermal output ± 2 $\mu\varepsilon/c^{o}$.

For each beam, two embedment gauges were placed 40 mm deep, one in the middle and the other 300 mm away. The embedment strain gauges are product of Vishay Micro-measurements Raleigh, North Carolina. The specification of the embedment strain gauge is as follows. Type is EGP-5-120, resistance in ohms is 120.0 ± 0.8%, gauge factor is 2.05 ± 1% and the code is 143911-16617. Figure 5.9 shows the embedment strain gauges used for all the beams in this study. The data recorded

from the embedment gauges were used to calculate strains at the top surface after the concrete cover spalled off.

Midspan deflection within the region of pure bending between the two loading points was measured using linear variable differential transformers (LVDTs). The LVDT was fixed to a U shaped steel plate attached to the bottom of the beams. This mechanism was used to prevent damage to the (LVDTs) when the concrete cover begins spalling off. Figure 5.10 and 5.11 show how the (LVDT) was fixed to the beam.

Five different measurements were taken at each load increment, strain at the top surface of the concrete, strain at 40 mm deep, the strains in the longitudinal reinforcement, strains in the helical reinforcement, and mid-span deflection. During the tests all the data was recorded by a Smart System installed in a PC computer.

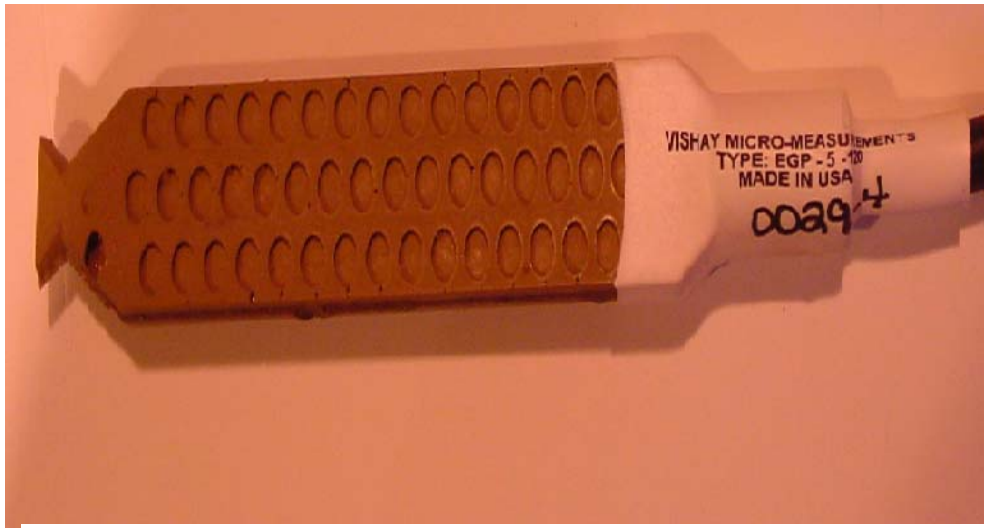

Figure 5.9 Embedment strain gauge

5.5 TESTING

5.5.1 Test Setup

The loading scheme was four-point. A load was applied to a stiff steel beam that distributed it into two equal parts applied on the third point of the tested beam. Figure 5.12 shows that the beams were tested under a four-point loading regime in the strong floor of the civil engineering laboratory at the University of Wollongong. The displacement controlled load was applied using 600 kN actuators.

Figure 5.10 Steel U shape from base side to support LVDT for measuring midspan deflection.

Figure 5.11 Steel U shape from rapper side to support LVDT to measure midspan deflection

Figure 5.12 Beam loading

5.5.2 Test Procedure

At least three cylinders were tested for each beam to obtain the concrete compressive strength. The LVDTs and other electronic devices were calibrated before starting the test. The load was applied at regular intervals of 30 seconds per millimetre. It continued until the beam was incapable of sustaining any further load but at each step the deflection and strain gauges were recorded. Finally every set of data was saved in the computer's hard disc and documented, with the photographs.

5.5.3 Test Observation

During testing, cracks were noticed on the surface under tension. It is worth noting that the flexural crack width did not exceed 0.3 mm as the requirements of the serviceability limits according to Australian Code of practice AS3600 (2001). The photographs in Figure 5.13 and 5.14 show the sequence of loading and pattern of surface cracks at ultimate load.

The behaviour of the helically confined beams is different from unconfined beams because of the spalling off phenomenon. It is noted that the load increased as the deflection increased until the spalling off phenomenon occurred and then the load dropped while deflection increased due to helical confinement. However, the load increased again as the deflection increased until the point where the load decreased gradually as the deflection increased. It is noted that the maximum load recorded for the well-confined beams is greater than the concrete cover spalling off load but

for beams where the helical pitch is high, the maximum load recorded was the concrete cover spalling off. Figures 5.15 and 5.16 show the general behaviour (load-midspan deflection) of the over-reinforced high strength concrete beams used in this study.

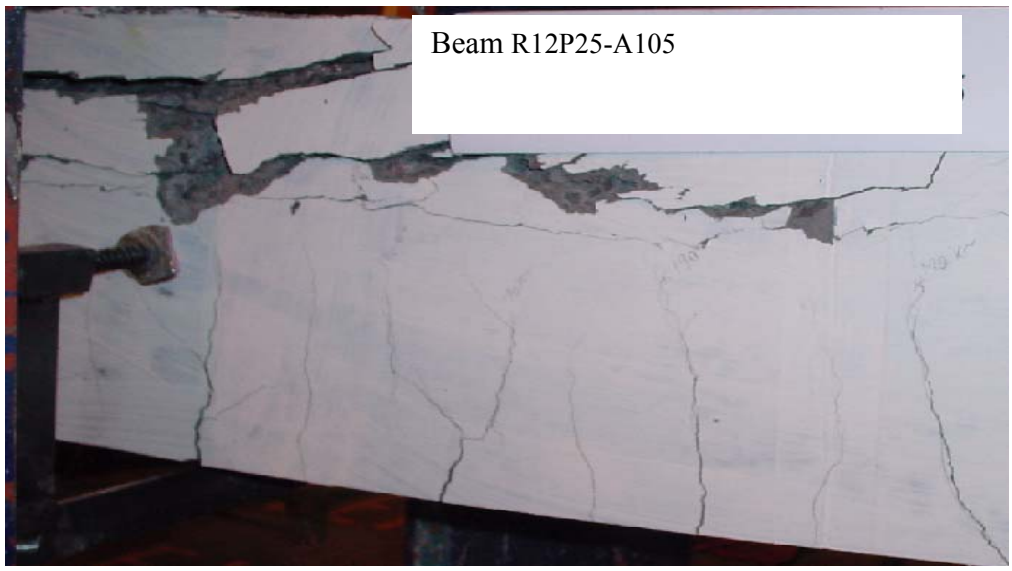

Figure 5.13 Cracks just after spalling off concrete cover

Figure 5.14 Cracking at ultimate load for beam R12P25-A105

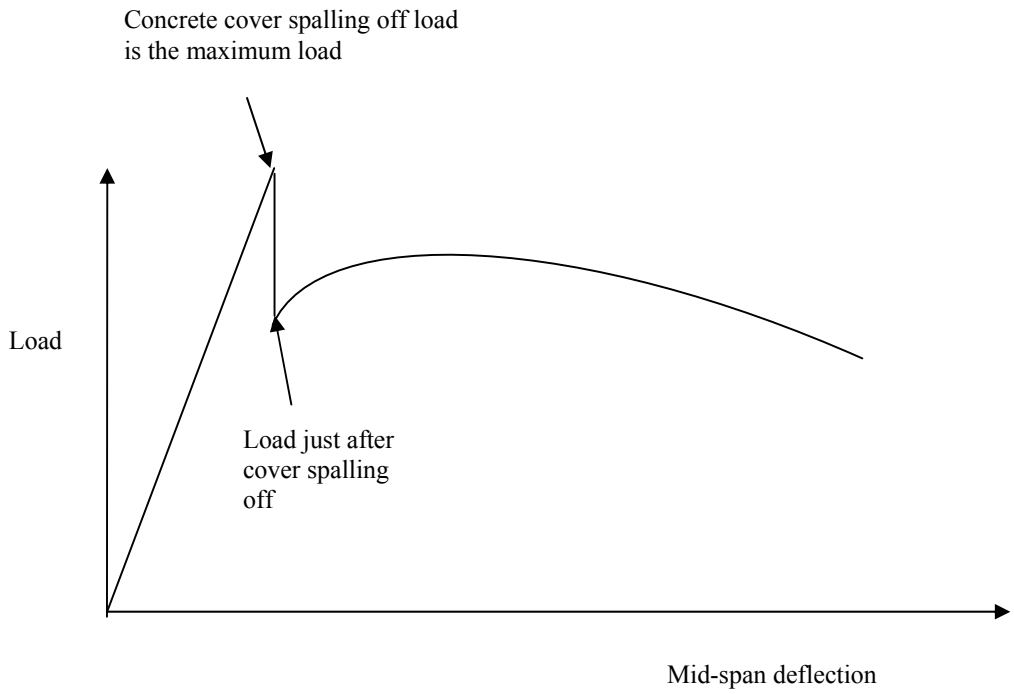

Figure 5.15 General behaviour of load-midspan deflection of not well confined beams

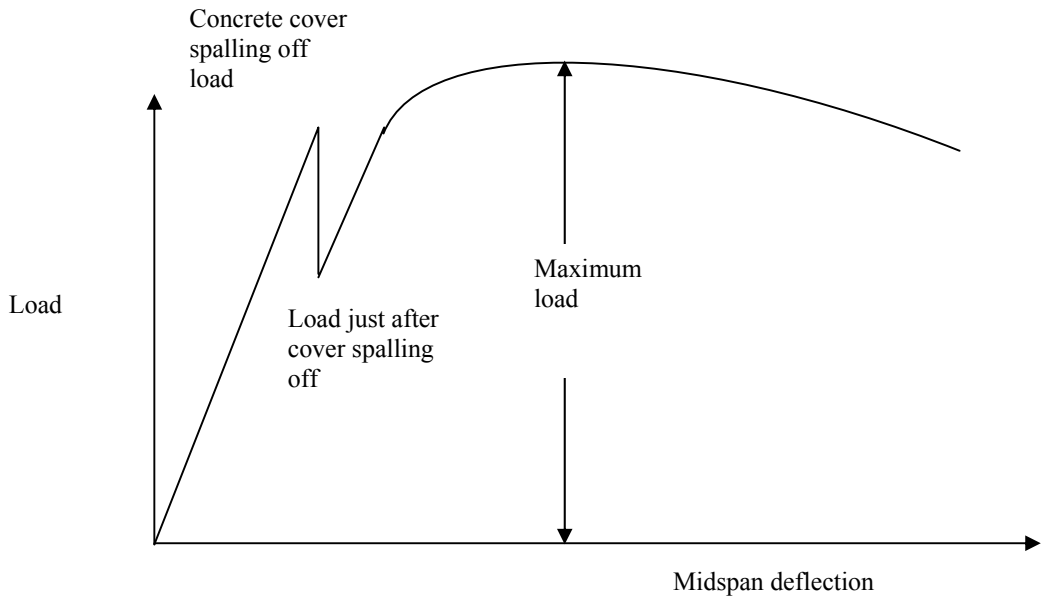

Figure 5.16 General behaviour of load-midspan deflection of well confined beams

5.6 SUMMARY

This chapter described the experimental program in detail. It presents the properties of the high strength concrete and high strength steel and discusses details of helical confinement used. The details of 20 beams are presented and the formwork, casting and curing, variables studied and instrumentation used are discussed. The test setup, test procedure and observations are presented and illustrated by figures and photographs.

The following chapter presents an analysis of the experimental results achieved.

CHAPTER 6

ANALYSIS AND DISCUSSION

6.1 GENERAL

The aim of the experimental programme in this study is to investigate the behaviour of over-reinforced HSC helically confined beams and to determine the effect of helical pitch, helix yield strength, helix diameter, tensile reinforcement ratio and concrete compressive strength on the strength and ductility of beams. The definition of HSC is not fixed with time. However, the most recent definition of HSC published in different studies, for example Bae and Bayrak (2003), define it as concrete that has a compressive strength that exceeds 55 MPa. In this study a minimum concrete compressive strength of 72 MPa is adopted for high strength concrete.

6.2 TEST RESULTS OF THE 20 BEAMS

Experimental results are presented in this chapter in the form of load versus midspan deflection, and load versus strain. Table 6.1 shows a summary of loads

and midspan deflections of the 20 beams where P_1 is the load at concrete cover spalling off, P_2 is the load just after spalling off the concrete cover, P_3 is the highest load recorded during the test, Δ_y is the yield deflection and $\Delta_{u,0.8}$ is the deflection at 80% of the highest load. Tables 6.2, 6.3 and 6.4 show a summary of load versus strains at 0, 20 and 40 mm depth from the top surface of the beam. An extensive number of beams were used in this experimental programme to study the effect of helical pitch on the behaviour of over-reinforced HSC helically confined beams.

6.2.1 Midspan deflection

The behaviour of the helically confined beams is different from unconfined beams because of the spalling off phenomenon. It is to be noted that the load increases as the deflection and strains increase until the concrete cover spalls off, and then the load drops while the midspan deflection and strain increase because of the helical confinement effect. However, the load increased again as the deflection increased until the point where the load decreases gradually as the deflection increases. It is to be noted that the maximum load recorded for some beams is greater than the concrete cover spalling off load but for the other beams the maximum load recorded was the load at concrete cover spalling off. Figures 5.15 and 5.16 in Chapter 5 show the two types of general behaviour (load-midspan deflection) of the HSC beams helically confined used in this research based on the experimental results. Appendix B shows the load-midspan deflection of the 20 tested beams.

Table 6.1 - Summary of loads and midspan deflections of the 20 tested beams

SPECIMEN	P_1, (kN)	P_2, (kN)	P_3, (kN)	$0.8P_3$, (kN)	Δ_y, (mm)	$\Delta_{u,0.8}$, (mm)	$\Delta_{u,0.8}/\Delta_y$
R12P25-A105	372	278	411	328	36	277	7.7
R12P50-A105	383	302	383	306	35	150	4.3
R12P75-A105	386	295	386	309	32	42	1.3
R12P100-A105	395	250	395	316	35	35	1.0
R12P150-A105	413	150	413	328	38	38	1.0
N8P25-A80	297	237	345	276	29	190	6.5
N8P50-A80	324	284	324	260	31	90	2.9
N8P75-A80	378	261	378	302	40	40	1.0
N8P100-A80	325	257	325	260	34	34	1.0
N8P150-A80	376	94	376	300	39	39	1.0
R10P35-B72	363	248	363	290	38	248	6.5
R10P35-B83	372	275	372	297	37	214	5.8
R10P35-B95	344	250	357	286	34	180	5.3
R10P35-C95	365	276	365	292	39	189	4.8
R10P35-D95	331	247	412	330	36	282	7.8
N12P35-D85	437	330	437	350	38	203	5.3
R12P35-D85	435	317	435	348	39	150	3.8
R10P35-D85	403	291	403	322	36	104	2.7
R8P35-D85	418	308	418	334	38	102	2.7
0P0-E85	292	80	292	234	45	45	1.0

P_1 is the load at concrete cover spalling off
P_2 is the load just after spalling off the concrete cover
P_3 is the highest load recorded during the test
Δ_y is the yield deflection and
$\Delta_{u,0.8}$ is the deflection at 80% of the maximum load

Table 6.2 - Summary of measured strains at 40 mm depth

SPECIMEN	Measured strain at 40 mm depth just before spalling off concrete cover	Measured strain at 40 mm depth just after spalling off concrete cover	Measured strain at 40 mm depth at 80% of maximum load
R12P25-A105	0.00154	0.00315	0.0146
R12P50-A105	0.00144	0.00296	0.011
R12P75-A105	0.0015	0.00361	0.008
R12P100-A105	0.00137	0.002	N/A
R12P150-A105	0.0014	0.0014	N/A
N8P25-A80	0.00139	0.002716	0.01246
N8P50-A80	0.00127	0.00163	0.009155
N8P75-A80	0.00207	0.0049	N/A
N8P100-A80	0.00169	0.0023	N/A
N8P150-A80	0.001824	0.001824	N/A
R10P35-B72	0.00136	0.0031	0.016
R10P35-B83	0.0014	0.0026	0.0158
R10P35-B95	0.00115	0.0026	0.01592
R10P35-C95	0.00135	0.0029	0.0135
R10P35-D95	0.0016	0.0028	0.016
N12P35-D85	0.0018	0.0031	0.016
R12P35-D85	0.0018	0.003	0.013
R10P35-D85	0.0018	0.0036	0.0158
R8P35-D85	0.0017	0.0029	0.0158
0P0-E85	0.001	0.001	N/A

Table 6.3 - Summary of calculated strains at top surface of the beam

SPECIMEN	Calculated strain at top surface just before spalling off concrete cover	Calculated strain at top surface just after spalling off concrete cover	Calculated strain at top surface at 80% of maximum load
R12P25-A105	0.0032	0.0086	0.032
R12P50-A105	0.0032	0.0075	0.025
R12P75-A105	0.0034	0.007	0.01
R12P100-A105	0.0034	0.004	N/A
R12P150-A105	0.0035	0.0035	N/A
N8P25-A80	0.0034	0.006	0.029
N8P50-A80	*	*	*
N8P75-A80	0.0034	0.008	0.0078
N8P100-A80	0.003	0.0046	N/A
N8P150-A80	0.0034	0.0034	N/A
R10P35-B72	0.0029	0.0066	0.034
R10P35-B83	0.0032	0.006	0.0359
R10P35-B95	0.003	0.0069	0.0419
R10P35-C95	0.0031	0.0065	0.03
R10P35-D95	0.0033	0.0058	0.032
N12P35-D85	0.00315	0.0054	0.028
R12P35-D85	0.0029	0.0048	0.02
R10P35-D85	0.003	0.006	0.027
R8P35-D85	0.003	0.0052	0.028
0P0-E85	0.0025	0.0025	N/A

* Not available

Table 6.4 - Summary of Calculated strains at 20 mm depth

SPECIMEN	Calculated strain at 20 mm depth just before spalling off concrete cover	Calculated strain at 20 mm depth just after spalling off concrete cover	Calculated strain at 20 mm depth at 80% of maximum load
R12P25-A105	0.0024	0.0051	0.023
R12P50-A105	0.0023	0.0058	0.018
R12P75-A105	0.0024	0.0055	0.009
R12P100-A105	0.0022	0.0036	N/A
R12P150-A105	0.0024	0.0024	N/A
N8P25-A80	0.0024	0.0045	0.021
N8P50-A80	*	*	*
N8P75-A80	0.0027	0.0065	0.007
N8P100-A80	0.0023	0.003	N/A
N8P150-A80	0.0029	0.0029	N/A
R10P35-B72	0.0021	0.0048	0.025
R10P35-B83	0.0023	0.0043	0.026
R10P35-B95	0.0021	0.0048	0.029
R10P35-C95	0.0044	0.0094	0.044
R10P35-D95	0.0024	0.0042	0.024
N12P35-D85	0.0025	0.0043	
R12P35-D85	0.0046	0.0077	0.033
R10P35-D85	0.0048	0.0095	0.043
R8P35-D85	0.0023	0.0041	0.022
0P0-E85	0.0018	0.0018	N/A

* Not available

6.2.2 Concrete beam strains

It is important to have confined compression strain data. This was achieved using embedment strain gauges. It was found that when the embedment strain gauge was fixed just under the helix reinforcement the readings could not have been obtained after the concrete cover spalled off. It was found that a suitable position for installing the embedment strain gauge is 40 mm from the top surface of the beam. Thus the strain 40 mm deep could be measured and the strain at top surface of the beam could be calculated with the help of the strain data recorded before the concrete cover spalled off, as explained in the next paragraph. The strain 20 mm deep could be estimated by taking the average of the top surface strain and the strain 40 mm deep.

The strain at the top surface of the beam (concrete cover) was recorded until the concrete cover spalled off. It was possible to estimate the data of strain at the top surface of the beam using the concrete strain data recorded 40 mm deep (Elbasha and Hadi, 2005). The strain at the top surface after concrete cover has spalled off (ε_0) was estimated by dividing the strain at depth 40 mm (ε_{40}) by a factor (F). The factor (F) was determined by using regression such that $\frac{\varepsilon_0}{(\varepsilon_{40}/F)} \cong 1$.

Table C.1 in Appendix C shows an example for the measured and calculated strain data between 336.9 kN and 258.1 kN for Beam R10P35-B95. From Table C.1, the load just before the concrete cover spalling off was 344.7 kN and dropped to 250 kN. The strain measured 40 mm deep just before the concrete cover spalled off was 0.0012, which increased to 0.0026 afterwards. The strain measured at the top surface just before concrete cover spalled off was 0.003 but it was impossible to measured the strain after the concrete cover spalled off. However the concrete strain at the top surface of the beam just after concrete cover spalled off was 0.0069 (calculated as mentioned above). The strain 20 mm deep increased from 0.0021 to 0.0048. Figures C.1-C.20 in Appendix C demonstrate the load-strains of the 20 beams tested.

6.2.3 Moment curvature

The mid-span curvature was determined using the average strain measured in the longitudinal steel and on the top surface concrete strain (measured top surface concrete strain up to concrete cover spalled off and calculated top surface strain after concrete cover spalled off). For reasons unknown, the strain gauges connected to the longitudinal steel bars, did not give reasonable output data. As such the moment-curvature curves could not be drawn using Equation 6.1. Of the 20 beams, only five have acceptable steel strain data which could be used to calculate the curvature. As a result this study focuses only on displacement ductility.

$$\chi = \frac{\varepsilon_o + \varepsilon_{st}}{d} \tag{6.1}$$

Where χ is the curvature; ε_o is the strain at top surface of the beam; ε_{st} is the average steel strain and d is the effective depth of a cross-section.

6.2.4 Concrete cover spalling off

It is a common belief that closely spaced reinforcement physically separates the concrete cover from the core causing the cover to fail early. That statement does not consider the effect of helical diameter or other variables such as helical yield strength, concrete compressive strength and longitudinal reinforcement ratio, which may have a significant effect. It may be the cover spalling off when the strain at the cover becomes less than the strain of the confined concrete, which does not follow the strain gradient as shown in Figure 6.1. In other words the stress-strain of the compression concrete zone (confined and unconfined) is the same for the beam up to the point where the stress-strain of confined concrete is significantly different from the stress-strain of unconfined concrete for the same beam. Concrete cover spalling off may occur at the point where the beam exhibits two different behaviours of stress-strain, one for confined and one for unconfined concrete. That is not the case for beams without confinement or when the confinement has a negligible effect. For example the Beam R12P150-A105 (where the effect of confinement is negligible) has no concrete cover spalling off where the maximum

load was recorded at 413 kN and dropped suddenly down to 150 kN (brittle failure), which indicates no differences of stress-strain behaviour (one for confined and the other for unconfined concrete). The Beam R12P150-A105 has no sudden change in strain (strain energy release) because of the negligible effect of confinement, where the maximum strain was at the top surface of the beam 0.0035 (no spalling off phenomenon).

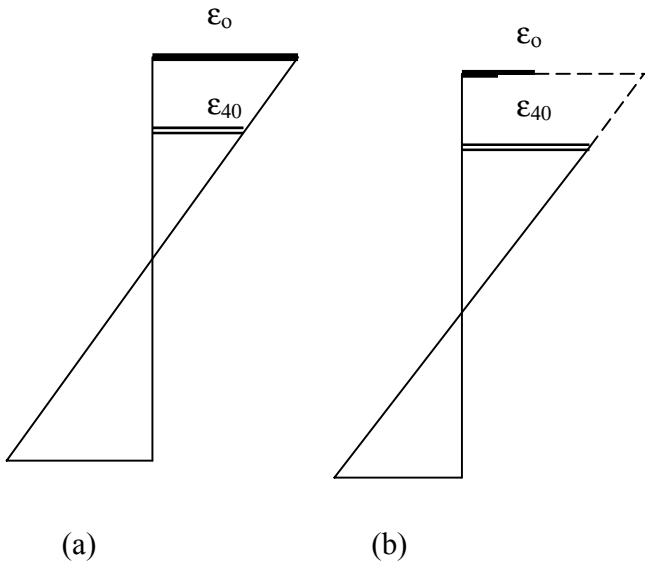

Figure 6.1 (a) Strain distribution before loss of the concrete cover
(b) Calculated strain distribution (ε_o) after spalling off the concrete cover

6.2.5 Helical pitch

It has been observed that helical pitch is an important parameter in enhancing the strength and ductility of beams. This observation is based on the results of an extensive experimental programme. However, building codes such as ACI 318R-02 (2002) and AS3600 (2001) do not take helical pitch or tie spacing as an explicit design parameter. For example Equation 6.2 is the ACI 318R-02 (2002) equation for the design of helical reinforcement of columns does not directly include helical pitch. The design is only for the quantity of lateral steel used (volumetric ratio), without specifying the pitch.

$$\rho_h = 0.45\left(\frac{A_g}{A_c} - 1\right)\frac{f_c'}{f_{yh}} \qquad (6.2)$$

where ρ_h is the total volumetric ratio of helices; A_g is the gross area of the section; A_c is the area of the core; f_c' is the concrete compressive strength and f_{yh} is the yield stress of helical reinforcement.

Equation 6.2 was derived to compensate for strength lost by the spalling off the concrete cover. An equation is needed to compensate for strength as well as the ductility and takes helical pitch into consideration.

6.3 THE EFFECT OF HELICAL PITCH

Sheikh and Uzumeri (1980) tested 24 specimens to examine the effect of different variables on the strength and ductility of columns. The results pointed to the significant influence of helical pitch on the behaviour of confined concrete. Shin et al. (1989) tested 36 beams, four of which were used to study the effect of tie spacing on ductility. The results did not clearly show the importance of confinement spacing. It may be because the spacings studied were only 75 and 150 mm, which did not provide adequate data to figure out the importance of confinement spacing. Hadi and Schmidt (2002) tested seven HSC beams helically confined in the compression zone to study different variables excluding the helical pitch, all with the same 25 mm helical pitch. However, the literature indicates the importance of helical pitch, but there is no quantitative data for over reinforced helically confined HSC beams.

This Section investigates ten of the 20 beams. These beams were used to investigate the effect of helical pitch on the behaviour of over-reinforced HSC helically confined beams and to determine their strength and ductility. The ten beams are divided into two groups of five, with 25, 50, 75, 100 and 150 mm pitches. The difference between the two groups are the helical confinement diameter and the concrete compressive strength. This is to study and confirm the effect of helical pitch on the behaviour of over-reinforced HSC helically confined

beams with different conditions, by using different helical confinement diameters and different concrete compressive strengths.

6.3.1 First group

The first five beams were constructed with R12 helical confinement diameter and five different pitches 25, 50, 75, 100 and 150 mm. All five beams had the same dimensions and material characteristics. To avoid repetition, all details are presented in Tables 5.3 and 5.4 in Chapter 5. A summary of the first test group results are presented in Tables 6.5 and 6.6. The observed load versus mid-span deflection and load versus strain are presented and discussed below.

Table 6.5 A summary of loads and mid-span deflection of first group beams

SPECIMEN	P_1, (kN)	P_2, (kN)	P_3, (kN)	$0.8P_3$, (kN)	Δ_y, (mm)	$\Delta_{u,0.8}$, (mm)	$\Delta_{u,0.8}/\Delta_y$
R12P25-A105	372	278	411	328	36	277	7.7
R12P50-A105	383	302	383	306	35	150	4.3
R12P75-A105	386	295	386	309	32	42	1.3
R12P100-A105	395	250	395	316	35	35	1.0
R12P150-A105	413	150*	413	328	38	38	1.0

* The load dropped suddenly from 413 to 150 kN
P_1 is the load at concrete cover spalling off
P_2 is the load just after spalling off concrete cover
P_3 is the highest load recorded during the test
Δ_y is the yield deflection and
$\Delta_{u,0.8}$ is the deflection at 80% of the maximum load

Table 6.6 - Summary of beam curvature results of first group beams

Beam specimen	Yield curvature X_y	Ultimate Curvature X_u	Curvature ductility index X_u/ X_y
R12P25-A105	0.0000145	0.00014	9.6
R12P50-A105	0.0000217	0.00013	6
R12P75-A105	0.0000217	0.000051	2.3
R12P100-A105	0.000025	0.000025	1
R12P150-A105	0.000015	0.000015	1

Figure 6.2 illustrates the load mid-span deflection for Beams R12P25-A105, R12P50-A105, R12P75-A105, R12P100-A105and R12P150-A105 and Figure 6.3 shows the moment mid-span curvature for the tested beams. From Figures 6.2 and 6.3, the remarkable effect that helical pitch has on displacement and curvature ductility could be noted. Beams, which have helical pitches of 25, 50 and 75 mm failed in a ductile manner. The level of ductility depends on helical pitch. The Beam R12P100-A105 failed in a brittle mode where the maximum load was 395 kN dropped to 250 kN, and then continued dropping significantly. Figure B.4 in Appendix B shows the complete recorded data of the mid-span deflection load for Beam R12P100-A105. Also the Beam R12P150-A105 failed in a brittle mode because the upper concrete in the compression zone was crushed and the maximum load was 413 kN, which then dropped to 150 kN. Thus it could be considered that

the effect of confinement is negligible when the helical pitch is equal to 70 percent of the confined concrete core diameter. This only happened for over-reinforced HSC helically confined beams, which does not agree with the experimental results conducted on columns by Iyengar et al. (1970) and Martinez et al. (1984). Iyengar et al. (1970) and Martinez et al. (1984) stated that the effect of confinement is negligible when the confinement spacing is equal to the confinement core diameter. Figure 6.4 shows the relation between the helical pitch and ultimate mid-span deflection. Beam R12P25-A105 had a maximum deflection of 277 mm and the deflection was reduced as the pitch was increased. It must be mentioned that the maximum deflection of Beam R12P25-A105 may be more than 277 mm because the test was stopped for safety reasons.

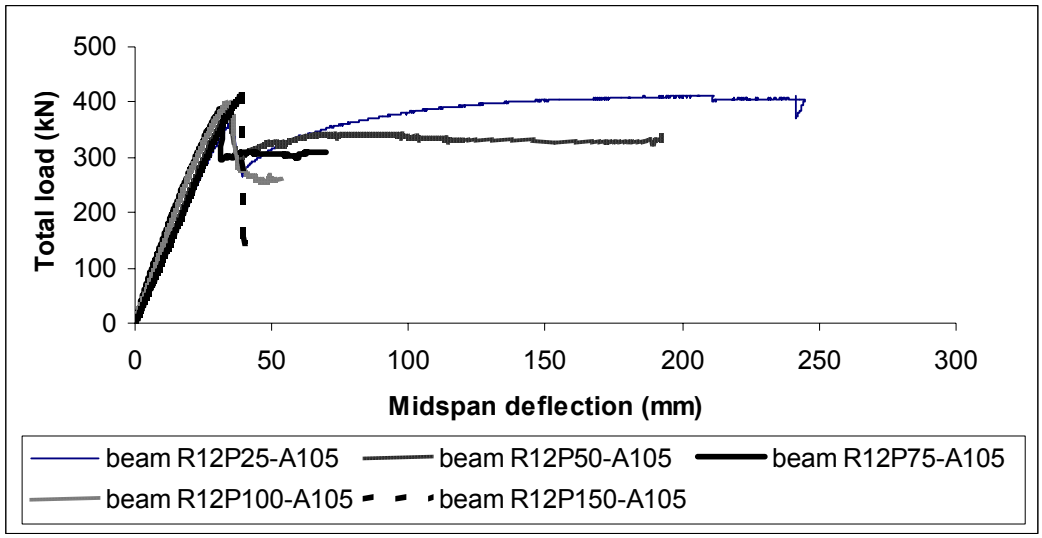

Figure 6.2 Load-deflection curves for beams with different helix pitch

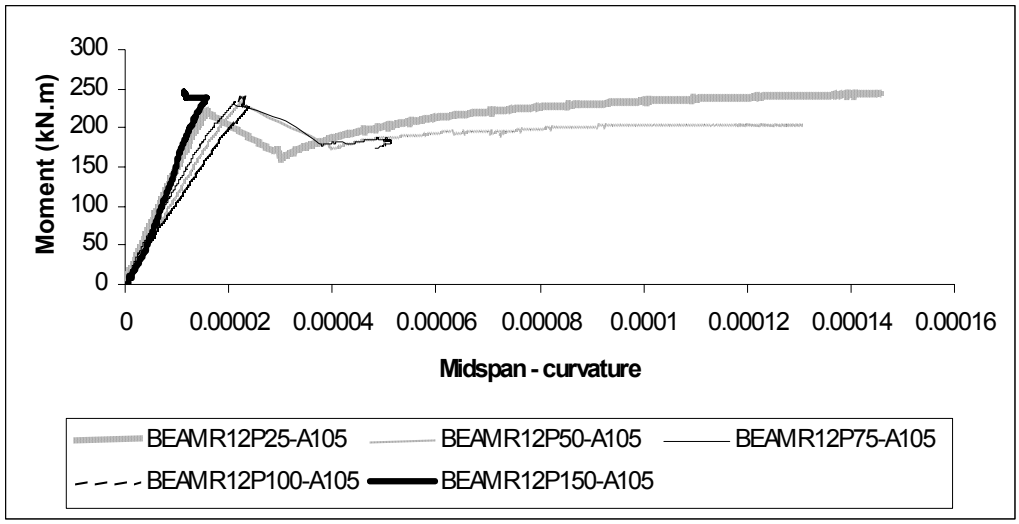

Figure 6.3 Moment-curvature curves for beams with different helix pitch

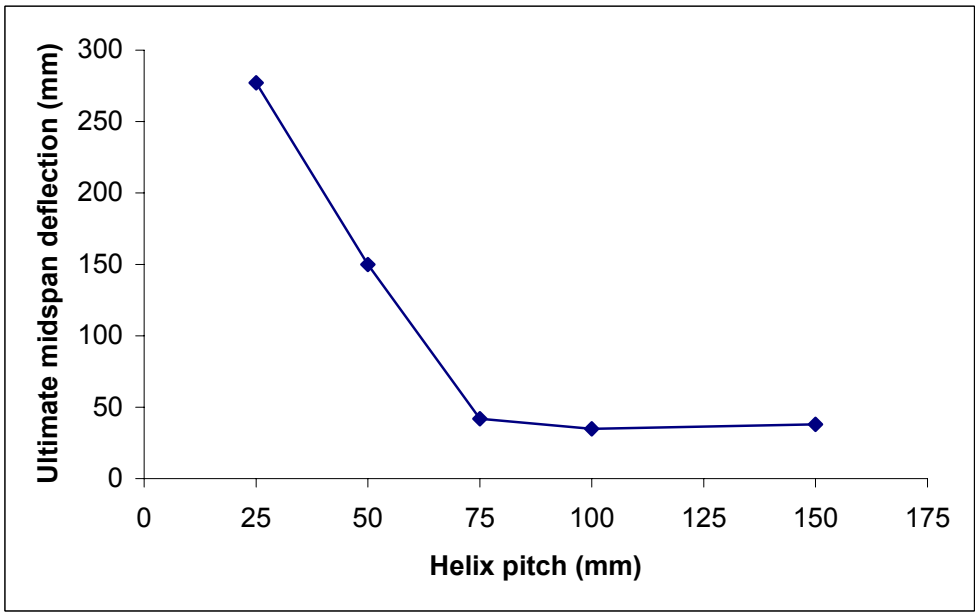

Figure 6.4 Ultimate deflection versus helix pitch

The deflection ductility index is defined as the ratio of ultimate deflection to yield deflection. Figure 6.5 shows that the deflection ductility index increases as the helical pitch decreases. The yield deflection for beams R12P25-A105, R12P50-A105, R12P75-A105, R12P100-A105 and R12P150-A105 was 36, 35, 32, 35 and 38 mm, respectively, and the ultimate corresponding deflections was 277, 150, 42, 35 and 38 mm. It could be noted that there is almost no difference between the yield deflections for the five beams compared to the ultimate deflection. Hence, it can be concluded that the deflection ductility index is significantly affected by the ultimate deflection. It could also be concluded that helical pitch has a significant effect on the ultimate deflection but less significant effect on the yield deflection (Elbasha and Hadi, 2005).

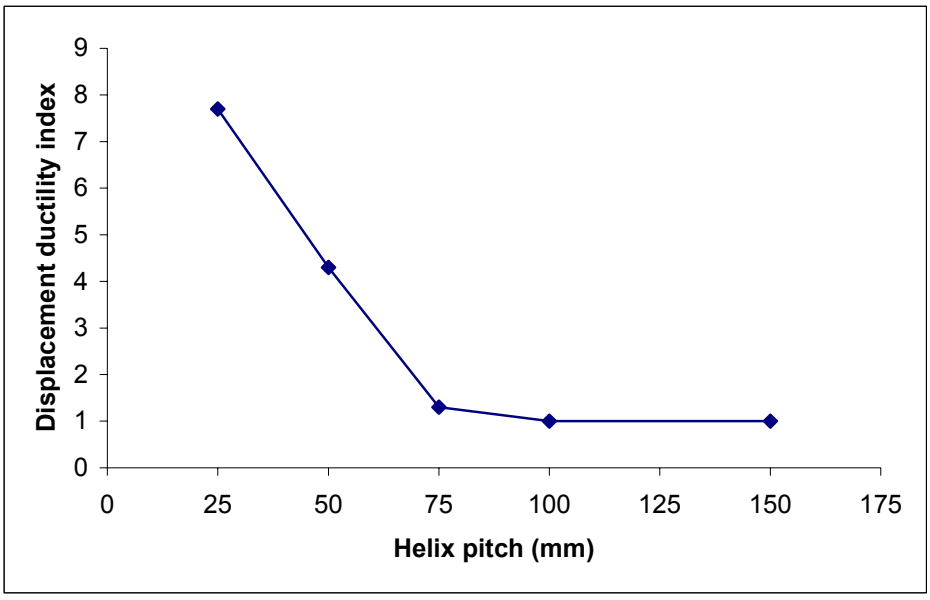

Figure 6.5 Effect of helix pitch on displacement ductility

Tables 6.2, 6.3 and 6.4 show the load versus strain at the top surface of the concrete and at, 20 mm and 40 mm deep. However the strain 20 mm deep is the average of the top surface strain (ε_0) and the strain 40 mm deep (ε_{40}). For the Beams R12P25-A105, R12P50-A105 and R12P75-A105 the strain generally increased as the load increased until the concrete cover spalled off at a strain equal to 0.0033 (measured strain at the surface of the beam) then the load dropped with a sudden increase in strain (measured strain 40 mm deep), the confined concrete core prevented the load from dropping further down and then the strains increased smoothly up to failure. However for the beams R12P100-A105 and R12P150-A105 the strain increased as the load increased until it reached about 0.0034 at the surface where the load suddenly dropped and the confined concrete core was not preventing the load from dropping further down because the helical pitch for beams R12P100-A105 and R12P150-A105 was ineffective (helical confinement has negligible effect when the helical pitch is more than or equal to the confinement core diameter). The interesting point is that there was no significant difference between the concrete cover spalling off strain (top surface). However, the average concrete cover spalling off strain for the five beams was 0.00332, which is in agreement with ACI 318R-02 (2002) and AS3600 (2001). The significant differences are between the calculated strains at top surface of 80% of the maximum load.

Figure 6.6 shows the relationship between the concrete spalling off load versus the helix pitch. It is worth noting that the spalling off load increased linearly as the

helical spacing increased. Based on these findings it can be concluded that the spalling off load is directly proportional to the helical pitch.

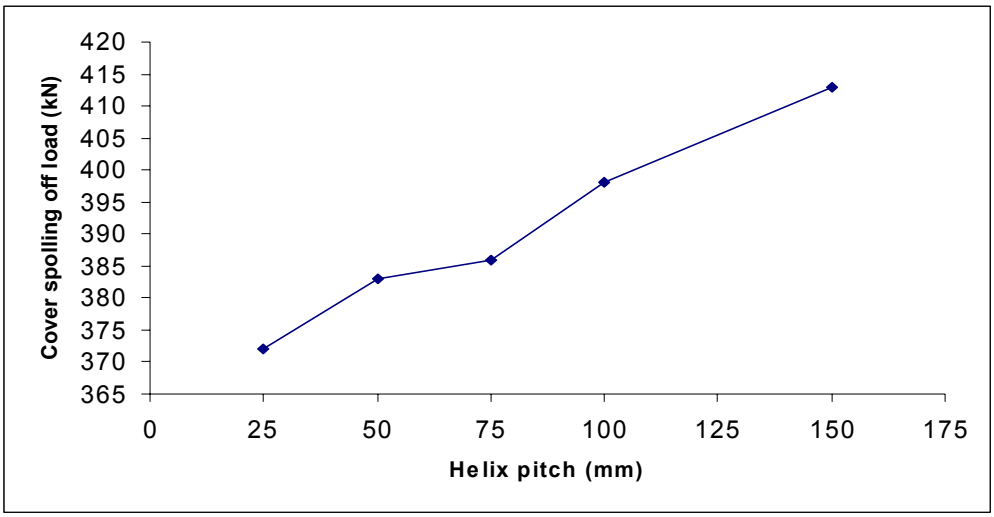

Figure 6.6 Cover spalling off load versus helix pitch

6.3.2 Second group

The second group of five beams was constructed with N8 helical confinement diameter and five different pitches 25, 50, 75, 100 and 150 mm. Every beam had similar dimensions and material, but dissimilar helical pitches. All beam details are shown in Tables 5.3 and 5.4, in Chapter 5. A summary of the test results, loads and deflections of Beams N8P25-A80, N8P50-A80, N8P75-A80, N8P100-A80 and N8P150-A80, is presented in Table 6.7. The observed load versus mid-span deflection and load versus strain are presented and discussed below.

Table 6.7 - Summary of second group beams results

SPECIMEN	P_1, (kN)	P_2, (kN)	P_3, (kN)	$0.8P_3$, (kN)	Δ_y, (mm)	$\Delta_{u,0.8}$, (mm)	$\Delta_{u,0.8}/\Delta_y$
N8P25-A80	297	237	345	276	29	190	6.5
N8P50-A80	324	284	324	260	31	90	2.9
N8P75-A80	378	261	378	302	40	40	1.0
N8P100-A80	325	257	325	260	34	34	1.0
N8P150-A80	376	94*	376	300	39	39	1.0

* The load dropped suddenly from 376 to 94 kN
P_1 is the load at concrete cover spalling off
P_2 is the load just after spalling off concrete cover
P_3 is the highest load recorded during the test
Δ_y is the yield deflection and
$\Delta_{u,0.8}$ is the deflection at 80% of the maximum load

From Figure 6.7 it should be noted that the helical pitch had remarkable affect on the displacement ductility. Beams N8P25-A80 and N8P50-A80, which have helical pitches of 25 and 50 mm failed in a ductile manner. The level of ductility depends on the helical pitch. Beam N8P75-A80 failed in a brittle mode, which was unexpected because from Group 1 it is noted that when the helical pitch is 75 mm, the failure mode was ductile. Also from Group 1 it is observed that the spalling off concrete cover load for the beams with 50 and 75 mm helical pitches were 383 and 386 kN, respectively. These loads are similar, but for Group 2 the spalling off the concrete cover load of Beam N8P75-A80 was 378 kN, which is more than the 324 kN spalling off concrete cover load of Beam N8P50-A80. Thus it could be considered that Beam N8P75-A80 had an experimental error.

Beams N8P100-A80 failed in a brittle mode, and the maximum load was 325 kN, which dropped to 257 kN at a 34 mm midspan deflection, and then dropped again to 102 kN at a 40 mm midspan deflection. Beam N8P150-A80 also failed in a brittle mode, as the upper concrete in the compression zone was crushed and the maximum load was 376 kN, which then dropped to 94 kN. There are no general levels of brittleness because brittle failure is not safe. Thus Beams N8P100-A80 and N8P150-A80 failed in brittle mode. As a result, the effect of confinement is negligible when the helical pitch is equal to or more than 70 percent of the confinement diameter, which agrees with the experimental results of the first group. Figure 6.8 shows the relationship between the helical pitch and ultimate mid-span deflection. Beam N8P25-A80 had a maximum deflection of 190 mm. The mid-span deflections of the beams are reduced as the pitch increases.

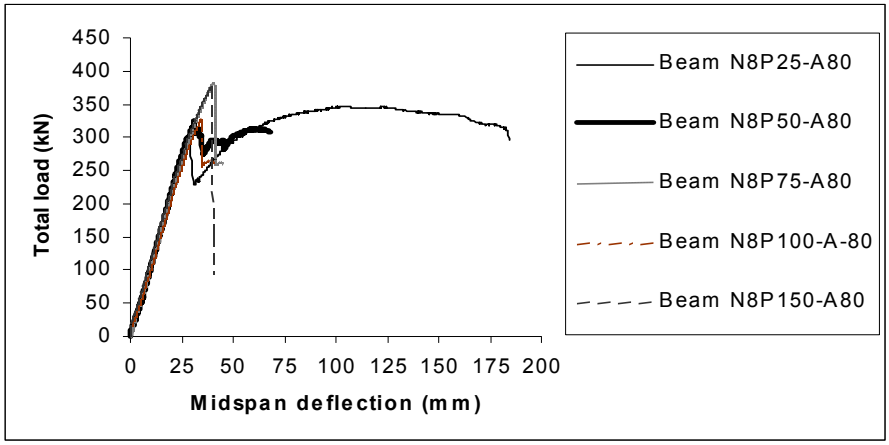

Figure 6.7 Load-deflection curves for beams with different helix pitch

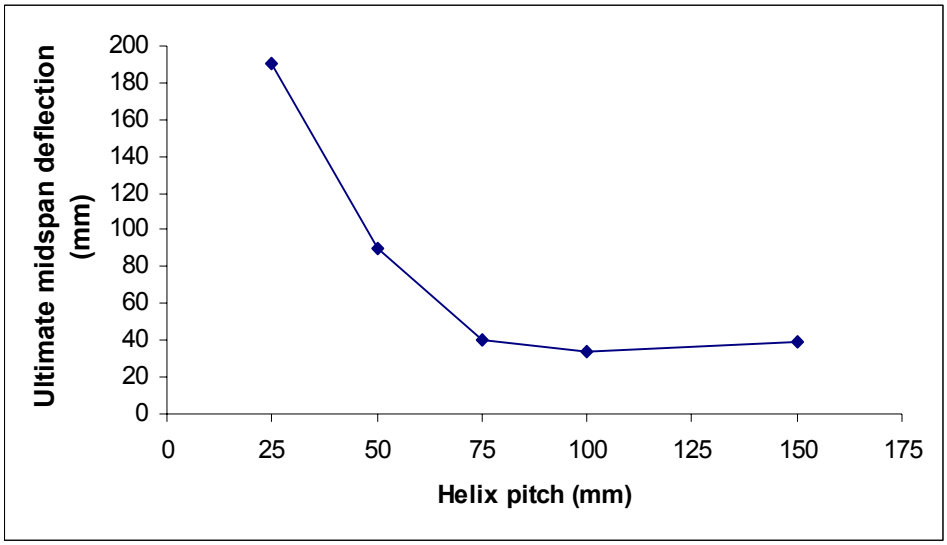

Figure 6.8 Ultimate deflection versus helix pitch

The deflection ductility index is defined as the ratio of ultimate deflection to the yield deflection. Figure 6.9 shows that the deflection ductility index increases as the helical pitch decreases. The yield deflection for Beams N8P25-A80, N8P50-A80, N8P75-A80, N8P100-A80 and N8P150-A80 were 29, 31, 40, 34 and 39 mm, respectively, and the ultimate corresponding deflections were 190, 90, 40, 34 and 39, respectively. It should be noted that there was no significant differences between the yield deflections for the five beams compared to the ultimate deflections where there was a considerable difference. Hence, it can be concluded that the deflection ductility index is significantly affected by ultimate deflection. It could also be concluded that helical pitch significantly affects ultimate deflection but less significantly on yield deflection. Figure 6.10 shows the ultimate deflection of Beams N8P25-A80, N8P50-A80, N8P75-A80 and N8P100-A80 and Figure 6.11

reveals the concrete core of Beam N8P25-A80. It can be noted that the 10 mm diameter steel bar, which was used to fix the helix pitch during casting has only buckled beams with high helix pitches, i.e., N8P75-A80 and N8P100-A80. Figure 6.12 shows that for Beam N8P100-A80 the steel bar used for holding the helix pitch has buckled. This probably occurred after cover spalled off, because the spalling off load for beams N8P75-A80 and N8P100-A80 was greater than for Beams N8P25-A80 and N8P50-A80. The helix diameter was small (8 mm) which could not resist the stress produced due expansion of the concrete core, which led to helix fracture. It can be noted that the helix of beams N8P25-A80, N8P50-A80 and N8P75-A80 had helix fracture. Figure 6.13 shows the helix fracture for beam N8P75-A80.

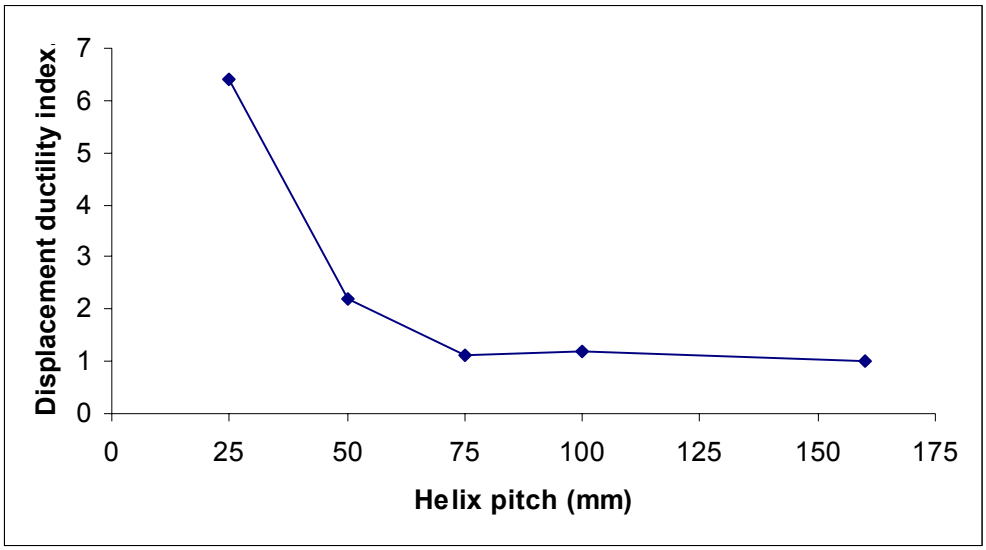

Figure 6.9 Effect of helix pitch on displacement ductility

Final deflection of
Beam N8P25-A80

Final deflection of Beam
N8P50-A80

Final deflection of Beam
N8P75-A80

Final deflection of Beam
N8P100-A80

Figure 6.10 Final deflection for beams helically confined with different helix pitch 25, 50, 75 and 100 mm

Figure 6.11 Core concrete of Beam 8HP25

Figure 6.12 Buckling in the steel bar of Beam 8HP100

Figure 6.13 Helix bar fracture of Beam 8HP75

The strain at the top surface of the beam (concrete cover) was recorded until the cover spalled off (Table 6.8). There was no significant difference between the concrete cover spalling off strain (top surface) for Beams N8P25-A80, N8P50-A80, N8P75-A80, N8P100-A80 and N8P150-A80. However, the average concrete cover spalling off strain for the five beams was 0.0033, which agrees with the test results of the first group, ACI 318R-02 (2002) and AS3600 (2001). Figures C.6-C.10 in Appendix C displays the load versus strain at a depth 0, 20 and 40 mm. The significant differences are between the confined strains measured 40 mm deep, for

example the strains measured were 0.012 and 0.009 of Beams N8P25-A80 and N8P50-A80, respectively.

Figure 6.14 shows the relationship between the concrete spalling off load versus helix pitch. It is worth noting that the spalling off load increased linearly as the helical pitch increased. The results of Beam N8P75-A80 were excluded as its results had an experimental error. Based on this finding, it can be concluded that the spalling off load is directly proportional to the helical pitch.

Table 6.8 - Summary of beam strains

Beam specimen	Measured top surface strain just before spalling off concrete cover	Measured strain at 40 mm depth just before spalling off concrete	Measured strain at 40 mm depth just after spalling off concrete	Measured strain at 40 mm depth at failure load
N8P25-A80	0.0034	0.001386	0.002716	0.012459
N8P50-A80	*	0.001273	0.00163	0.009155
N8P75-A80	0.0034	0.002077	0.0049	N/A
N8P100-A80	0.003	0.00119	0.00157	N/A
N8P150-A80	0.0035	0.001824	0.001824	N/A

* Not available

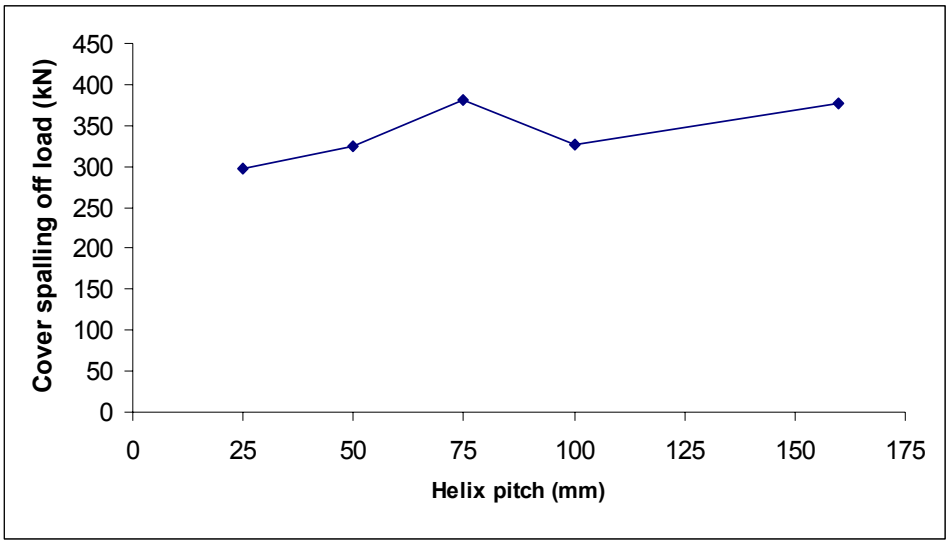

Figure 6.14 Cover spalling off load versus helix pitch

6.4 THE EFFECT OF CONCRETE COMPRESSIVE STRENGTH

The ultimate deflection shown in Table 6.9 was taken as the value corresponding to 80% of the maximum load capacity. Figure 6.15 shows the load versus deflection of the three beams, which have the same longitudinal reinforcement ratio but a different concrete compressive strength. It is to be noted that the yield deflection decreased slightly as the concrete compressive strength increased but ultimate deflection decreased significantly. For Beam R10P35-B72, which has a 72 MPa concrete compressive strength, the ultimate deflection recorded was 248 mm, but for Beam R10P35-B83, where the concrete compressive strength was 83 MPa, ultimate deflection was 214 mm, which is 86% of the ultimate deflection of Beam

R10P35-B72. However, the ultimate deflection of Beam R10P35-B95 was 72% of Beam R10P35-B72. It must be noted that Beam R10P35-B72 had an ultimate deflection higher than the other two beams, even though Beam R10P35-B72 had a higher value of (ρ/ρ_{max}).

Table 6.9 Summary of beam results having different concrete compressive strength.

SPECIMEN	P_1, (kN)	P_2, (kN)	P_3, (kN)	$0.8P_3$, (kN)	Δ_y, (mm)	$\Delta_{u,0.8}$, (mm)	$\Delta_{u,0.8}/\Delta_y$
R10P35-B72	363	248	363	290	38	248	6.5
R10P35-B83	372	275	372	297	37	214	5.8
R10P35-B95	344	250	357	286	34	180	5.3

P_1 is the load at concrete cover spalling off
P_2 is the load just after spalling off concrete cover
P_3 is the highest load recorded during the test
Δ_y is the yield deflection and
$\Delta_{u,0.8}$ is the deflection at 80% of the maximum load

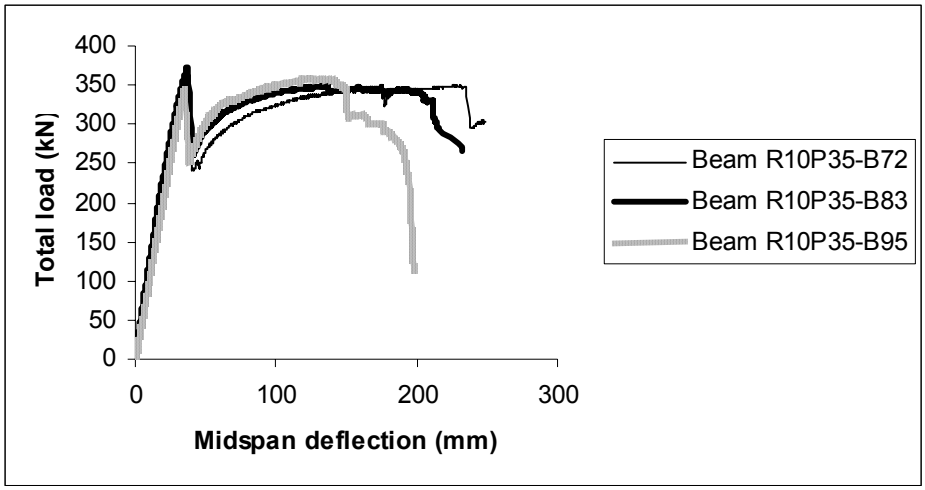

Figure 6.15 Load- deflection curves for beams that have different concrete compressive strength R10P35-B72, R10P35-B83 and R10P35-B95

Beams R10P35-B72, R10P35-B83 and R10P35-B95 have the same longitudinal reinforcement ratio (ρ) but the maximum longitudinal reinforcement ratio (ρ_{max}) increased as the concrete compressive strength increased, therefore the (ρ/ρ_{max}) is decreased. (ρ/ρ_{max}) for Beams R10P35-B72, R10P35-B83 and R10P35-B95 was 2.30, 2.0 and 1.75, respectively, but the ultimate deflection was 248, 214 and 180 mm respectively. It could be concluded that for over reinforced HSC helically confined beams, increasing the concrete compressive strength decreases the yield deflection slightly, and decreases ultimate deflection significantly.

The displacement ductility index is defined as the ratio of ultimate deflection (corresponding to 80% of the maximum load capacity recorded) over yield deflection. Figure 6.16 shows the effect of concrete compressive strength on the displacement ductility index. It is noted that as the concrete compressive strength increases, the displacement ductility index decreases. The same trend has been reported by Ashour (2000) that the displacement ductility index decreases slightly as concrete compressive strength increases from 78 to 102 MPa. The displacement ductility index for Beams R10P35-B83 and R10P35-B95 was 89% and 81% respectively of the displacement ductility index of Beam R10P35-B72. However, Saatcioglu and Razvi (1993) and Pessiki and Pieroni (1997) reached similar conclusions that as the concrete compressive strength increases, a significantly higher lateral reinforcement ratio is required to enhance ductility. Also Galeota et

al. (1992) affirmed that ductility is decreases as the concrete compressive strength increases.

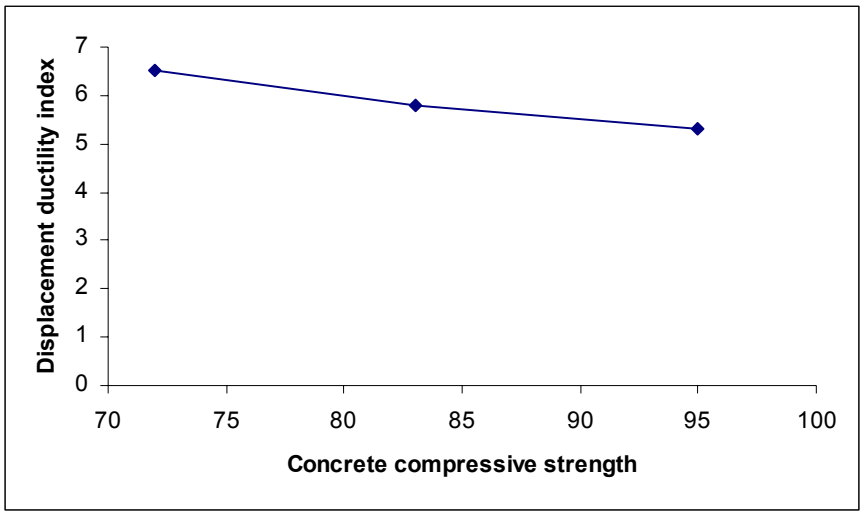

Figure 6.16 Effect of concrete strength on displacement ductility index

The recorded load at the spalling off the concrete cover for R10P35-B72, R10P35-B83 and R10P35-B95 was 363, 372 and 344 kN, respectively and the load just afterwards dropped to 68%, 74% and 73%, respectively. The maximum loads recorded during the experimental test for Beams R10P35-B72 and R10P35-B83 were those at which the concrete cover spalled off as 363 and 372 kN, respectively. However, it was not the same for Beam R10P35-B95 where the maximum load recorded was 357 kN, which is higher than the load at spalling off because Beam R10P35-B95 has a higher concrete compressive strength. Figure 6.17 shows the

effect of concrete compressive strength on the concrete cover spalling off load using three beams with different concrete compressive strengths. The load at spalling off the concrete cover increases as the concrete compressive strength increases up to the point where the concrete compressive strength is 83 MPa, after which the load decreases as the concrete compressive strength increases. It could be concluded that the load at spalling off the concrete cover is increased as the concrete compressive strength increases up to a particular concrete compressive strength, but if the concrete compressive strength increases after that the concrete cover spalling off load is decreased but the maximum load will be higher than the load at spalling off.

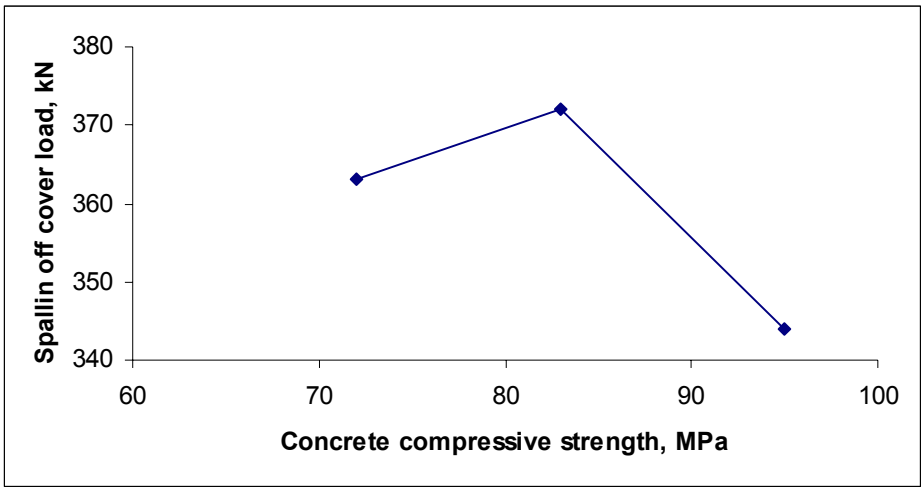

Figure 6.17 Effect of concrete strength on concrete cover spalling off load

Tables 6.2, 6.3 and 6.4 display the summary of Beams R10P35-B72, R10P35-B83 and R10P35-B95 top surface strain just before spalling off concrete cover and the

strains at 20 and 40 mm depth. The measured top surface concrete strain just before spalling off concrete cover for Beams R10P35-B72, R10P35-B83 and R10P35-B95 were 0.0029, 0.0032 and 0.003, respectively which is in agreement with ACI 318R-02 (2002) and AS3600 (2001). The difference between the strain measured 40 mm deep just before spalling off the concrete cover and the strains measured just after spalling off the concrete cover, for example at 40 mm deep, just before the cover of Beam R10P35-B72 spalled off was 0.00135 and the strain just after spalling off concrete cover was 0.00307. The strain just after spalling off the concrete cover was 2.3 times the strain just before the cover of Beam R10P35-B72 spalled off. It has been noted that the strains at 40 mm depth from top surface of the beams just before spalling off the concrete cover had increased slightly as the concrete compressive strain increased. The strains measured 40 mm deep just before spalling off were 0.00135, 0.00141 and 0.0015 for those beams with concrete compressive strength of 72, 83 and 95 MPa, respectively. However, the strains just after spalling off concrete cover decreased. The maximum strain measured 40 mm deep was almost the same value. These readings did not represent the strains versus 80% of the maximum load because of premature damage to the embedment gauges before the loads reached that point.

6.5 THE EFFECT OF REINFORCEMENT RATIO

The ultimate deflection shown in Table 6.10 was taken as the value corresponding to 80% of the maximum load capacity. Figure 6.18 presents the load deflection of the three beams which have the same concrete compressive strength but a different longitudinal reinforcement ratio. It can be observed that the ultimate deflection increases significantly as the longitudinal reinforcement ratio increases, which is different from the influence of concrete compressive strength. Bjerkeli et al. (1990) noted that for well-confined column, as the longitudinal reinforcement ratio increases a column member sustains ultimate load. Whereas with a lower longitudinal reinforcement ratio the load decreased immediately after reaching maximum load. Beam R10P35-C95 with 95 MPa compressive strength and longitudinal reinforcement ratio of 0.051, recorded 189 mm the ultimate deflection but Beam R10P35-B95 with 95 MPa compressive strength ultimate deflection was 180 mm, which is 95% of Beam R10P35-C95. However, Beam R10P35-D95 has 157% of the ultimate deflection of Beam R10P35-C95. It must be noted that Beam R10P35-D95 has a higher ultimate deflection than Beam R10P35-C95 even though Beam R10P35-D95 has a higher value of ρ/ρ_{max}. Figure 6.19 presents the ultimate deflection of Beam R10P35-D95. Beams R10P35-C95, R10P35-B95 and R10P35-D95 have the same concrete compressive strength of 95 MPa but a different longitudinal reinforcement ratio (ρ) although the maximum longitudinal reinforcement ratio (ρ_{max}) was the same. (ρ/ρ_{max}) for Beams R10P35-C95, R10P35-

B95 and R10P35-D95 was 1.40, 1.75 and 2.09, respectively, while the ultimate deflection was 189, 180 and 282 mm, respectively. It could be concluded that increasing the longitudinal reinforcement ratio of an over-reinforced HSC helically confined beam, increases the ultimate deflection although (ρ/ρ_{max}) has increased. This is not the case for Beams R10P35-B72, R10P35-B83 and R10P35-B95 where increasing the concrete compressive strength decreased ultimate deflection.

Figure 6.20 shows the effect of longitudinal reinforcement ratio on the displacement ductility index. It is noted that as the longitudinal reinforcement ratio increases the displacement ductility index increases. The displacement ductility index for Beams R10P35-B95 and R10P35-D95 was 110% and 163%, respectively of the displacement ductility index of Beam R10P35-C95, and even though it has a higher longitudinal reinforcement ratio displacement ductility index is higher. It was also found that a larger amount of long and wide cracks appeared in the lower reinforced beams. Figure 6.21 shows their patterns for Beam R10P35-C95 and the strong concrete core

Table 6.10 Summary of beam results having different longitudinal reinforcement ratio

SPECIMEN	P_1, (kN)	P_2, (kN)	P_3, (kN)	$0.8P_3$, (kN)	Δ_y, (mm)	$\Delta_{u,0.8}$, (mm)	$\Delta_{u,0.8}/\Delta_y$
R10P35-C95	365	276	365	292	39	189	4.8
R10P35-B95	344	250	357	286	34	180	5.3
R10P35-D95	331	247	412	330	36	282	7.8

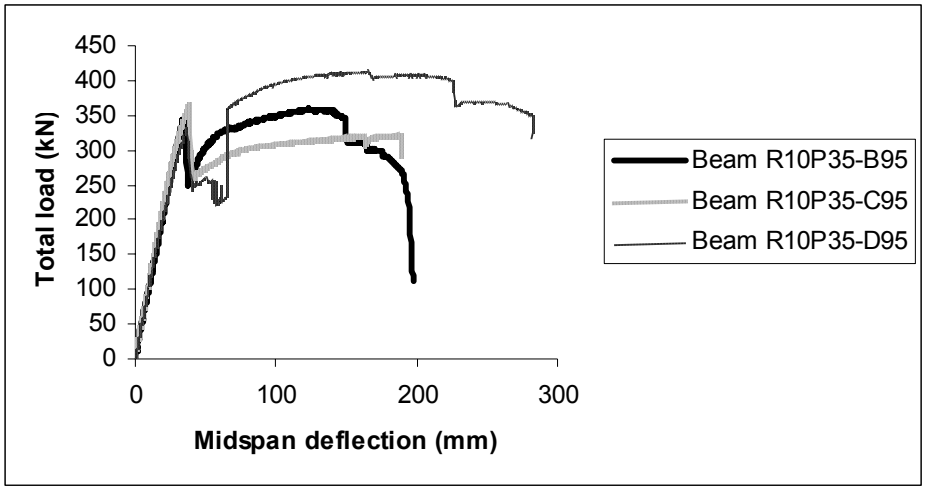

Figure 6.18 Load-midspan deflection curves for beams that have different longitudinal reinforcement ratio, Beams R10P35-C95, R10P35-B95 and R10P35-D95

Figure 6.19 Ultimate deflection of Beam R10P35-D95

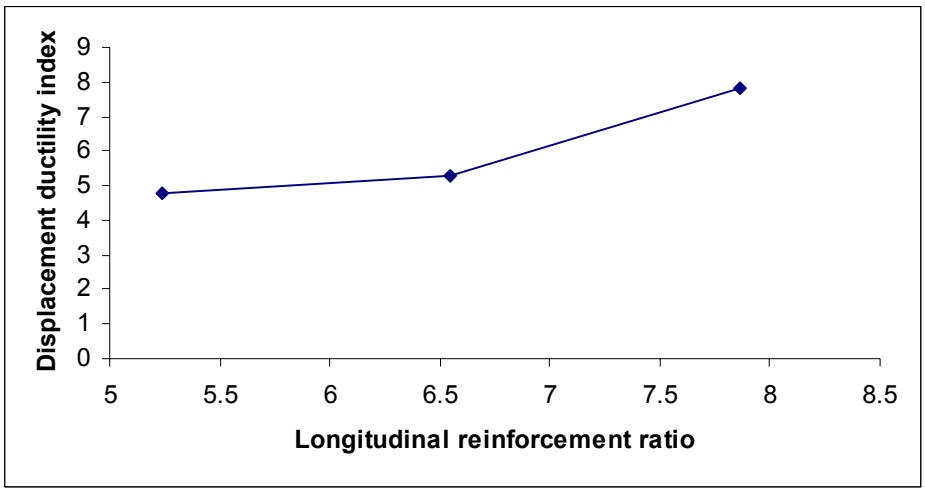

Figure 6.20 Effect of longitudinal reinforcement ratio on displacement ductility index

Figure 6.21 Crack patterns for Beam R10P35-C95

The load recorded at spalling off the concrete cover for Beams R10P35-C95, R10P35-B95 and R10P35-D95 was 365, 344 and 331 kN, respectively and the load just after spalling off dropped to 76%, 73% and 75%, respectively. The maximum load for Beam R10P35-C95 was at spalling off load of 365 kN. However, it is noted that for Beams R10P35-B95 and R10P35-D95 where the maximum load recorded was 357 and 412 kN, respectively which is higher than the load at spalling off. These results are similar to the experiments results conducted by Cusson and Paultre (1994) where they found that for well confined columns the strength and ductility enhanced by 7% and 56%, respectively when the longitudinal reinforcement ratio increased from 2.2 to 3.6%, respectively. Saatcioglu and Razvi (1993) reported that the strength and ductility of HSC is enhanced as the longitudinal reinforcement ratio increases. Figure 6.22 shows the effect of longitudinal reinforcement ratio on the concrete cover spalling off load using three beams with different longitudinal reinforcement ratios and the same concrete compressive strength. The load at spalling off the concrete cover is decreased as the longitudinal reinforcement ratio increased for the three beams which have the same concrete compressive strength of 95 MPa. As a result of increasing the longitudinal reinforcement ratio, the load capacity (maximum load) is increased and because the helical confinement effect the concrete cover spalling off phenomenon will occur at a load less than the maximum load. The maximum load of Beams R10P35-B95 and R10P35-D95 was 1.04 and 1.24 times the load at spalling off, respectively. Cusson and Paultre (1994) conclude that after the concrete cover has completely spalled

off, important gains in strength and ductility have been recorded for the concrete core of well-confined specimens. It can be concluded that the load at spalling off the concrete cover is decreases as the longitudinal reinforcement ratio increases but the maximum load will be higher than the load at spalling off the concrete cover for higher longitudinal reinforcement ratio. This conclusion differs from the influence of concrete compressive stress studied above.

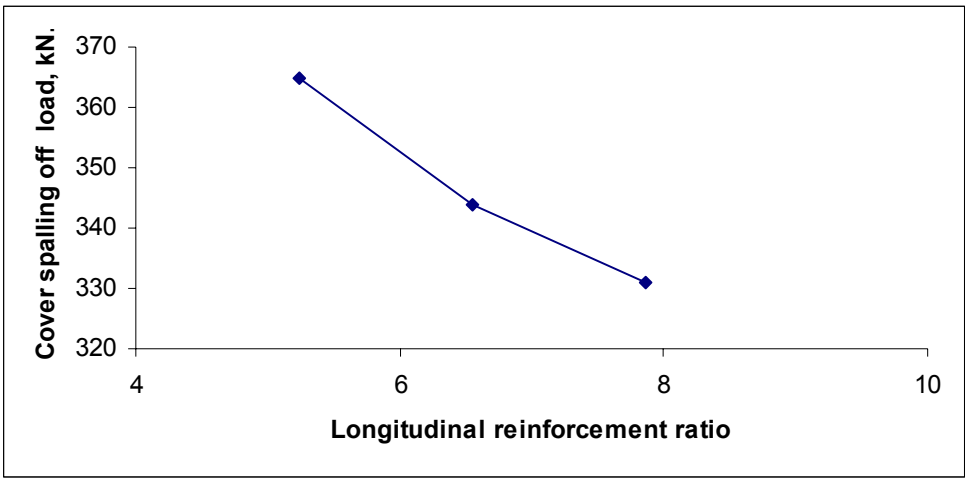

Figure 6.22. Effect of concrete strength on concrete cover spalling off load

The top surface concrete strain measured just before spalling off the concrete cover for Beams R10P35-B95, R10P35-C95 and R10P35-D95 were 0.003, 0.0031 and 0.00328, respectively which is very similar to the strains of Beam R10P35-B72, R10P35-B83 and R10P35-B95 which have different concrete compressive strength

and the same longitudinal reinforcement ratio. Also Ibrahim and MacGregor (1997) stated that for lightly confined HSC columns the surface concrete strain just before spalling off the concrete cover ranged from 0.003 to 0.004. The significant difference is between the measured strain at 40 mm depth just before spalling off the concrete cover and measured strains just after spalling off the concrete cover. For example the strain at 40 mm depth just before spalling off the concrete cover of Beam R10P35-D95 was 0.00163 and the strain just after spalling off the concrete cover was 0.0028. It is to be noted that the strains at 40 mm depth from the top surface of the beams just before spalling off the concrete cover slightly increased as the longitudinal reinforcement ratio increased and the strains just after spalling off the concrete cover increased. The measured maximum strains at 40 mm depth recorded were almost the same 0.0159 and 0.01589 for Beams R10P35-B95 and R10P35-D95, respectively. However, Beam R10P35-C95 had a lower recorded strain of 0.0135.

Figure 6.23 shows the effect of ρ/ρ_{max} on the concrete cover spalling off load for beams with different longitudinal reinforcement ratios and beams with different concrete compressive strengths. It is to be noted that the effect of ρ/ρ_{max} on concrete cover spalling off load for beams that have the same concrete compressive strength and different longitudinal reinforcement ratios is significantly different from the effect of ρ/ρ_{max} on the concrete cover spalling off load for beams that have the same longitudinal reinforcement ratio and different concrete compressive

strengths. Also Figure 6.24 shows the effect of ρ/ρ_{max} on the displacement ductility index. It can be noted that the relationship between ρ/ρ_{max} and the displacement ductility index (for beams with the same concrete compressive strength but different longitudinal reinforcement ratio) is different from the relationship between ρ/ρ_{max} and the concrete cover spalling off load (for beams with the same longitudinal reinforcement ratio and different concrete compressive strength). However, the significant difference between the influence of concrete compressive strength and the influence of longitudinal reinforcement ratio can be proved theoretically from the basic Equations 5.1 and 5.2 in Chapter 5 as follows:

Here the five beams with the same concrete cross section and the same steel strength

Then b, d, γ and f_{sy} are constants

By dividing Equation 5.2 by Equation 5.1

Then $$\frac{\rho}{\rho_{\max}} = \lambda \times \frac{A_s}{f_c'}$$

Where λ is a proportion constant which depends on b, d, γ and f_{sy}. As a result ρ/ρ_{max} is directly proportional with the longitudinal reinforcement ratio and inversely proportional with the concrete compressive strength.

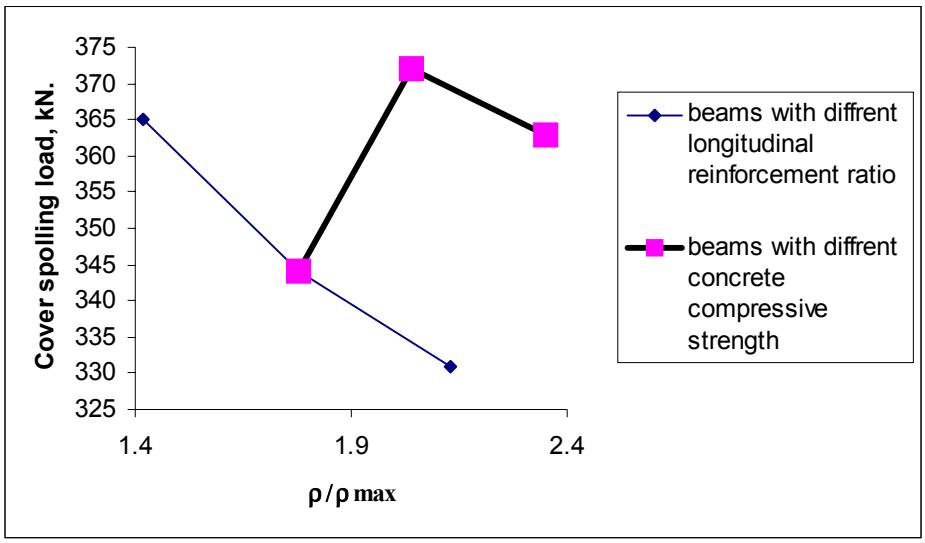

Figure 6.23 Load at spalling off concrete cover versus ρ/ρ_{max}

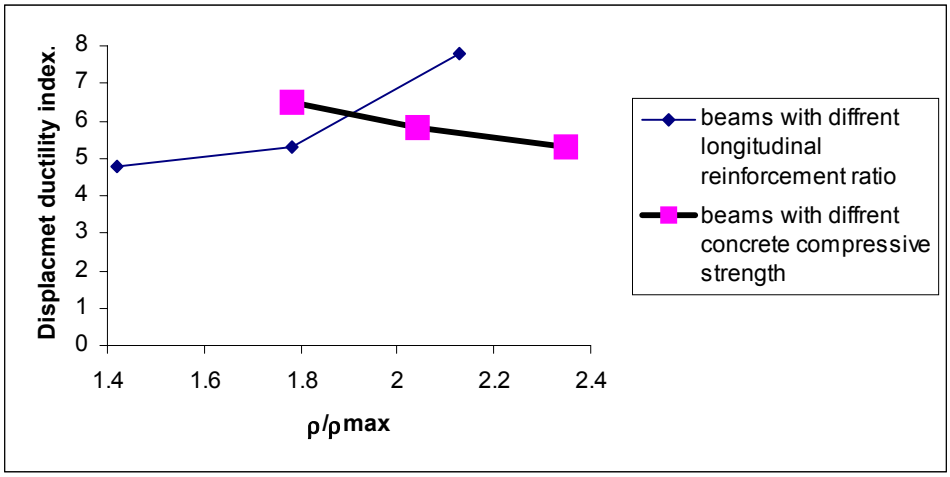

Figure 6.24 Displacement ductility index versus ρ/ρ_{max}

6.6 THE EFFECT OF HELICAL YIELD STRENGTH

The lateral expansion of concrete in helically confined beams produces tensile stress on the helical reinforcement. The amount of stress depends on the size of the concrete core, position of the neutral axis (in other words whether the concrete core is under pure compression or tension and compression) and the mechanical property of the concrete. However there are different views about the effect of helical yield strength. Foster and Attard (1997) have doubts that the yield strength of lateral confinement affects the level of confinement. On the other hand Muguruma et al. (1990) stated that well confined columns using high strength confinement steel show very high ductility. Also Razvi and Saatcioglu (1994) found that the displacement ductility factor was enhanced by 250% when the yield strength of lateral confinement increased from 328 to 792 MPa. This was for high strength concrete columns (86 to 116 MPa) where the lateral volumetric reinforcement ratio was 4.4 %.

This section examines the effect of helical yield strength on the behaviour of helically confined high strength concrete beams. Figure 6.25 shows the load deflection of the two beams, which have the same concrete compressive strength, longitudinal reinforcement ratio and helical diameter but different helical yield strengths. It was observed that the ultimate deflection increases significantly as the helical yield strength increases. For Beam N12P35-D85 with a concrete

compressive strength of 85 MPa, a longitudinal reinforcement ratio of 0.077 and a helical yield strength of 500 MPa, deflection at 80% of the maximum load could not be reached because of the helical rupture at the welding point, probably due to poor pentration. Figure 6.26 displays the rupture of the helical confinement of Beam N12P35-D85 at the welding point. However the midspan deflection at the load 407 kN which is 93% of the maximum load was 203 mm, but for Beam R12P35-D85 which has the same concrete compressive strength and longitudinal reinforcement ratio and different helical yield strength (310 MPa), the ultimate deflection was 150 mm which is 70% of the deflection of Beam N12P35-D85. It should be noted that the Beam R12P35-D85 suffers from slight buckling at the core. Thus the 150 mm deflection may not represent the exact value for the deflection of Beam R12P35-D85, but the load did not suddenly drop. From Figure 6.25 it must be noted that Beam N12P35-D85 has a midspan deflection higher than R12P35-D85 even though Beam N12P35-D85 recorded a midspan deflection at 93% of the maximum load. It could be concluded that for an over reinforced HSC helically confined beams, increasing the yield strength of helical confinement reinforcement increases the strength as well as the ductility. This is similar conclusion to the experimental study conducted by Cusson and Paultre (1994), where the two different yield strengths of the tie confinement was 392 and 770 MPa. Cusson and Paultre (1994) concluded that increasing the confinement yield strength enhances the strength and toughness in well confined specimens.

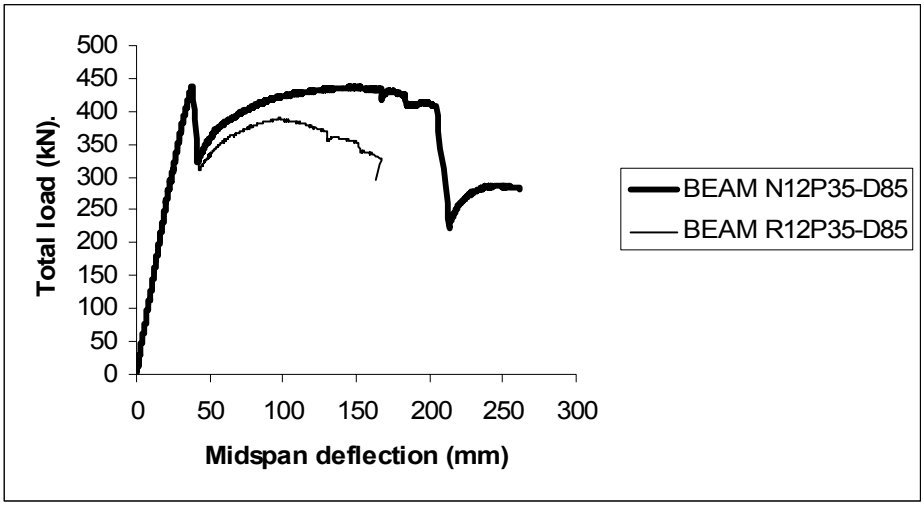

Figure 6.25 Load midspan deflection curve for beam N12P35-D85 and R12P35-D85

Figure 6.26 The rupture of the helical confinement of Beam N12P35-D85 at welding point.

Table 6.11 demonstrates the effect of helical yield strength on the displacement ductility index. It should be noted that as the helical yield strength increases the displacement ductility index increases. However the displacement ductility index is not affected by the yield deflection because the yield deflections for both beams were almost the same. On the other hand, a displacement ductility index was affected by the ultimate deflection whether at helical rupture or 80% of the maximum load. The displacement ductility index for Beams N12P35-D85 was 139% of the displacement ductility index of Beam R12P35-D85 even though the midspan deflection for Beam N12P35-D85 was determined at 93% of the maximum load at the helical rupture (weak welded point).

Table 6.11 - Summary of beam results for Beams N12P35-D85 and R12P35-D85.

SPECIMEN	P_1, (kN)	P_2, (kN)	P_3, (kN)	$0.8P_3$, (kN)	Δ_y, (mm)	$\Delta_{u,0.8}$, (mm)	$\Delta_{u,0.8}/\Delta_y$
N12P35-D85	437	330	437	350	38	203	5.3
R12P35-D85	435	317	435	348	39	150	3.8

P_1 is the load at concrete cover spalling off
P_2 is the load just after spalling off concrete cover
P_3 is the highest load recorded during the test
Δ_y is the yield deflection and
$\Delta_{u,0.8}$ is the deflection at 80% of the maximum load

The load recorded at spalling off the concrete cover for Beams N12P35-D85 and R12P35-D85 was 437 and 435 kN respectively, and the load just after spalling off the concrete cover dropped down to 330 kN and 317 kN, respectively. The

maximum load for beams N12P35-D85 and R12P35-D85 was the load at which the concrete cover spalled off, 437 and 435 kN, respectively. However, it should be noted that for Beam N12P35-D85 the load dropped down to 330 kN and then started to increase as the deflection increased until failure due to helical rupture at the welding point where the maximum load recorded was 436 kN which is equal to the load at which the concrete cover spalled off. The load of Beam R12P35-D85 dropped to 317 kN and then started to increase as the deflection increased until the maximum load was 388 kN, which is 80% of the load at which concrete cover spalled off and then the load started to drop gradually.

The strain measured at the top surface concrete just before spalling off the concrete cover for Beams N12P35-D85 and R12P35-D85 were 0.00315 and 0.0029, respectively which are very similar. The measured strain at 40 mm depth just before spalling off the concrete cover for Beam N12P35-D85 was 0.0018 and the measured strain at 40 mm depth just after spalling off the concrete cover was 0.0031. For Beam R12P35-D85, the measured strain at 40 mm depth just before spalling off the concrete cover was 0.0018 and the measured strain at 40 mm depth just after spalling off the concrete cover was 0.003. Thus for both beams N12P35-D85 and R12P35-D85, the measured strain at 40 mm depth just before spalling off concrete cover was the same 0.0018. Also the measured strain at 40 mm depth just after spalling off concrete cover was the same 0.003. Thus it could be concluded that the helical yield strength has little or no effect on the behaviour of over-

reinforced helically confined beams before or when covers spall off. This also indicates that the helical reinforcement yielded after the cover spalled off. This agrees with Han et al. (2003). Han et al. (2003) found that the transverse reinforcement yields at the descending branch of load-deflection curve after maximum load.

The measured maximum strain at 40 mm depth for beams N12P35-D85 and R12P35-D85 was 0.016 and 0.013, respectively. Figures C.15 and C.16 in Appendix C show the load versus concrete compressive strain at 0, 20 and 40 mm depth from the top surface of the beams N12P35-D85 and R12P35-D85.

6.7 EFFECT OF HELIX DIAMETER

The effect of the helix bar diameter could be studied using Beams R12P35-D85, R10P35-D85 and R8P35-D85 and Table 6.12 summarises their loads and displacement deflection results. Figure 6.27 demonstrates the load deflection of the three beams. These beams have the same concrete compressive strength, longitudinal reinforcement ratio and helical yield strength but different helical diameters. It has been observed that the midspan deflection at 80% of the maximum load increases as the helical diameter increases. For Beam R12P35-D85 with a 12 mm helical diameter and a helical yield strength of 310 MPa, the deflection at 80% of the maximum load was 150 mm. For Beam R10P35-D85 with

a 10 mm helical diameter and 300 MPa helical yield strength, deflection was 104 mm at 80% of the maximum load. For Beam R8P35-D85 with an 8 mm helical diameter and 410 MPa helical yield strength, deflection was 102 mm at 80% of the maximum load. As mentioned above the concrete core of Beam R12P35-D85 buckled to the right side so the 150 mm deflection may not represent the exact value of the deflection for this beam. Beam R10P35-D85 has a midspan deflection of 104 mm at 80% of the maximum load while Beam R10P35-D85 is 234 mm at 70% of the maximum load. Beam R10P35-D85 could have had an experimental error due to compaction of the concrete. However, for comparison purposes the midspan deflection at 80% of the maximum load is considered. Thus the midspan deflection for R12P35-D85 is higher than R10P35-D85. Beam R8P35-D85 has an 8 mm helical diameter and 410 MPa helical yield strength, which is higher than helices in Beams R12P35-D85 and R10P35-D85. However it is possible to study the effect of helix bar diameter through Beams R12P35-D85, R10P35-D85 and R8P35-D85, which had the same nominal yield strength of 250 MPa. The midspan deflection of Beam R8P35-D85 was 102 mm at 80% of the maximum load. From Figure B.19 in Appendix B, the ultimate failure of Beam R8P35-D85 was due to helical rupture at 70% of the maximum load, after which the load suddenly dropped to 23% of the maximum load. Figure 6.28 illustrates the helical rupture of Beam R8P35-D85.

Table 6.12 - Summary of beam results for Beams R8P35-D85, R10P35-D85 and R12P35-D85.

SPECIMEN	P_1, (kN)	P_2, (kN)	P_3, (kN)	$0.8P_3$, (kN)	Δ_y, (mm)	$\Delta_{u,0.8}$, (mm)	$\Delta_{u,0.8}/\Delta_y$
R8P35-D85	418	308	418	334	38	102	2.7
R10P35-D85	403	291	403	322	36	104	2.7
R12P35-D85	435	317	435	348	39	150	3.8

P_1 is the load at concrete cover spalling off
P_2 is the load just after spalling off concrete cover
P_3 is the highest load recorded during the test
Δ_y is the yield deflection and
$\Delta_{u,0.8}$ is the deflection at 80% of the maximum load

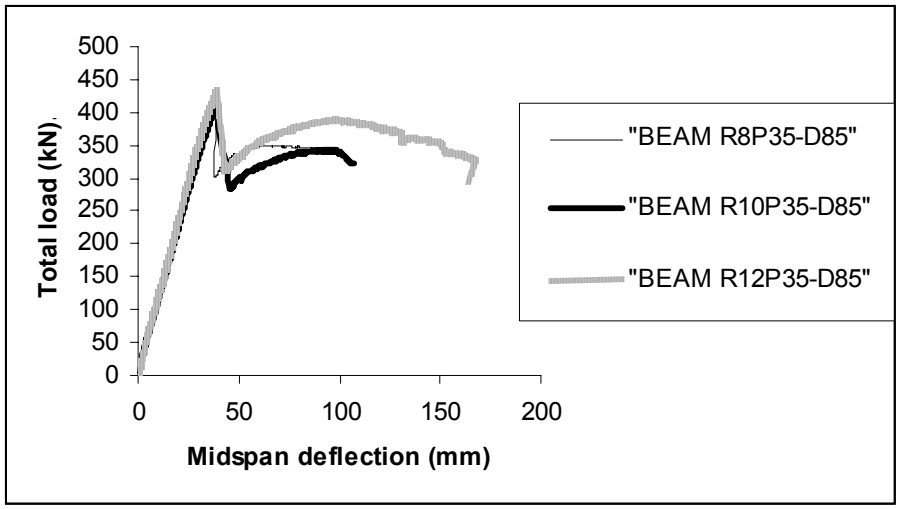

Figure 6.27 Load-midspan deflection curves for beams R12P35-D85, R10P35-D85 and R8P35-D85

Figure 6.28 The rupture of the helical confinement of Beam R8P35-D85

The recorded load at spalling off the concrete cover for Beams R12P35-D85, R10P35-D85 and R8P35-D85 was 435, 403 and 418 kN, respectively and the load just after spalling off the concrete cover dropped to 317, 291 and 308 kN, respectively. The maximum load for Beams R12P35-D85, R10P35-D85 and R8P35-D85 was that at which the concrete cover spalled off 435, 403 and 418 kN, respectively. However, it is to be noted that the load at which the cover spalled off Beam R10P35-D85 is less than for Beam R8P35-D85, which is incorrect because it should be greater. The spalling off load of Beam N10P35-D85 should be in the range 418-435 kN. Thus Beam R10P35-D85 could have some experimental error due to concrete compaction or other reasons. In conclusion, the helical diameter has a significant effect on the concrete cover spalling off load of helically confined

high strength concrete beams. Generally a well-confined beam could resist loads higher than that at which the concrete cover spalls off. A well-confined beam is defined as the beam with a well-confined compression zone using a suitable helical pitch, helical yield strength, and helical diameter. Figure 6.29 illustrates disintegration of the confined core of Beam R8P35-D85 and Figure 6.30 shows the strong confined core of Beams R12P35-D85 and N12P35-D85 where Beam N12P35-D85 has a strong confined concrete core. The only problem with Beam N12P35-D85 was the early helical rupture at the weak welding point.

Figure 6.29 Disintegration of the confined core of Beam R8P35-D85

Figure 6.30 The confined core of Beams N12P35-D85 and R12P35-D85

The strain measured on the top surface just before the concrete cover spalled off for Beams R12P35-D85, R10P35-D85 and R8P35-D85 was 0.0029, 0.003 and 0.003, respectively, which is very close. The strain measured at 40 mm deep just before the concrete cover spalled off for Beam R12P35-D85 was 0.0018 and 0.003 just after. For Beam R10P35-D85, the strain measured at 40 mm deep just before the cover spalled off was 0.0018 and 0.0036 just after. For Beam R8P35-D85, the strain measured at 40 mm deep just before the cover spalled off was 0.0017 and 0.0029 just after.

Thus for Beams R12P35-D85, R10P35-D85 and R8P35-D85, the strain measured was slightly different. Also there were differences in the strain 40 mm deep just after the cover spalled off. It could be concluded that helical diameter affects over-reinforced helically confined beams before and after spalling off the concrete cover. This conclusion differs from the influence of helical yield strength studied earlier. However, the effect of the helical pitch is higher than the helical diameter.

Figures C.17, C.18 and C.19 in Appendix C show the load versus concrete compressive strain at 0, 20 and 40 mm depth from the top surface of the three beams with a different helical diameter. The measured maximum strain at 40 mm depth was recorded for Beams R12P35-D85, R10P35-D85 and R8P35-D85 as 0.013, 0.015 and 0.015, respectively. No further results could be obtained because the strain gauges failed.

Over-reinforced concrete beams behave differently than over-reinforced helically confined HSC beams. The test results of this study proved that the ductility of over-reinforced helically confined HSC beams were significantly enhanced. As the behaviour of an over-reinforced beam differs from an over-reinforced helically confined HSC beam so its analysis and design processes are also different. Thus to design over-reinforced helically confined HSC beams raises three issues. The first is the concrete cover spalling off phenomenon, the second is the stress block

parameters and the third is the enhanced confined concrete strength. Chapter 7 discusses these issues in detail.

The strength of confined concrete differs from the concrete cover and the rest of the beam. Based on this the behaviour of over-reinforced helically confined HSC beams could be non-linear. So it is difficult to predict the moment capacity of the beams using the internal resisting couple through strain compatibility.

6.8 STRENGTH AND DUCTILITY ENHANCEMENT

Installing helical confinement in the compression zone of beams enhances their strength and ductility by providing a longitudinal reinforcement ratio (ρ) more than the maximum longitudinal reinforcement ratio (ρ_{max}).

Codes of practice such as AS3600 (2001) and ACI 318R-02 (2002) do not allow for design of over-reinforced beams, because they fail in a brittle way where safety is the main concern. In this study, Beam 0P0-E85 was designed to be just into the over-reinforced section, where the longitudinal reinforcement ratio (ρ) is 0.036 and the maximum longitudinal reinforcement ratio (ρ_{max}) is 0.035 as specified by Australian standred AS3600 (2001). As such ρ/ρ_{max} was equal to 1.04. Beam failure was brittle when the load suddenly dropped from 292 kN to 26 kN. Figure 6.31 illustrates the load deflection of Beam 0P0-E85. Table 6.13 demonstrates that a comparison of strength between Beam 0P0-E85 which is just into the over

reinforced section and Beams N12P35-D85, R12P35-D85, R10P35-D85 and R8P35-D85, which are over-reinforced concrete sections, where ρ/ρ_{max} is 2.65. It has been found that the strength of Beams N12P35-D85, R12P35-D85 was 1.5 times Beam 0P0-E85 and Beam R10P35-D85 and Beam R8P35-D85 were 1.4 times stronger than Beam 0P0-E85. This increase in strength is accompanied by an increase in the displacement ductility. It is important to keep in mind that the displacement deflection of Beams N12P35-D85, R12P35-D85 and R10P35-D85 are not representative of the actual values because of the rupture mentioned above. The actual values are higher than the recorded ones. However, the relative values in Table 6.13 show the significant role of helical confinement in enhancing the strength as well as ductility.

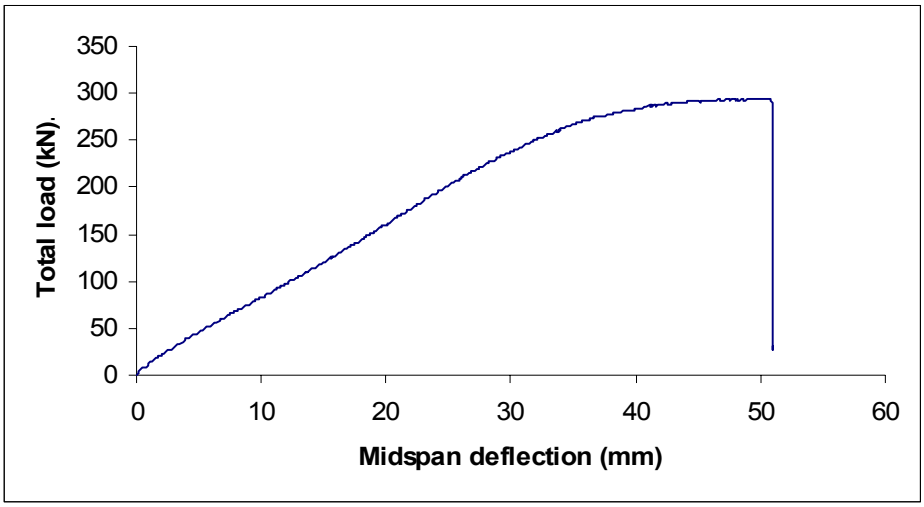

Figure 6.31 Load-midspan deflection curves for Beams 0P0-E85

Table 6.13. Effect of installing helical confinement on the strength and the displacement ductility factor.

SPECIMEN	Maximum load, kN	Relative value	Displacement ductility factor	Relative value
N12P35-D85	437	1.5	5.3	5.3
R12P35-D85	435	1.5	3.8	3.8
R10P35-D85	403	1.4	2.7	2.7
R8P35-D85	418	1.4	2.7	2.7
0P0-E85	292	1.0	1.0	1.0

6.9 SUMMARY

In this chapter, the experimental results of over-reinforced HSC helically confined beams are presented and analysed as tables and figures. The summary of load deflection and load strains is available as tables within this chapter. The figures of load deflection and load strains are enclosed in Appendices B and C, where these figures were obtained from the experimental results recorded. In other words the figures of Appendices B and C represent the whole data recorded from the beginning and end of each test for each beam. The effects of helical pitch, helical yield strength, helical diameter, tensile reinforcement ratio and compressive strength on the behaviour of over-reinforced HSC helically confined beams were examined. Each variable was examined alone by comparing the beam results (load-deflection and load-strains).

The next chapter presents a method for predicting the flexure strength capacity of over-reinforced helically confined HSC beams.

CHAPTER 7

PREDICTING FLEXURE STRENGTH OF OVER REINFORCED HELICALLY CONFINED HSC BEAMS

7.1 GENERAL

The use of an over-reinforced concrete beam is vital when the beam is under extreme loads or when there is a restriction on beam size. In these circumstances, the code of practice allows the use of over-reinforced concrete beams with strict conditions. In regards to safety, these conditions are applied to predict and design the flexural strength capacity of over-reinforced concrete beams. There is potential for discovering efficient ways of enhancing the ductility of over-reinforced concrete beams with economic advantages. However, installing helical confinement in the compression zone significantly enhances ductility. Nevertheless, predicting the flexural capacity of over-reinforced helically confined HSC beams is difficult. This is due to complexities such as enhanced concrete compressive strength, confined compressive strain and the concrete cover spalling off phenomenon. This chapter addresses these factors.

7.2 AS3600 (2001) RECOMMENDATION FOR OVER REINFORCED CONCRETE BEAMS

With over-reinforced concrete beams the tensile steel is generally in the elastic region even though the ultimate flexural strength is reached. Thus the AS3600 (2001) procedure for predicting flexural strength of over-reinforced concrete beams does not consider the yield strength of steel because longitudinal reinforcement steel never yields. The strength reduction factor (ϕ) is considered in the procedure for predicting flexural strength of over-reinforced concrete beams because they fail suddenly, without warning (compression failure). The strength reduction factor has different values in different codes of practice, for example ACI318-02 (2002) recommends that it be 0.9 for a tension controlled section but AS3600 (2001) recommends 0.8. The value of the strength reduction factor depends on the level of warning (mode of failure). Under-reinforced concrete beams have the highest strength reduction factor because they fail in a ductile manner when the tension steel yields. ACI318-02 (2002) has suggested that the strength reduction factor for tension controlled sections be 0.9 and 0.65 for compression controlled sections.

This section examines the prediction of strength capacity of over-reinforced helically confined HSC beams based on neglecting the effect of the helical confinement and using the strength reduction factor as recommended by Clause 8.1.3 (c) of AS 3600 (2001). The strength reduction factor depends on the neutral

axis parameter (K_u). If $K_u \leq 0.4$, then ϕ is 0.8 and if $K_u > 0.4$, then ϕ is equal to $0.8M_{ud}/M_u \geq 0.6$. Where M_{ud} is the reduced ultimate strength in bending, M_u is the ultimate strength in bending. M_{ud} is calculated by assuming that the concrete strain at the extreme compression fibre is 0.003 and K_u is equal to 0.4. The steps for calculating moment capacity of an over-reinforced section using AS3600 (2001) are explained in Section D.1 of Appendix D. Also, Table D.1 demonstrates the calculated strength reduction factor.

Table 7.1 displays the comparison between the calculated bending moment according to the AS 3600 (2001) recommendation, and the experimental moment for confined beams. It has to be noted that the experimental moment is significantly higher than the calculated moment capacity by 30% to 60%. The difference depends on variables helical confinement, the concrete compressive strength and the longitudinal reinforcement ratio. However, the ductility of these beams was significantly enhanced because of the helical confinement installed in the compression zone with an effective pitch at the mid span of the beam. It has to be noted that using the AS 3600 (2001) recommendation for predicting the flexure strength capacity of over reinforced helically confined HSC beams is safe but not economic because the AS 3600 (2001) recommendation is based on the behaviour of over-reinforced beams without helical confinement, where there is lack of ductility. It is uneconomical to predict the flexure strength capacity of over-reinforced helically confined HSC beams using the AS 3600 (2001)

recommendation unmodified because over-reinforced beams behave differently than over-reinforced helically confined HSC beams. Once the ductility of an over-reinforced beam is improved by installing helical confinement in the compression zone then there is a need to improve the predictive method to minimise the differences between the experimental and predicted results. The test results of this study proved that the ductility of over-reinforced helically confined HSC beams was significantly enhanced. As the behaviour of an over-reinforced beam differs from an over-reinforced helically confined HSC beams so their design processes are also different. Thus there is a need to develop a simple method with an appropriate assumption for predicting the flexural strength capacity of over-reinforced helically confined HSC beams.

Using AS3600 (2001) to predict the flexural strength of over-reinforced helically confined HSC beams raises three issues. First is concrete cover spalling off phenomenon, Second is the stress block parameters and third the enhanced confined concrete strength. The next sections discuss these issues.

Table 7.1 – Comparison between calculated and experimental moment

SPECIMEN	K_u	M_{cal} (kN.m)	M_{exp} (kN.m)	M_{exp}/ M_{cal}
R12P25-A105	0.562	176.6	246.6	1.40
R12P50-A105	0.562	176.6	229.8	1.30
R12P75-A105	0.562	176.6	231.6	1.31
N8P25-A80	0.608	143.0	207	1.45
N8P50-A80	0.608	143.0	194.4	1.36
R10P35-B72	0.616	135.5	217.8	1.61
R10P35-B83	0.591	151.5	223.2	1.47
R10P35-B95	0.568	168.2	214.2	1.27
R10P35-C95	0.530	159.2	219	1.38
R10P35-D95	0.599	175.1	247.2	1.41
N12P35-D85	0.618	160.4	262.2	1.63
R12P35-D85	0.618	160.4	261	1.63
R10P35-D85	0.618	160.4	241.8	1.51
R8P35-D85	0.618	160.4	250.8	1.56

K_u is the neutral axis parameter
M_{cal} is the calculated moment
M_{exp} is the experimental moment

7.3 THE EFFECT OF SPALLING OFF THE CONCRETE COVER

The experimental results proved that helical reinforcement in the compression region of over-reinforced beams enhances their ductility significantly. It is encouraging not to be restricted by the maximum longitudinal reinforcement ratio. The issue of spalling off the concrete cover affects the prediction the moment capacity of helically confined beams using AS3600 (2001). However, there is no satisfactory answer to why and when the concrete cover spalls off. Cusson and Paultre (1994) suggested that for confined HSC columns, the concrete cover should be excluded when calculating the axial compression strength. Ziara et al. (2000)

predicted the moment capacity without considering the concrete cover. Also Elbasha and Hadi (2004) and Hadi and Elbasha (2004) predicted the moment capacity for over-reinforced helically confined HSC beams without considering the concrete cover. Based on these previous studies, this study similarly neglects the concrete cover when modifying the code equations of AS3600 (2001).

For well-confined over-reinforced helically confined HSC beams, the second peak load after the concrete cover has spalled off is greater than the first peak load. For example Beam R12P25-A105 with a 25 mm helical pitch, the second peak load was 9% higher than the first peak load and for Beam N8P25-A80 with a 25 mm helical pitch the second peak load was 14% higher than the first peak load. Cusson and Paultre (1994) and Razvi and Saatcioglu (1994) conclude that for well-confined HSC columns, the second peak load is approximately equal to the first. Thus one could consider the differences between the first and second peak loads to be insignificant. Most of the literature such as Mansur et al. (1997), Foster and Attard (1997), Pessiki and Pieroni (1997) and Ziara et al. (2000) compared predicted strength with the experimental ultimate strength (whatever was maximum, the first or the second peak). Thus one could design an over-reinforced helically confined HSC beam to reach its maximum load regardless of the spalling off the concrete cover phenomenon. However, the confined strain is enhanced significantly for over-reinforced helically confined HSC beams. Then for predicting

flexural strength of over-reinforced helically confined HSC beams one must consider confined strain rather than the 0.003 which is used for normal design.

7.4 STRESS BLOCK PARAMETERS

The rectangular stress block was introduced by Hongnestad et al. (1955). There is on going research to study rectangular stress block parameters to predict the strength capacity as close as possible to the experimental results. Figure 7.1 demonstrates the distribution of concrete stress at ultimate load. The rectangular stress block is defined by two parameters, γ (ratio of the depth of the assumed rectangular compressive stress block to $K_u d$) and α (the intensity of the equivalent stress block factor). γ and α were developed based on the experimental results. These parameters have either fixed values or are calculated using empirical formulas. However there is no agreement between researchers about a certain value of γ or α. Also there are different values of γ and α in different code provisions. Table 7.2(a) shows the different values of γ and α in the different code provisions and Table 7.2(b) shows different values of γ and α reported in the literature. However, the calculated moments using the values of γ and α of CEB-FIP-1990 (1990) are the closest moments to experimental moments. Thus the stress block parameters γ and α of CEB-FIP-1990 (1990) are adopted for predicting the flexure capacity of over-reinforced helically confined HSC beams.

It must be noted that predicting flexural strength of beams is significantly affected by the parameter (α) but is unaffected by the parameter (γ). The parameter (γ) is only used to determine the location of the neutral axis and then to determine the longitudinal reinforcement strain.

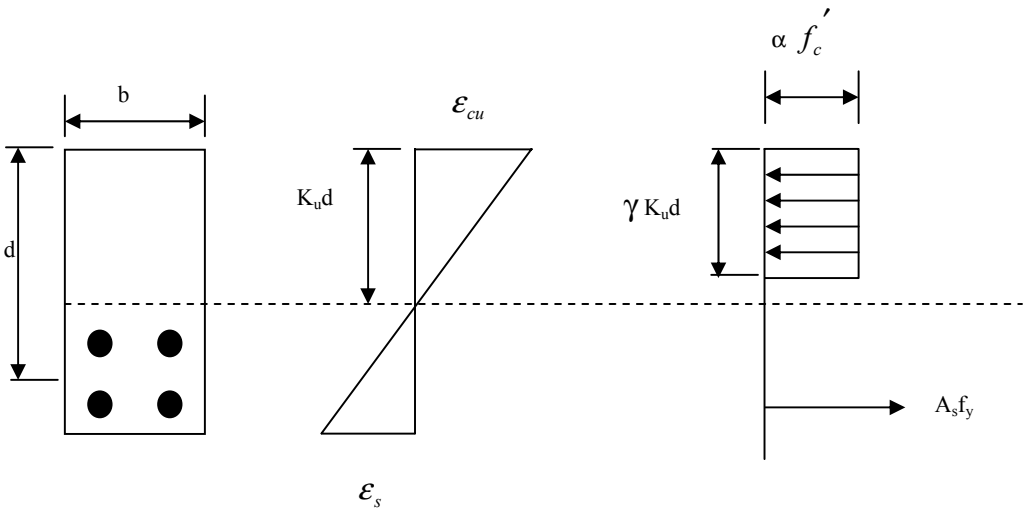

Figure 7.1 Rectangular stress block

Table 7.2(a)- Concrete stress block parameters in different codes provisions

Please see print copy for Table 7.2 (a)

Table 7.2(b)- Concrete stress block parameters in different literature

Please see print copy for Table 7.2 (b)

The limiting confined compressive strain is considered for predicting the longitudinal reinforcement strain of over-reinforced helically confined HSC beams rather than the 0.003 used for normal design. When the longitudinal steel strain of over-reinforced helically confined HSC beam is greater than the yield strain, then the beam is ductile and the flexural capacity could be predicted as proposed in this thesis. However if the longitudinal steel strain of the over-reinforced helically confined HSC beam is less than the yield strain, then the failure of the beam is brittle and the flexural capacity could be predicted by using equations from the codes of practice. The model proposed by the Kaar et al. (1977) presented in Chapter 3 in Equation 3.18 is modified to predict the confined compressive strain (ε_{con}). It has to be noted that the confined compressive strain predicted by the Kaar et al. (1977) model is more than 0.003 even though the effect of confinement is negligible. Thus the Kaar et al. (1977) model needs to be modified to satisfy the condition that confinement is negligible when the helical pitch is greater than 70% of the concrete core diameter.

Equation 7.1 is a modified equation which could be used to predict the confined concrete compressive strain (ε_{con}) of over-reinforced helically confined HSC beams. This equation needs verification with a considerable amount of experimental data. The confined compressive strains presented in this study do not represent the real value because the embedment gauge failed early. The embedment

gauge cannot resist high beam deflection which is where most embedment gauges broke during the test. Thus to gain good confined compressive strain results using similar quality embedment gauges the size of the beam must be reduced. If a full size beam is desired then the embedment gauges must be made from flexible material like plastic, that does not break under deflection. However the confined compressive strain predicted by Equation 7.1 is used in the stress block instead of the 0.003 strain recommended by most codes of practice. Confined compressive strain determines whether the tension steel strain is greater than the yield strain.

$$\varepsilon_{con} = 0.003 + \left(\frac{\rho_h f_{yh}}{50}\right)^2 \left(0.7 - \frac{S}{D}\right) \qquad (7.1)$$

Where ρ_h is the volumetric helical reinforcement steel ratio and f_{yh} is the helical steel yield stress expressed in MPa; D is the diameter of the confined core and S is the helical pitch.

7.5 MODELS FOR PREDICTING THE ENHANCED STRENGTH OF CONFINED CONCRETE

Most of research carried out on confinement of the compression zone in beams is based on research done on columns, because the idea of a confined compression zone in beams has only recently been developed. There is a need to use the column

models for comparison purposes because no model had been developed for helically confined beams. The helical confinement enhancements of the compressive strength of concrete can be expressed as ($K_s f_c'$) where K_s is the strength gain factor and f_c' is the concrete compressive strength. K_s depends on many variables such as the helical pitch, the diameter and characteristics of steel used for helical confinement. In this study five models for predicting the strength gain factor are examined. These models were developed by Ahmad and Shah (1982), Martinez et al. (1984), Mander et al. (1984), Issa and Tobaa (1994), and Bing et al. (2001), and are presented in Chapter 4. All these models were developed based on variables such as spiral spacing, spiral volumetric ratio and core diameter. However, the difference between models' prediction comes through different the relationship between the variables. For example the Martinez et al. (1984) model was based on the observation that confinement is negligible when the spacing between the spirals is equal to the diameter of confinement. That is different from Ahmad and Shah (1982) who neglected confinement when the spiral pitch exceeded 1.25 times the diameter of the confined core. Also the difference between the models' prediction comes through the coefficients obtained from regression analysis of particular experimental results. Sakai and Sheikh (1989) stated, "Predictions from various models differ significantly because different sets of variables are considered in different models".

7.6 MODELS COMPARISON

A comparison between the five models is between the predicted moment capacities using the strength gain factor with the experimental moment capacity of the beams tested. There is a general agreement about which variables affect the confined concrete strength, but a disagreement about the magnitude of the increased strength. Tables 7.3, 7.4, 7.5, 7.6 and 7.7 show different magnitudes of strength gain factor by using the different models. The accumulative difference between the experimental and the calculated bending moments using Ahmad and Shah (1982), Martinez et al. (1984), Mander et al. (1984), Issa and Tobaa (1994), and Bing et al. (2001) models by applying AS3600 (2001) was -31%, 1%, 28%, -9% and 20%, respectively. These results show that the difference between experimental and predicted moment is high. However, the model by Martinez et al. (1984) for predicting compressive strength of confined concrete gave better results when compared with the other models. It is important to note that comparing the models is a result of comparing predicted moment capacities using proposed stress block parameters and those models used to predict the strength gain factor. The purpose of the comparison is to choose the model that gives results that are close to the test results.

TABLE 7.3– Summary of using Ahmad and Shah (1982) Model to predict strength gain factor, which is used for calculating the moment capacity

Please see print copy for Table 7.3

Cumulative difference between experimental and calculated moment as a percentage for the 19 beams)

$$= \sum \frac{(M_{test} - M_{cal})}{M_{test}} = -31\%$$

D* is the Difference between experimental and calculated moment as a percentage

TABLE 7.4– Summary of using Martinez et al. (1984) Model to predict strength gain factor, which is used for calculating the moment capacity

Please see print copy for Table 7.4

Cumulative difference between experimental and calculated moment as a percentage for the 19 beams)

$$= \sum \frac{(M_{test} - M_{cal})}{M_{test}} = 1\%$$

D* is the Difference between experimental and calculated moment as a percentage

TABLE 7.5– Summary of using Mander et al. (1984) Model to predict strength gain factor, which is used for calculating the moment capacity

Please see print copy for Table 7.5

Cumulative difference between experimental and calculated moment as a percentage for the 19 beams)

$$= \sum \frac{(M_{test} - M_{cal})}{M_{test}} = 28\%$$

D* is the Difference between experimental and calculated moment as a percentage

TABLE 7.6 – Summary of using Issa and Tobaa (1994) Model to predict strength gain factor, which is used for calculating the moment capacity

Please see print copy for Table 7.6

Cumulative difference between experimental and calculated moment as a percentage for the 19 beams)

$$= \sum \frac{(M_{test} - M_{cal})}{M_{test}} = \text{-9\%}$$

D* is the Difference between experimental and calculated moment as a percentage

TABLE 7.7 – Summary of using Bing et al. (2001) Model to predict strength gain factor, which is used for calculating the moment capacity

Please see print copy for Table 7.7

Cumulative difference between experimental and calculated moment as a percentage for the 19 beams)

$$= \sum \frac{(M_{test} - M_{cal})}{M_{test}} = 20\%$$

D* is the Difference between experimental and calculated moment as a percentage

7.7 A NEW MODEL

From Tables 7.3-7.7 it has to be noted that is possible to gain an acceptable prediction of the moment capacity of helically confined beams by using the proposed stress block parameters, while considering confinement, to predict the strength gain factor using Martinez et al. (1984) model. However there is a need to modify this model according to where the experimental results of over-reinforced helically confined HSC beams are, where confinement is negligible when the helical pitch is greater than or equal to 0.7 times the diameter of the confined core. The effectiveness of helical confinement of columns is different from beams because the column confinement is usually throughout, whereas its limited to the upper portion of the cross section of the beam (short depth). Thus a new model to predict the strength gain factor for over-reinforced helically confined HSC beams is proposed as follows.

$$f_{cc} = f_c^{'} + 4f_2\left(0.7 - \frac{S}{D}\right) \qquad (7.2)$$

Where f_2 is the confinement stress, $f_2 = 2A_h f_{yh} / DS$; f_{cc} is the enhanced compressive strength of over-reinforced helically confined HSC beams; $f_c^{'}$ is the compressive strength of the concrete; D is the diameter of the confined core; S is

the helical pitch; f_{yh} is the yield strength of the helical steel and A_h is the area of helical steel.

Table 7.8 shows a comparison between the experimental and the calculated moments using a proposed new model (achieved by modifying the Martinez et al. (1984) model) to predict the strength gain factor for the 15 beams (where the helical pitch is less than or equal to 0.7 times the diameter of the confined core). The cumulative difference between the experimental and the predicted moment as a percentage for the 15 beams, $D_1 = \sum \frac{(M_{test} - M_{cal})}{M_{test}} = -7$. Also the average difference between the experimental and the predicted moments as a percentage, $D_2 = -0.46\%$. Table 7.9 shows the comparison between the experimental and the calculated moments using Martinez et al. (1984) model to predict the strength gain factor for the 15 beams (where the helical pitch is less than or equal to 0.7 of the diameter of the confined core). The cumulative difference between the experimental and the predicted moment as a percentage for the 15 beams, $D_1 = \sum \frac{(M_{test} - M_{cal})}{M_{test}} = -17$. Also the average difference between the experimental and the predicted moment as a percentage, $D_2 = -1.13\%$.

Table 7.8 demonstrates a good agreement between the calculated and the experimental results. It is therefore concluded that Equation 7.2 could be used to

predict the strength gain factor for high strength concrete beams confined with helix (short depth). Section D.2 in Appendix D demonstrates the whole process of predicting the moment capacity for over-reinforced helically confined HSC beams using Beam R12P50-A105 as a prototype example.

In conclusion, improving the prediction of moment capacity could be achieved by considering the code equations but neglecting the concrete cover as well as modifying Martinez et al. (1984) model. Modifications to their model are based on the experimental results of this research. The test results proved that the behaviour of an over-reinforced helically confined HSC beam is dissimilar to over-reinforced concrete beams. The over-reinforced helically confined HSC beams fail in a ductile mode. The significant improvements to ductility by helical confinement in the compression zone and the predictive process presented in this chapter encourage taking the strength redaction factor as 0.9 when designing over-reinforced helically confined HSC beams. This is based on the ACI318-02 (2002) recommendation that the strength reduction factor for tension control section is 0.9.

TABLE 7.8 – Summary of using modified Martinez et al. (1984) Model to predict strength gain factor, which is used for calculating the moment capacity

Please see print copy for Table 7.8

Cumulative difference between experimental and calculated moment as a percentage for the 15 beams)

$= \sum \frac{(M_{test} - M_{cal})}{M_{test}} =$ -7%, when delete the 4 beams

D* is the Difference between experimental and calculated moment as a percentage

TABLE 7.9– Summary of using Martinez et al. (1984) Model to predict strength gain factor, which is used for calculating the moment capacity

Please see print copy for Table 7.9

Cumulative difference between experimental and calculated moment as a percentage for the 15 beams)

$$= \sum \frac{(M_{test} - M_{cal})}{M_{test}} = \text{-17\%},$$

D* is the Difference between experimental and calculated moment as a percentage

7.8 SUMMARY

In this chapter, the AS3600 (2001) recommendation of over-reinforced concrete beams are presented and the effect of the spalling off the concrete cover on predicting the flexure strength of over-reinforced helically confined HSC beams is discussed. The stress block parameters have been chosen to predict the flexural strength of over-reinforced helically confined HSC beams. The enhanced strength of confined concrete was predicted using five different models and the model, which give results closest to the experimental results, was modified. A new model is proposed based on the effectiveness of helical confinement. A summary of the predicted moment capacities compared to the experimental moment capacities are presented in this chapter as tables. The process of calculating and predicting the flexure strength of over-reinforced helically confined HSC beams are available in Appendix D. The next chapter presents a model to predict the displacement ductility factor of over-reinforced helically confined HSC beams.

CHAPTER 8

PREDICTING DISPLACEMENT DUCTILITY INDEX

8.1 GENERAL

The experimental programme of this study has proven that helices confinement provided in the compression zone of over-reinforced HSC beams improves their ductility, the progression of this concept into the engineering industry should be considered. According to the codes of practice, there is a limit to the ratio of longitudinal reinforcement for a particular cross section. However more longitudinal reinforcement can be installed if the flexural strength required is more than the capacity of a particular cross section, where such a section becomes under-reinforced rather than over-reinforced section. It is basic knowledge that over-reinforced sections fail in a brittle mode but installing helical reinforcement with a suitable pitch in the compression zone will reduce this unwanted effect.

Formulating the displacement ductility index for an over-reinforced helically confined HSC beam is required to study and focus on non-dimensional factors. The relationship between displacement ductility index and non-dimensional factors involves a large number of variables, most of which are related to helical confinement. The behaviour of over-reinforced helically confined HSC beams is

complex and therefore numerous variables must be investigated to develop an empirical formula.

The development of a model to predict displacement ductility index of over-reinforced helically confined HSC beams is presented in this chapter. The displacement ductility index is affected by variables such as the volumetric ratio of helical reinforcement, helical pitch and helical yield strength. The results obtained from this model are compared with the experimental results.

8.2 DUCTILITY

Ductility is an important property of structural members as it ensures that large deflections will occur during overload conditions prior to the failure of the structure. A large deflection warns of the nearness of failure. Ductility is a very important design requirement for structures subjected to earthquake loading. It could be estimated by the displacement ductility factor, which is defined as the ratio of deflection at ultimate load to the deflection when the tensile steel yields. Measuring displacement ductility of confined concrete is important, especially for high strength concrete beams confined with helical reinforcement. Thus there is a need to develop a model to predict the displacement ductility of over-reinforced helically confined HSC beams. This developed model is to be based on

experimental results from realistic sized over-reinforced helically confined HSC beams.

8.3 DEVELOPMENT OF A MODEL TO PREDICT THE DISPLACEMENT DUCTILITY

The experimental results (full scale beams presented in this study) were used to obtain an analytical description for predicting the displacement ductility index. Several variables such as helical reinforcement ratio, concrete compressive strength, longitudinal reinforcement ratio, helical yield strength and helical pitch were considered. However, the relationship between the displacement ductility and the non-dimensional ratios ($\frac{\rho_h f_{yh}}{f_c'}$), ($\frac{\rho}{\rho_{\max}}$) and ($0.7-\frac{S}{D}$) can be expressed as follows:

$$\mu_d = 1 + \mathrm{f}\left(\left(\frac{\rho_h f_{yh}}{f_c'}\right), \left(\frac{\rho}{\rho_{\max}}\right), \left(0.7-\frac{S}{D}\right)\right) \qquad (8.1)$$

where ρ_h is the total volumetric ratio of helices; f_c' is the concrete compressive strength; f_{yh} is the yield stress of helical reinforcement; ρ_{max} is the maximum allowable tensile reinforcement; ρ is the longitudinal reinforcement ratio; D is the diameter of the confined core and S is the helical pitch.

8.3.1 Effect of $\frac{\rho_h f_{yh}}{f_c'}$

Razvi and Saatcioglu (1994) and Sugano et al. (1990) reported correlation between the non-dimensional parameter $\frac{\rho_h f_{yh}}{f_c'}$ and the displacement ductility of HSC columns. This parameter can be used to indicate the level of displacement ductility of over-reinforced helically confined HSC beams. However, Ahmad and Shah (1982), Naaman et al. (1986), Leslie et al. (1976), Tognon et al. (1980) and Shuaib and Batts (1991) showed that concrete compressive strength has no effect on the ductility of reinforced concrete beams. Some authors indicate that as the concrete compressive strength increases, the displacement ductility index decreases but others showed the converse relation to be true. The experimental results presented in Chapter 6 proved that the displacement ductility index increases as the helical reinforcement ratio increases and as the helical yield strength increases, but the displacement ductility index decreases as the concrete compressive strength increases. In other words the displacement ductility index increases as the $\frac{\rho_h f_{yh}}{f_c'}$ increases. Thus the non-dimensional parameter $\frac{\rho_h f_{yh}}{f_c'}$ is an important parameter to be included in the model for predicting the displacement ductility of over-reinforced helically confined HSC beams.

8.3.2 Effect of $\frac{\rho}{\rho_{\max}}$

$\frac{\rho}{\rho_{\max}}$ is a major factor in determining whether a beam is an under or over-reinforced section. Also $\frac{\rho}{\rho_{\max}}$ could be used to indicate the flexural ductility of a beam section. It is well known that, for under-reinforced concrete beams the displacement ductility index decreases as $\frac{\rho}{\rho_{\max}}$ increases. Thus the non-dimensional parameter $\frac{\rho}{\rho_{\max}}$ could be used for predicting the displacement ductility. Suzuki et al. (1996) proposed a model, Equation 3.15 in Chapter 3 to predict beam's ductility. This model is a function in $\frac{\rho}{\rho_b}$ only.

Kwan et al. (2004) proposed a model to predict the beam flexural ductility and one of the main parameters used is $\frac{\rho}{\rho_{\max}}$. Kwan et al. (2004) model is as follows:

$$\mu = 10.7(\lambda)^{-1.25}(f_{co})^{-0.45}(f_{yt}/460)^{-0.25}(1+95.2(f_{co}))^{-1.1}\left((f_{yc}\rho_c)/(f_{yt}\rho_t)\right)^3 \quad (8.2)$$

where λ is the degree of beam sections being under or over-reinforced. λ may be measured in terms of the tension to the balanced steel ratio, as given below:

$$\lambda = \frac{\rho_t}{\rho_{bo}}$$

However, for doubly reinforced sections with equal tension and compression steel yield strengths, λ should be evaluated as:

$$\lambda = \frac{(\rho_t - \rho_c)}{\rho_{bo}}$$

while in the case of a doubly reinforced section with unequal tension and compression steel yield strengths, λ should be evaluated as:

$$\lambda = \frac{\left(\rho_t - \left(f_{yc} / f_{yt}\right)\rho_c\right)}{\rho_{bo}}$$

Where λ is the degree of beam section being under or over-reinforced; ρ_b, ρ_{bo} are the balanced steel ratio of beam section with and without compression steel; ρ_c, ρ_t are the compression steel ratio and tension steel ratio; f_{yc}, f_{yt} are the yield strength of compression and tension steel reinforcement.

Shehata and Shehata (1996) and Pastor (1984) stated that the effect of confinement is negligible for under-reinforced concrete beams. However for well confined over reinforced concrete beams, the concrete core is strong, which enhances the ultimate

confined concrete strain and allows the longitudinal reinforcement to yield. It has been noted that if the longitudinal reinforcement ratio increases, the load strength capacity increases. Also the interval between ultimate deflection (ultimate mid-span deflection at 80% of the maximum load) and yield deflection increases as the longitudinal reinforcement ratio increases. In other words for well-confined beams, the displacement ductility increases as the reinforcement ratio increases up to a certain point (Hadi and Elbasha, 2005). It has been found through the experimental programme presented in Chapter 6 that the displacement ductility increases as reinforcement ratio increases. This result is based on testing three over-reinforced helically confined HSC beams with different reinforcement ratios. The $\frac{\rho}{\rho_{max}}$ for three tested beams was 1.4, 1.75 and 2.09.

8.3.3 Effect of $(0.7-\frac{S}{D})$

The last parameter in the displacement ductility model is $(0.7-\frac{S}{D})$. The effect of this parameter is developed based on the test results of over-reinforced helically confined HSC beams presented in Chapter 6. The effect of the helical pitch on the displacement ductility index is significant because it affects the distribution of confinement pressure. The experimental results presented in this research confirm the significant effect of helix pitch on the displacement ductility index for over-

reinforced helically confined HSC beams. This parameter shows how decreasing the helical pitch increases the effectiveness of helical confinement. Also $(0.7-\frac{S}{D})$ indicates that helical confinement is negligible when the helical pitch is 70% of the confined concrete core diameter.

8.4 AN ANALYTICAL ANALYSIS OF DISPLACEMENT DUCTILITY

The analytical analysis is based on the experimental results presented in Chapter 6. Table 8.1 shows the 14 beams which were used for regression analysis. However, the other five over-reinforced helically confined HSC beams were excluded from this regression analysis. Four of the excluded beams (12HP100, 12HP160, 8HP100 and 8HP160) have helical confinement with negligible effect. As such the result of these beams are not applicable for regression analysis. The fifth excluded beam, N8P75-A80 had experimental errors as explained in Chapter 6. Excluding these beams could improve the correlation between the predicted and experimental results.

Table 8.1 Experimental data used for regression analysis

Specimen	f_c' ,MPa	f_{yh} ,MPa	d , mm	S ,mm	ρ_h	ρ/ρmax	μd
R12P25-A105	105	310	12	25	0.120	1.47	7.7
R12P50-A105	105	310	12	50	0.060	1.47	4.3
R12P75-A105	105	310	12	75	0.040	1.47	1.3
N8P25-A80	80	500	8	25	0.054	1.94	6.5
N8P50-A80	80	500	8	50	0.0268	1.94	2.9
R10P35-B72	72	300	10	35	0.060	2.30	6.5
R10P35-B83	83	300	10	35	0.060	2.0	5.8
R10P35-B95	95	300	10	35	0.060	1.75	5.3
R10P35-C95	95	300	10	35	0.060	1.40	4.8
R10P35-D95	95	300	10	35	0.060	2.09	7.8
N12P35-D85	85	500	12	35	0.086	2.34	5.3
R12P35-D85	85	310	12	35	0.086	2.34	3.8
R10P35-D85	85	300	10	35	0.060	2.34	2.7
R8P35-D85	85	410	8	35	0.038	2.34	2.7

f_c' is the concrete compressive strength, MPa

f_{yh} is the helical yield strength, MPa

d is the helical diameter, mm

S is the helical pitch, mm

ρ_h is the helical reinforcement ratio

ρ is the actual reinforcement ratio

ρ_{max} is the maximum allowable tensile reinforcement as defined by AS 3600 (2001)

μ_d is the displacement ductility index

The first is to examine the significance of the factors $\frac{\rho_h f_{yh}}{f_c'}$, $\frac{\rho}{\rho_{max}}$ and $0.7-\frac{S}{D}$ using JMP software (Cary, 2002). The variable is significant when the P-value (a measure of the significance of the variable which is denoted by "Prob>F" at output of the programme analysis) is less than or equal to 0.05. The 14 beams results presented in Table E.1 at Appendix E is used as input data, where the dependent variable y is μ_d and the independent variables, x1, x2 and x3 are as follows: x1 is

$\frac{\rho_h f_{yh}}{f_c'}$, x2 is $\frac{\rho}{\rho_{\max}}$ and x3 is $0.7-\frac{S}{D}$. The output of analysing the data using (Fit y by x) is presented in Section E-1 at Appendix E. This result shows that the factors x1and x2 are insignificant because the P-value was 0.1164 and 0.9044 which is greater than 0.05 but the factor x3 is significant because the P-value is 0.0066 which is less than 0.05. It must be noted that the correlation factors for x1, x2 and x3 are 0.192673, 0.00125 and 0.473073, which prove that the factor $0.7-\frac{S}{D}$ has a significant effect. x1 and x2 are statistically insignificant may be because the size of the data is not sufficient to show their importance (small data). However, in this study enforces the use $\frac{\rho_h f_{yh}}{f_c'}$ and $\frac{\rho}{\rho_{\max}}$ in modelling even though they are statistically insignificant.

The relationship proposed above (Equation 8.1) to predict the displacement ductility index of over-reinforced helically confined HSC beams can be modelled as follows:

$$\mu_d = 1+\alpha\left(\frac{\rho_h f_{yh}}{f_c}\right)^{\beta}\left(\frac{\rho}{\rho_{\max}}\right)^{\gamma}\left(0.7-\frac{S}{D}\right)^{\phi} \qquad (8.3)$$

where α,β,γ and ϕ are the unknown constants of confinement for the displacement ductility index. A regression analysis on the experimental results was

performed to find the best combination of α, β, γ and ϕ. The test results of the displacement ductility index of the 14 beams were used to determine the best correlation between the predicted and the experimental values.

The regression analysis has been conducted using JMP software (Cary, 2002) where the first step was to transfer the equation into the form $y = f(x_1, x_2, x_n)$ by taking the logarithm for both sides of the equation as follows:

$$Ln(\mu_d - 1) = Ln\alpha + \beta Ln\left(\frac{\rho_h f_{yh}}{f_c}\right) + \gamma Ln\left(\frac{\rho}{\rho_{\max}}\right) + \phi Ln\left(0.7 - \frac{S}{D}\right) \qquad (8.4)$$

Or simply:

$$y = c + \beta x_1 + \gamma x_2 + \phi x_3$$

Where

$$y = Ln(\mu_d - 1)$$

$c = Ln\alpha$ and then $\alpha = e^c$

$$x_1 = Ln\left(\frac{\rho_h f_{yh}}{f_c}\right)$$

$$x_2 = Ln\left(\frac{\rho}{\rho_{\max}}\right)$$

$$x_3 = Ln\left(0.7 - \frac{S}{D}\right)$$

Applying the method of regression (Fit model) using the experimental results presented in Table 8.1, the output of analysing is presented in the Section E-2 at Appendix E. This result shows that only the factor x3 is significant where the P-value is 0.0013 which is less than 0.05. However the correlation factors for the model is 0.78

Then the unknown constants of Equation 8.3 are determined as

$\alpha = 96.139$ $\gamma = -0.976$

$\beta = 0.247$ $\phi = 2.914$

Thus, the displacement ductility index is a function expressed as Equation 8.5.

$$\mu_d = 1 + 96.139\left(\frac{\rho_h f_{yh}}{f_c}\right)^{0.247}\left(\frac{\rho}{\rho_{\max}}\right)^{-0.976}\left(0.7 - \frac{S}{D}\right)^{2.914} \qquad (8.5)$$

Values for the displacement ductility index determined from Equation 8.5 are listed in Table 8.2 and are compared with the experimental values. It has to be noted that, when $\frac{S}{D}$ is greater than or equal to 0.7, the second part of the Equation 8.5 has a negative or zero value. This indicates that the effect of the helical confinement is negligible when the ratio $\frac{S}{D}$ is greater than or equal to 0.7. For example the

displacement ductility index for Beams 12HP100, 12HP160, 8HP100 and 8HP160 is equal to 1.0 because the second part of equation 8.5 is equal to zero. Also the experimental displacement ductility index was 1.0. It has been noted that predicting the displacement ductility using Equation 8.5 has an average error of -2.5% (average error is a summation of the error divided by the number of beams). Also the absolute average error is 22.3% (the absolute average error is the summation of the absolute value of error divided by the number of beams).

Table 8.2 – Comparison between the experimental results and values predicted using Equation 8.5

	μ_d experimental	μ_d predicted	Error
R12P25-A105	7.7	9.189618	-19%
R12P50-A105	4.3	3.315911	23%
R12P75-A105	1.3	1.358213	-4%
N8P25-A80	6.5	7.172544	-10%
N8P50-A80	2.9	2.742308	5%
R10P35-B72	6.5	4.289511	34%
R10P35-B83	5.8	4.640166	20%
R10P35-B95	5.3	5.010846	5%
R10P35-C95	4.8	5.986779	-25%
R10P35-D95	7.8	4.372705	44%
N12P35-D85	5.3	4.849746	8%
R12P35-D85	3.8	4.420998	-16%
R10P35-D85	2.7	4.104686	-52%
R8P35-D85	2.7	3.995915	-48%

$\mu_{\exp}$ = Experimental displacement ductility index

μ_{prd} = predicted displacement ductility index

$$\text{Error} = \frac{(\mu_{\exp} - \mu_{prd})}{\mu_{\exp}}$$

It has been noted that some beams have high error such as the beam R10P35-D85 has a maximum error of -52%, which could be due to low compaction of the concrete, but if these beams were not included in the regression analysis the correlated data can be improved. Thus by excluding these beams and applying the regression analysis again, the model will be as follows:

$$\mu_d = 1 + 41.223\left(\frac{\rho_h f_{yh}}{f_c}\right)^{-0.004}\left(\frac{\rho}{\rho_{\max}}\right)^{0.099}\left(0.7 - \frac{S}{D}\right)^{3.092} \qquad (8.6)$$

Section E-3 at Appendix E shows the output of analysing eight beams. This result shows that the only factor x3 is significant where the P-value is 0.0001 and the correlation factor for the model is 0.99.

Table 8.3 shows a comparison between the experimental results and values predicted by Equation 8.6. Here the regression analysis was conducted by using eight beams. It is to be noted that the average error is -0.12% whereas the average error was –2.5% when Equation 8.5 was used. Also the absolute average error is reduced from 22.3% (by using Equation 8.5) to 0.12% (by using Equation 8.6). Also the correlation factor has improved from 0.78 to 0.99 by using Equation 8.6. Considering the scatter in the experimental results, the performance of the model (Equation 8.6) is quite satisfactory. It is therefore concluded that Equation 8.6

could be used to predict the displacement ductility index for high strength concrete beams confined with helix (short depth) within the range of the experimental data. However further data from over-reinforced helically confined HSC beams is needed. It is obvious that more experimental data would give a model with a higher degree of confidence (correlation factor). However such accuracy is not warranted within the scope of this study.

Table 8.3 – Comparison of experimental results with the values predicted by the proposed model (Equation 8.6)

	μ_d experimental	μ_d predicted	Error
R12P25-A105	7.7	7.16	7%
R12P75-A105	1.3	1.30	0%
N8P25-A80	6.5	7.33	-13%
N8P50-A80	2.9	2.99	-3%
R10P35-B83	5.8	5.21	10%
R10P35-B95	5.3	5.16	3%
R10P35-C95	4.8	5.07	-6%
N12P35-D85	5.3	5.26	1%

$\mu_{\exp}$ = Experimental displacement ductility index

μ_{prd} = predicted displacement ductility index

$$\text{Error} = \frac{(\mu_{\exp} - \mu_{prd})}{\mu_{\exp}}$$

8.5 APPLICATION OF THE MODEL IN PRACTICE

The analytical model provided in this chapter would have an immense potential for future application for estimating the displacement ductility index for over-reinforced helically confined HSC beams. This section explains how the proposed model was applied to over-reinforced helically confined HSC beams with the help of two simple examples. The first example deals with the analysis in which the displacement ductility index is predicted while the second example uses the proposed model to design the helical confinement of over-reinforced confined HSC beams.

8.5.1 Example 1:

Determine displacement ductility index, if the following information is given:

Beam concrete cross-section is 200×300 mm

Concrete cover is 20 mm

Longitudinal reinforcement is 4N32

Yield strength of longitudinal reinforcement is 500 MPa

Concrete compressive strength is 80 MPa

Helical details:

Helical diameter is 12 mm

Yield strength of helical reinforcement is 250 MPa

Helical pitch is 30 mm

Helical confinement concrete core diameter is 150 mm

Step 1: Calculate $\frac{\rho_h f_{yh}}{f_c'}$

Where $\rho_h = \frac{\pi d_h^{\,2}}{DS} = 0.10$

Then $\frac{\rho_h f_{yh}}{f_c'} = 0.313$

Step 2, Calculate $\frac{\rho}{\rho_{\max}}$

$\frac{\rho}{\rho_{\max}} = 1.93$

Step 3, Calculate $0.7 - \frac{S}{D}$

$$0.7-\frac{S}{D}=0.5$$

Then the displacement ductility index for the above reinforced helically confined HSC beams could be predicted using the Equation 8.6 as follows:

$$\mu_d = 1+41.223\left(\frac{\rho_h f_{yh}}{f_c}\right)^{-0.004}\left(\frac{\rho}{\rho_{\max}}\right)^{0.099}\left(0.7-\frac{S}{D}\right)^{3.092}=6.18$$

8.5.2 Example 2:

The data used here is the same as that in the analysis problem (Example 1), but here the displacement ductility index is given and helical pitch is required (unknown).

Firstly, substitute for the value of ρ_h and simplify

$$\mu_d = 1+41.223\left(\frac{\rho_h f_{yh}}{f_c}\right)^{-0.004}\left(\frac{\rho}{\rho_{\max}}\right)^{0.099}\left(0.7-\frac{S}{D}\right)^{3.092}$$

$$\mu_d = 1+43.589\times\left(0.7-\frac{S}{D}\right)^{3.092}\left(\frac{1}{S}\right)^{-0.004}$$

$$6.18 = 1+43.589\left(0.7-\frac{S}{D}\right)^{3.092}\left(\frac{1}{S}\right)^{-0.004}$$

$$0.0958 = \left(0.7 - \frac{S}{150}\right)^{3.092} \left(\frac{1}{S}\right)^{-0.004}$$

S is the only unknown in the above equation but by trial and error, the value of S is found to be 30 mm. Thus to gain a displacement ductility index of 5.18 with the concrete compressive strength, the longitudinal and helical reinforcement details given above, the helical pitch must be 30 mm.

8.6 SUMMARY

In this chapter, the experimental data presented in Chapter 6 was used to predict displacement ductility index. It has been noted that the mechanical behaviour of confined concrete is affected by various variables related to helical confinement. This study introduces three non-dimensional ratios and proposes an analytical model to predict and determine the displacement ductility index. The proposed model is reasonable at estimating experimental data and was applied to practical problems such as analysis and design over-reinforced HSC beams. The next chapter is the conclusion of the thesis.

CHAPTER 9

CONCLUSIONS AND RECOMMENDATIONS

9.1 GENERAL

High strength concrete and high strength steel have benefits for different structures such as high rise structures and larger span girders but these materials lack ductility. This thesis has shown that helical confinement in the compression zone of beams enhances the strength and the ductility of over-reinforced HSC beams. However, as development in material science and computational technology is somewhat unimaginable, it is believed that over-reinforced helically confined HSC beams will become a very important design concept for safeguarding structures.

This chapter summarises the conclusions drawn from both the experimental and analytical parts, which were carried out during this study. This chapter concludes with a brief list of areas of further research needed.

9.2 CONCLUSIONS FROM THE EXPERIMENTAL WORK

The experimental component of this study involved 20 full size over-reinforced helically confined HSC beams. Their cross section was 200×300 mm, the length was 4 m and the clear span was 3.6 metres. They were subjected to four point loading with an emphasis on midspan deflection. The following conclusions are drawn from this study:

Using steel helices to encase concrete in the compression zone increases ductility and improves overall performance of HSC beams. The experimental testing conducted in this research proved that using helices to enhance the characteristics of high strength concrete beams is an effective technique.

Helical confinement will restrain transverse stress in concrete under compression, and delay compression failure which allows the longitudinal reinforcement to yield before the confined concrete fails. The interval between the longitudinal steel yielding and failure depends on the characteristics of helical confinement especially helical pitch.

This thesis has shown that when there is helical confinement in the compression zone of an over-reinforced concrete beam, it fails in a ductile manner. Therefore, when the strength and/or ductility of a beam must be increased, helical confinement

can be added into the compression area. In these instances the tensile reinforcement can be increased above the maximum ratio of longitudinal reinforcement imposed by design standards such as (AS3600, 2001). The concept behind this is that longitudinal reinforcement significantly affects the behaviour of under-reinforced concrete beams while the characteristics of helical confinement have a major effect on over-reinforced helically confined HSC beams

Beams with a 25, 35, 50 and 75 mm helical pitch are ductile based on the level of the helical pitch. The helices were affectively confined in the compressive region when the helical pitch was reduced. It is interesting to note that the displacement ductility index is inversely proportional to the helical pitch. However, confinement is negligible when the helical pitch is greater than or equal to 70% of the core diameter of helically confined beams.

There was no significant difference between the yield deflections of the beams but there was between the ultimate deflections which indicates that the helix effect occurs after yield deflection, after which the strength is enhanced (confined concrete strength). The change of strength of confined concrete depends on many factors such as helix pitch.

The common reason for the spalling off phenomenon is that closely pitched helices physically separate the concrete cover from the core. However, experimental results

show that spalling off occurred when the strain between the confined and unconfined concrete changed significantly. This change is affected by the helical pitch and parameters such as helical diameter and tensile strength of the helix bar. In other words a considerable release of strain energy causes the concrete cover to spall off. The quantity of strain energy released is affected by different factors, one of which is helical pitch.

Increasing the concrete compressive strength of over-reinforced helically confined HSC beams decreases the yield deflection slightly, but decreases ultimate deflection significantly. The displacement ductility index is decreased as the concrete compressive strength is increased. Also, increasing the concrete compressive strength increases the load at spalling off the concrete cover up to a particular concrete compressive strength.

Increasing the longitudinal reinforcement ratio of over-reinforced well-confined HSC beams increases ultimate deflection and the displacement ductility index although the (ρ/ρ_{max}) is increased (within the range of ρ/ρ_{max} used in the test). However, the load at spalling off the concrete cover is decreased as the longitudinal reinforcement ratio increases. The maximum load was higher than the load at spalling off the concrete cover for beams that had a high longitudinal reinforcement ratio.

Within the range used in the test, helical pitch has a greater effect on over-reinforced HSC helically confined beams than helical diameter, helical yield strength and concrete compressive strength. This significant influence of helical pitch on the behaviour of over-reinforced HSC helically confined beams encourages using it as an important parameter in design equations.

9.3 ANALYTICAL STUDY

9.3.1 Predicting flexure strength

In order to predict the flexure strength of over-reinforced helically confined HSC beams, there is a need to find suitable rectangular stress block parameters, and suitable model to predict the enhanced concrete compressive strength and ultimate concrete confined strain.

There are on going studies to investigate the rectangular stress block parameters to predict the strength capacity in close agreement with experimental results. In this study, the stress block parameters γ and α of CEB-FIP-1990 (1990) were adopted for predicting flexure capacity of over-reinforced helically confined HSC beams. Also a new model for predicting the strength gain factor for over- reinforced helically confined HSC beams are developed. This new model is proposed based on the effectiveness of helical confinement.

The confined compressive strain predicted by Equation 7.1 is used in the stress block instead of the strain recommended by most codes of practice as 0.003. The agreement between the experimental and the predicted flexure strength of over-reinforced helically confined HSC beams was found to be reasonably accurate.

9.3.2 Predicting displacement ductility index

Variables such as helical reinforcement ratio, concrete compressive strength, longitudinal reinforcement ratio, helical yield strength and helical pitch have already been studied experimentally. In addition, the effect of each of the non-dimensional ratios $(\frac{\rho_h f_{yh}}{f_c'})$, $(\frac{\rho}{\rho_{\max}})$ and $(0.7-\frac{S}{D})$ on the displacement ductility index have been investigated. The model was derived from a better understanding of the behaviour of over-reinforced HSC beams within the range of the experimental data. The three non-dimensional ratios have been used to propose an analytical model to predict a displacement ductility index. The proposed model is reasonable at estimating the experimental data. The model was also applied to practical problems such as the analysis and design of over-reinforced HSC beams.

9.4 RECOMMENDATION FOR FUTURE RESEARCH

The following is a summary of the recommendations associated with these areas:

1- Further research to study the behaviour of over-reinforced helically confined HSC beams under cyclic loading

2- Further experimental research to apply the concepts presented in this study to light weight concrete and prestressed concrete.

3- The effect of helical confinement on over-reinforced HSC beams has been studied in this research, where the concrete compression strength was in the range 70 - 105 MPa. For future research it is recommended that the effect of helical confinement on over-reinforced HSC beams when concrete compression strength exceeds 130 MPa be investigate.

4- There is a need for more experimental data on over-reinforced helically confined HSC beams. The results of experiments on a large number of over-reinforced helically confined HSC beams could help to develop an acceptable analytical model using statistical analysis.

5- It has been noted that the concrete cover spalling off phenomena effects the strength of beams. Further research to study this phenomena with different thicknesses of concrete cover is required, but it could be solved by providing steel fibre in the concrete cover or both cover and confined core.

6- This study provides valuable information about the effect of helical pitch on the cover spalling off and the effectiveness of helical confinement. However, installing a double helical confinement (one helix inside the other) in the compression zone of the beam could enhance its effectiveness and delay cover spalling. This idea is based on the idea that reducing the concrete core enhances the effectiveness of helical confinement. This method divides the compression concrete area in two, with each area controlled by helical confinement. The helical pitch of outer confinement should delay the concrete cover from spalling off. This new idea warrants further research.

REFERENCES

ACI 318-02. Building Code Requirements for Structural Concrete. American Concrete Institute, Michigan, 2002.

ACI 318-95. Building Code Requirements for Reinforced Concrete. American Concrete Institute, Detroit, 1995.

ACI Committee 363R- State of Art Report on High-Strength Concrete "State of the Art Report on High-Strength Concrete", American Concrete Institute, Detroit, 1992.

Ahmad, S. H. and Shah, S. P. (1982). "Stress-Strain Curves of Concrete Confined By Spiral Reinforcement." ACI Structural Journal, 79(6), 484-490.

AL-Jahdali, F. A., Wafa, F. F. and Shihata, S. A. (1994). "Development length for straight deformed bars in high strength concrete", proceeding, ACI International conference on High performance concrete, Singapore, ed. V.M. Malhotra, ACI SP-149, American Concrete Institute, 507-521.

American Society for testing and materials, (1994). Annual Book of ASTM Standards, Part 4, Concrete and Mineral Aggregates, ASTM, Philadelphia, Pa.

AS3600. Australian Standard for Concrete Structures. Standards Association of Australia. North Sydney, 2001.

Ashour, S. A. (2000). "Effect of Compressive Strength and Tensile Reinforcement Ratio on Flexural Behaviour of High-Strength Concrete Beams." Engineering Structural Journal, 22(5), 413-423.

AS/NZS 4671. Australian Standards for Steel Reinforcing Materials. Standards Association of Australia, North Sydney, 2001.

Azizinamini, A., Kuska, S. S. B., Brungardt, P. and Hatfield, E. (1994). "Seismic Behaviour of Square High-Strength Concrete columns." ACI Structural Journal, 91(3), 336-345.

Bae, S. and Bayrak, O. (2003). "Stress Block Parameters for High Strength Concrete Members." ACI Structural Journal, 100(5), 626-636

Bartlett, M. and MacGregor, J. G. (1995). "In Place Strength of High Performance Concrete." proceeding, ACI International conference on High An International Perspective, Montreal, ed. J. A. Bickley, ACI SP-167, American Concrete Institute, 211-228.
Base, G. D. and Read, J. B. (1965) "Effectiveness of Helical Binding in the Compression Zone of Concrete Beams." Journal of the American Concrete Institute, Proceedings, 62, 763-781.

Bayrak, O., Sesmic (1998). "Performance of Rectilinearly angular Confined High-Strength Concrete Columns." Thesis submitted in conformity with the requirements for the Degree of Doctor of Philosophy in the University of Toronto.

Bhanja, S. and Sengupta, B. (2003). "Investigations On the Compressive Strength of Silica Fume Concrete Using Statistical Methods." Cement and Concrete Research Journal, 33(3), 447-450

Bing, L., Park R. and Tanaka, H. (2001). "Stress-Strain Behaviour of High-Strength Concrete Confined by Ultra High and Normal-Strength Transverse Reinforcements." ACI Structural Journal, 98(3), 395-406.

Bjerkeli, L., Tomaszewicz, A. and Jensen, J. J. (1990). "Deformation Properties and Ductility of High Strength Concrete." Utilization of High Strength concrete– Second International Symposium, SP-121, ACI, Detroit, 215-238.

Blick, R. L. (1973). "Some factors influencing High Strength Concrete." Modern Concrete, 36(12) 38-41.

CAN 3-A23.3-M94. (1994). "Design of Concrete Structure in Buildings Canadian Standards Association." Rexdale, Ontario, Canada.

Carrasquillo, R. L., Nilson, A. H. and Slate, F. O. (1981) "Properties of high strength concrete subjected to short term loads." ACI Journal proceedings, 78(3), 171-178.

Cary, N. C. (2002). "JMP discovery software, version 5." SAS Institute Inc.

CEB-FIP Model Code (1990), Comite Euro-International du Beton, 1990, Thomas Telford.

CEB/FIP Working Group on High Strength/ High Performance Concrete, " Application of High Performance Concrete." CEB Bulletin d' Information 222, Nov. 1994, Lausanne, Switzerland.

Chan, S. Y. N., Feng, N. Q. and Tsang K. C. (2000). "Mechanical properties of high strength concrete incorporating carrier fluidifying agent." ACI Material Journal, 97 (2), 108-114.

Chan, S. Y. N. and Anson, M. (1994). "The Ultimate Strength and Deformation of Plastic Hinges in Reinforced Concrete Frameworks." Magazine of Concrete Research, 46(169), 235-236.

Chan, W. W. L. (1955). "High-Strength Concrete: The Hong Kong Experience." Magazine of Concrete Research, 7(21), 121-132.

Corley, W. G. (1966). "Rotational Capacity Of Reinforced Concrete Beams." ASCE proceedings, 92(5), 121-146.

Cusson, D. and Paultre P. (1994). "High-Strength Concrete Columns Confined by Rectangular Ties." ACI Structural Journal, 120(3), 783-804.

Elbasha, N. M. and Hadi, M. N. S. (2004). "Investigating the Strength of Helically Confined HSC Beams." Int. Conf. Of Structural & Geotechnical Engineering, and Construction Technology, IC-SGECT'04, Mansoura, Egypt, 23-25 March 2004, pp. 817-828.

Elbasha, N. M. and Hadi, M. N. S. (2004). "Effects of the Neutral Axis Depth on Strength Gain Factor for Helically Confined HSC Beam." Int. Conf. on Bridge Engineering & Hydraulic Structures, BHS2004. Kuala Lumpur, Malaysia. ISBN 983-2871-62-X. 26-27 July 2004, pp. 213-217.

Elbasha, N. M. and Hadi, M. N. S. (2005). "Flexural Ductility of Helically Confined HSC Beams." ConMat'05 Third International Conference on Construction Materials: Performance, Innovations and Structural Implications Vancouver, Canada, August 22-24, 2005. Paper number 50. 10 pages.

Elbasha, N. M. and Hadi, M. N. S. (2005). "Experimental testing of helically confined HSC beams." Structural Concrete Journal (Thomas Telford and *fib*), 6(2), 43-48.

Foster, S. J., Liu, J., and Sheikh, S. A. (1998). "Cover spalling in HSC columns load in concrete compression." Structural Engineering Journal, 124 (12), 1431-1437.

Foster, S. J. and Attard, M. M. (1997) "Experimental Tests On Eccentrically Loaded High Strength Concrete Columns." ACI Structural Journal, 94(3), 783-804.

Galeota, D., Giammatteo, M. M. and Marino, R. (1992). "Strength and Ductility of Confined High Strength Concrete." Proceedings of 10th World Conference, Toronto, On Earthquake Engineering, Madrid, 5, 2609-2613.

Hadi, M. N. S. and Schmidt, L. C. (2002). "Use of Helixes In Reinforced Concrete Beams." ACI Structural Journal, 99(2), 304-314.

Hadi, M. N. S. and Elbasha, N. M. (2004). "A New Model for Helically Confined High Strength Concrete Beams." 7th International Conference on Concrete Technology in Developing Countries. Modelling and Numerical Methods for Concrete Materials. 5-8 October 2004. Kuala Lumpur, Malaysia. University of Technology MARA. pp. 29-40.

Hadi, M. N. S. and Elbasha, N. M. (2005). **"**Effect of Tensile Reinforcement Ratio and Compressive Strength on the Behaviour of Over Reinforced HSC Helically Confined." Construction and Building Materials Journal, (In Press). Letter of acceptance 2 Sept 2005

Hadi, M. N. S. and Elbasha, N. M (2005). "The Effect of Helical Pitch on the Behaviour of Helically Confined HSC Beams." Australian Structural Engineering Conference, ASEC 2005. Newcastle. Editors: MG Stewart and B Dockrill. 11-14 September. Paper 54. 10 pages.

Han, B. S., Shin, S. W. and Bahn, B. Y. (2003). " A Model of Confined Concrete in High Strength Concrete Tied Columns." Magazine of Concrete Research, 55(3), 203-214.

Hatanaka, S. and Tanigawa, Y. (1992). "lateral pressure requirements for compressive concrete." Proceedings of 10th World Conference on Earthquake Engineering, Madrid, 2603-2608.

Haug, A. K. (1994). "Concrete Technology, the Key to Current Concrete Platform Concepts." proceeding, ACI International Conference on High performance Concrete, Singapore, ed. V.M. Malhotra, ACI SP-149, American Concrete Institute, 63-80.

Helland, S. (1995). " Application of High Strength Concrete in Norway." proceeding, ACI International Conference on High An International Perspective, Montreal, ed. J. A. Bickley, ACI SP-167, American Concrete Institute, 27-53.

Hognestad, E., Hanson, N. W. and MacHenry, D. (1955). "Concrete stress Distribution in Ultimate Strength Design." ACI Journal, Proceedings, 455-479

Huo, X. S., Al-Omaishi, N. and Tadros, M. K. (2001). "Creep, Shrinkage and Modulus of Elasticity of High Performance Concrete." ACI Material Journal, 98(6), 440-449.

Ibrahim, H.H. and MacGregor, J. G. (1997). "Modification of the ACI Rectangular Stress Block For High Strength Concrete." ACI Structural Journal, 94(1), 40-48.

Iyengar, K. T., Sundra, R. Desayi, P. and Reddy, K. N. (1970). "Stress-Strain Characteristics of Concrete Confined in Steel Binders." Magazine of Concrete Research, 22(72), 173-184.

Issa, M. A. and Tobaa, H. (1994). "Strength and Ductility Enhancement in High-Strength Confined Concrete." Magazine of Concrete Research, 46(168), 177-189.

Kaar, P. H., Fiorato, A. E., Carpenter, J. E. and Corley, W. G. (1977). "Limiting Strains of Concrete Confined by Rectangular Hoops." Tentative Report, Research and Development, Construction Technology Laboratories, Portland Cement Association, PCA R/D Ser. 1557.

King, J. W. H. (1946). "The effect of lateral reinforcement in reinforced concrete columns." Structural Engineer Journal, 24(7), 355-388.

Kwan, A., Ho, J. and Pam, H. (2004). "Effect of concrete grade and steel yield strength on flexural ductility of reinforced concrete beams." Australian Journal of structural engineering, proceedings, 5(2), 119-138.

Legeron, F. and Paultre, P. (2000). "Predicting of modulus of rupture of concrete." ACI Material Journal, 97(2), 193-200.

Leslie, K. E., Rajagopalan, K. S. and Everard, N. J. (1976). "Flexure Behaviour of High Strength Concrete Beams." ACI Journal, proceedings, 73(9), 517-521.

Malhotra, V. M., Zhang, M. H. and Leaman, G. H. (2000). "Long-Term Performance of Steel Reinforcing Bars in Portland Cement Concrete and Concrete Incorporating Moderate and High Volumes of ASTM Class F Fly Ash." ACI Material Journal, 97 (4), 407-417.

Malier, Y. and Richard, P. (1995). "High Performance Concrete- Custom Designed Concrete: A Review Of The French Experience and Prospects For Future Development." proceeding, ACI International Conference on High An International Perspective, Montreal, ed. J. A. Bickley, ACI SP-167, American Concrete Institute, 55-80.

Mander, J. B., Priestley, M. J. N., and Park, R. (1984). "Seismic Design of Bridge piers." Research Report 84-2, Department of Civil Engineering, University of Canterbury, New Zealand, 444 pp.

Mansur, M. A., Chin, M. S. and Wee, T. H. (1997). "Flexural Behaviour of High-Strength Concrete Beams." ACI Structural Journal, 97(6), 663-674.

Martinez, S. Nilson, A. H. and Slate, F. O. (1984). "Spirally Reinforced High-Strength Concrete Columns." ACI Structural Journal, 81(5), 431-442.

Mattock, A. H., Kriz, L. B. and Hognestad, E. (1961). " Rectangular Concrete Stress Distribution in Ultimate Strength Design." ACI Structural Journal, 56, 875-928.

Mokhtarzadeh, A. and French, C. (2000) "Mechanical Properties of High Strength Concrete with Consideration for Precast Applications." ACI Material Journal, 97(2), 136-147.

Montes, P., Bremner, T. W. and Mrawira, D. (2005). " Effect Of Calcium Nitrate-Based Corrosion Inhibitor and Fly Ash On Compressive Strength of High-Performance Concrete." ACI Material Journal, 102(1), 3-8.

Muguruma, H., Watanabe, F., Tanaka, H., Sakurai, K. and Nakamura, E. (1979). "Effect of Confinement by High Yield Strength Hoop Reinforcement Upon the Compressive Ductility of Concrete." 22nd Japan Congress on Material Research, 377-382.

Muguruma, H. Watanabe, F. and Komuro, T. (1990). "Ductility Improvement of High Strength Concrete Columns with lateral Confinement." Utilization of High Strength Concrete–Second International Symposium, SP-121, American Concrete Institute, Detroit, 47-60.

Naaman, A. E., Harajli, M. H. and Wight, J. K. (1986). "Analysis Of Ductility in Partially Prestressed Concrete Flexural Members." PCI Journal, 31(3), 64-87.

Nagataki, S. (1995). "High Strength Concrete in Japan: History and Progress." proceeding, ACI International Conference on High An International Perspective, Montreal, ed. J. A. Bickley, ACI SP-167, American Concrete Institute, 1-25.

Nawy, E. G. (2001). "Fundamentals of High-Performance Concrete." Second edition. John Wiley & Sons, Canada.

Nilson, A. H. (1985). “Design Implications of Current Research On High Strength Concrete.” ACI Special publication SP-87, American Concrete Institute, 85-118.

Nilson, A. H. (1994). “Structural Members.” Published in the Book High Performance Concrete and Applications, Edited by Shah, S. P and Ahmad, S. H., published by Edwards Arnold, London, 213-233.

NS 3473E, (1992), Concrete Structures, Design Rules, Norwegian Standard for Building Standardisation, Oslo, 1992.

NZS 3101-1995 “The Design Of Concrete Structures, New Zealand Standard, Wellingoton, New Zealand 1995.

Park, R. and Paulay, T. (1975). “Reinforced concrete structures.” John Wiley and Sons.

Pastor, J. A., Nilson, A. H. and Floyd, S. O. (1984). “Behaviour of High-Strength Concrete Beams, Research Report No. 84-3, School of Civil and Environmental Engineering, Cornell University.

Paulay, T. and Priestley, M. J. N. (1990). Seismic Design of Reinforced Concrete Masonry Buildings, John Wiley& Sons, London, UK, 744 PP.

Pendyala, R., Mendis, P. and Patnaikuni, I. (1996). “Full Range Behaviour of High Strength Concrete Flexural Members: Comparison of Ductility Parameters of High and Normal-Strength Concrete Members.” ACI Structural Journal, 93(1), 30-35.

Pessiki, S., Pieroni, A. (1997). “Axial Load Behaviour of Large-Scale Spirally-Reinforced High Strength Concrete Columns.” ACI Structural Journal, 94(3), 304-314.

Priestly, M. J. N. and Park, R. (1987). “Strength and Ductility of Concrete Bridge Columns Under Seismic Loading.” ACI Structural Journal, 84(1), 69-76.

Razvi, S. R. and Saatcioglu, M. (1994). “Strength and deformability of Confined High Strength Concrete Columns.” ACI Structural Journal, 91(6), 678-687.

Richart, F. E., Brandtzaeg, A. and Brown, R. l. (1929). “A Study of the Failure of Concrete Under Combined Compressive Stresses.” University of Illinois Engineering Experimental Station, Bulletin No. 185, 104 pp.

Saatcioglu, M. and Razvi, S. R. (1994). "Behavior of Confined High Strength Concrete Columns." Proceedings Structural Concrete Conference, Toronto, Ontario, May 19-21,pp 37-50.

Sakai, K., and Sheikh, S. (1989). "A comparative study of confinement models." ACI Structural Journal, 79(4) 296-306.

Sargin, M. (1971). "Stress-Strain Relationships for Concrete and the Analysis of Structural Concrete Sections." Solid Mechanics Division Study No 4, university of Waterloo, 167pp.

Schmidt, W. and Hoffman, E. S. (1975). "Nine thousand-Psi." Civil Engineering Magazine, 45(5), 52-55.

SEAOC, "Recommended Lateral Force Requirements and Commentary." Seismology Committee, Structural Engineers' Association of California, San Francisco, 1973, 146 pp.

Shah, S. P. and Rangan, B. V. (1970). "Effects of Reinforcements on Ductility of Concrete." Journal of The Structural Division, 96(6), 1167-1184

Shehata, I. A. E. M. and Shehata, L. E. D. (1996). "Ductility of HSC Beams in Flexure." Proc. Of Fourth International Symposium On the Utilisation of High Strength/ High Performance Concrete (BHP-96), Paris, pp945-954.

Sheikh, S. A. and Uzumeri, S. M. (1980). "Strength and Ductility of Tied Concrete Columns." Journal Of The Structural Division, 106(5), 1079-1102.

Sheikh, S. A. (1978). "Effectiveness of Rectangular Tie as Confinement Steel in Reinforced Concrete Columns." Thesis submitted in conformity with the requirements for the Degree of Doctor of Philosophy in the University of Toronto.

Sheikh, S. A. and Yeh, C. C. (1990). "Tied Concrete Columns Under Axial Load and Flexura." Journal Of The Structural Engineering, 116(10), 2780-2800.
Sheikh, S. A. and Yeh, C. C. (1986). "Flexura Behaviour of Confinement Concrete Columns Subjected to High Axial Load." ACI Structural Journal 83(5), 389-404.

Shin, S. W., Ghosh, S. K. and Moreno, J. (1989). "Flexural Ductility of Ultra-High Strength Concrete Members." ACI Structural Journal, 86(4), 394-400.

Shuaib, H. A. and Batts, J. (1991). "Flexural Behaviour of Doubly Reinforced High Strength Lightweight Concrete Beams With Web Reinforcement." ACI Structural Journal, 88(3), 351-358.

Sugano, S., Nagashima, T., Kimura, H., Tamura, A. and Ichikawa, A. (1990). "Experimental Studies on Seismic Behaviour of Reinforced Concrete Members of High Strength Concrete-Second International Symposium." SP-121, American Institute, Detroit, 61-87.

Suzuki, M., Suzuki, M., Abe, K. and Ozaka, Y. (1996). "Mechanical Properties of Ultra High Strength Concrete" Proc. Of Conference Fourth International Symposium on the Utilisation of High Strength/ High performance Concrete, BHP 96, Paris, pp 835-844.

Swartz, S. E., Nikaeen, A., Naryana Babu, H. D., Periyakaruppan, N. and Refai, T. E. M. (1985). "Structural Bending Properties of High Strength Concrete." ACI Special Publication 87, High Strength Concrete, 147-178.

Tan, T. H. and Nguyen, N. B. (2005). "Flexural Behaviour of Confined High Strength Concrete Columns." ACI Structural Journal, 102(2), 198-205

Thornton, C. T., Mohamad, H., Hungspruke, U. and Joseph, L. (1994). "High Strength Concrete for High-Rise Towers." proceeding, ACI International Conference on High Performance Concrete, Singapore, ed. V.M. Malhotra, ACI SP-149, American Concrete Institute, 769-784.

Tognon, G., Ursella, P. and Coppetti, G. (1980). "Design and Properties of Concretes with Strength Over 1500 kgf/cm^2." ACI Journal, proceedings,77(3), 171-178.

Walraven, J. (1995). "High strength concrete in the Netherlands." Proceeding, ACI International Conference on High Strength Concrete, An International Perspective, Montreal, ed. J. A. Bickley, ACI SP-167, American Concrete Institute, 103-126.

Wang, C. K. and Salmon, C. G. (1985). "Reinforced Concrete Design." Harper International Edition; 1985:pp 39-88.

Warner, R. F., Rangan, B. V., Hall, A. S., Faulkes, K. A. (1999). "Concrete Structures." Longman, South Melbourne.

Webb, J. (1993). "High Strength Concrete: Economics, Design and Ductility. Australia: Concrete International; 1993:pp 27-32.

Whitehead, P. A. and Ibell, T. J. (2004). "Deformability and Ductility in Over-Reinforced Concrete Structures." Magazine of Concrete Research, 56(3), 167-177.

Ziara, M. M., (1993). “Influence of Confining the Compression Zone in the Design of Structural Concrete Beams.” Ph.D thesis, Department of Civil and Offshore Engineering, Heriot-Watt University, Edinburgh.

Ziara, M. M., Haldane, D., and Kuttab A. S. (1995). “Flexural Behaviour of Beams with Confinement.” ACI Journal, 92(1), 103-114.

Ziara, M. M., Haldane, D. and Hood, S. (2000). “Proposed Changes to Flexural Design in BS 8110 to allow Over-Reinforced Sections to Fail in a Ductile Manner.” Magazine of Concrete Research, 52(6), 443-454.

Appendix A:

Stress-strain of longitudinal, helical confinement and shear reinforcing steel bars

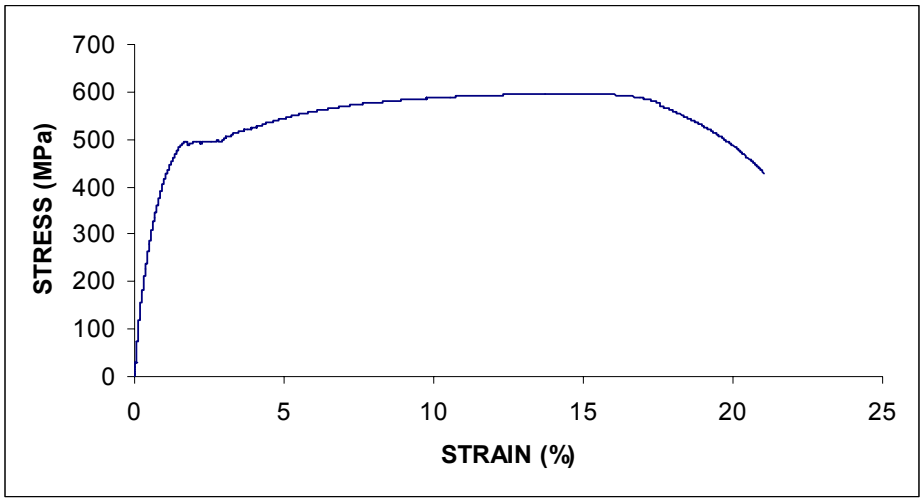

Figure A.1. Tensile stress-strain curve for the longitudinal steel with 32 mm diameter

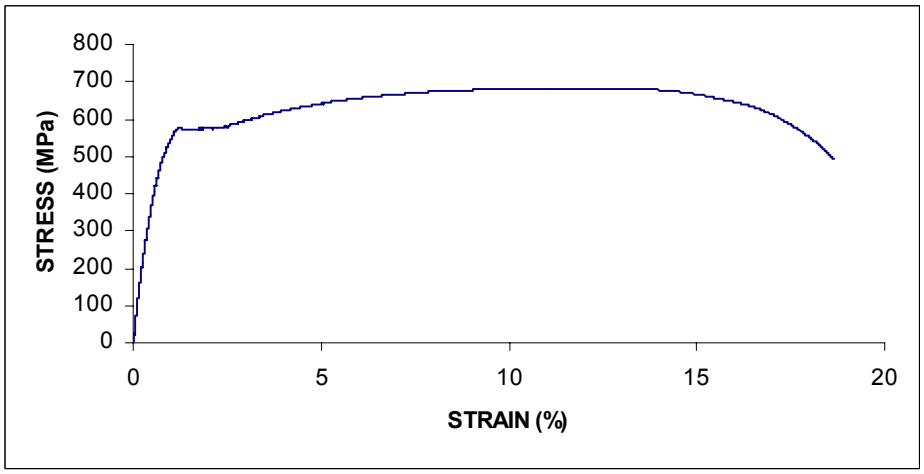

Figure A.2. Tensile stress-strain curve for longitudinal steel with 28 mm diameter

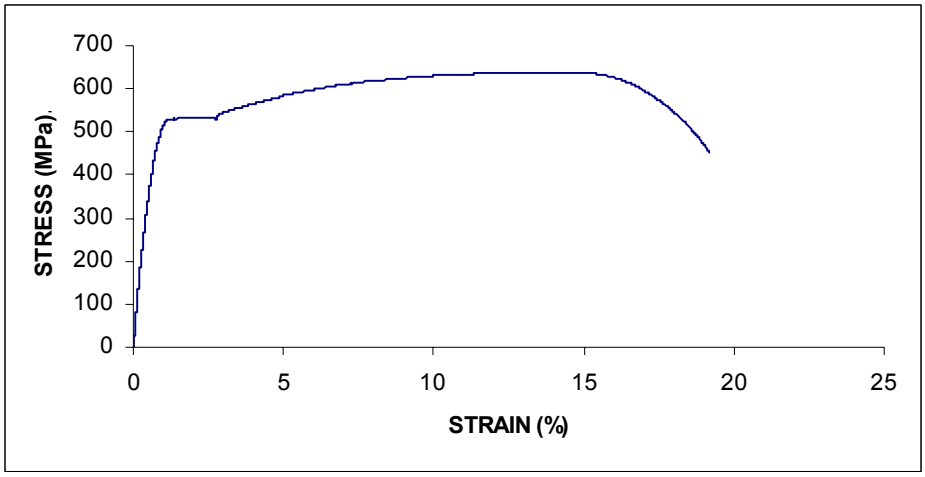

Figure A.3. Tensile stress-strain curve for longitudinal steel with 24 mm diameter

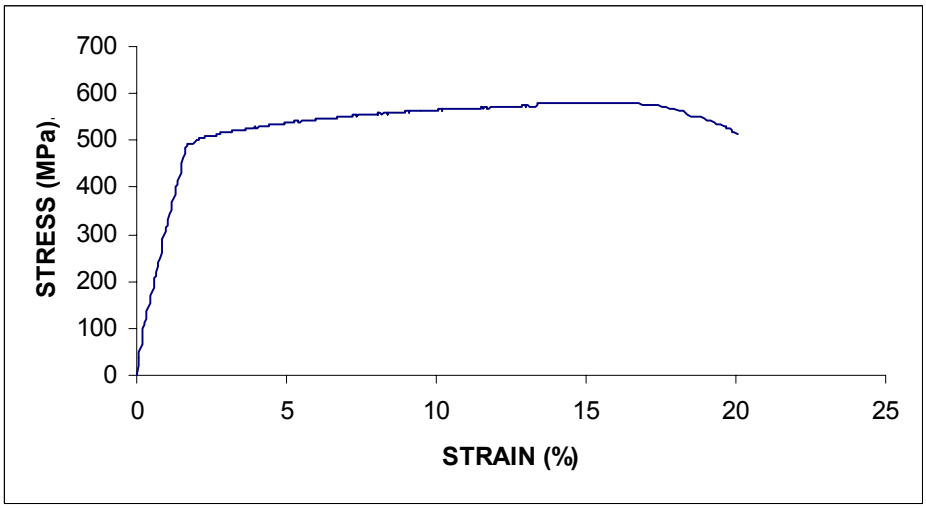

Figure A.4. Tensile stress-strain curve for the helical steel with 8 mm diameter (plain bar)- N8

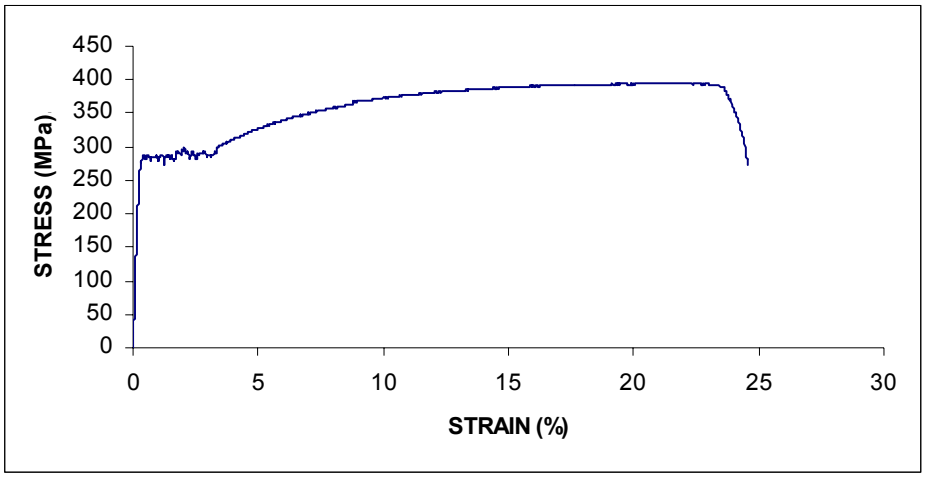

Figure A.5. Tensile stress-strain curve for the helical steel with 10 mm diameter (plain bar)- R10

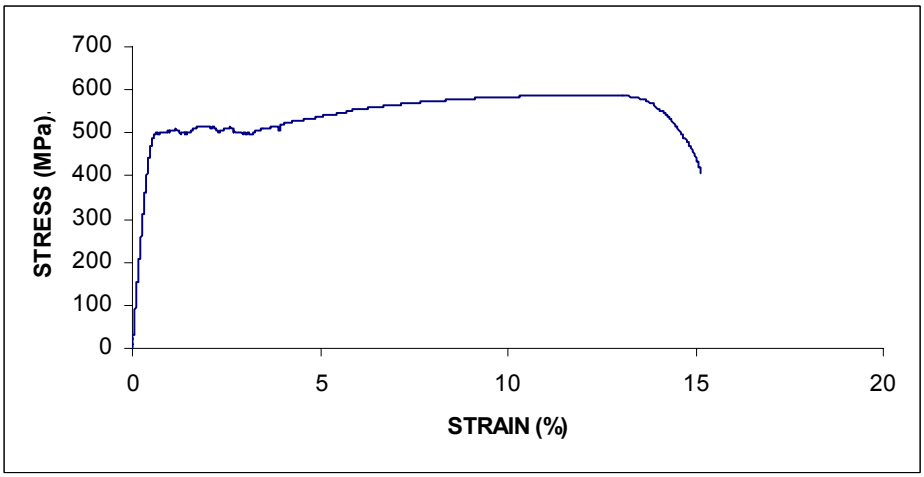

Figure A.6. Tensile stress-strain curve for the helical steel with 12 mm diameter (deformed bar)- N12

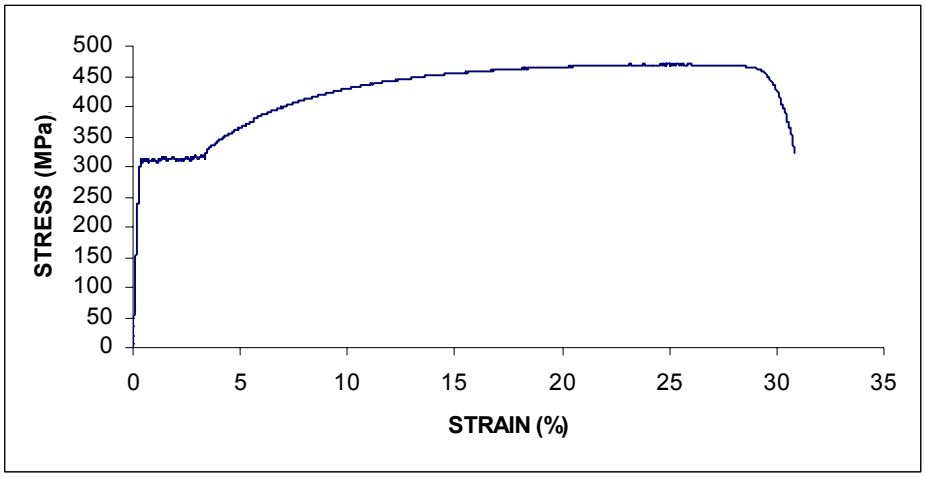

Figure A.7. Tensile stress-strain curve for the helical steel with 12 mm diameter (plain bar)- R12

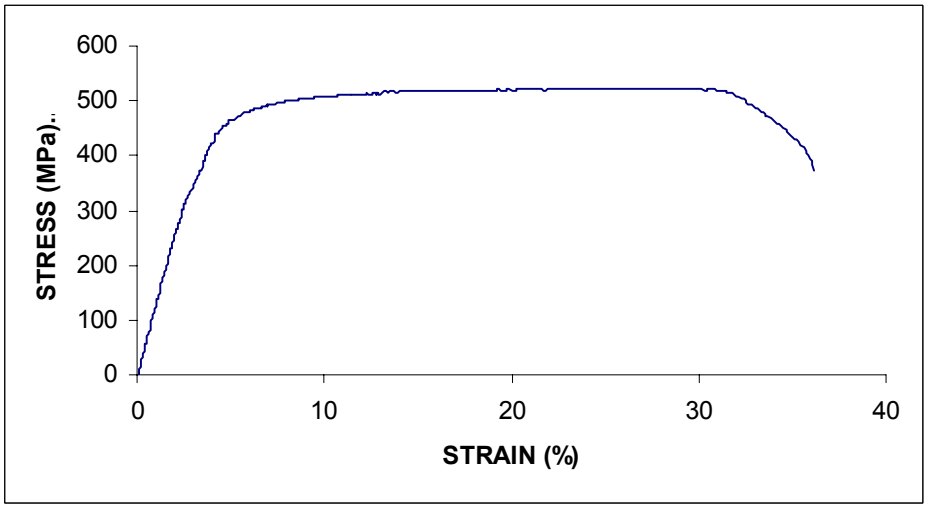

Figure A.8. Tensile stress-strain curve for the helical steel with 7.8 mm diameter (ribbed bar)- R8

Appendix B:

Load-midspan deflection of the 20 tested beams

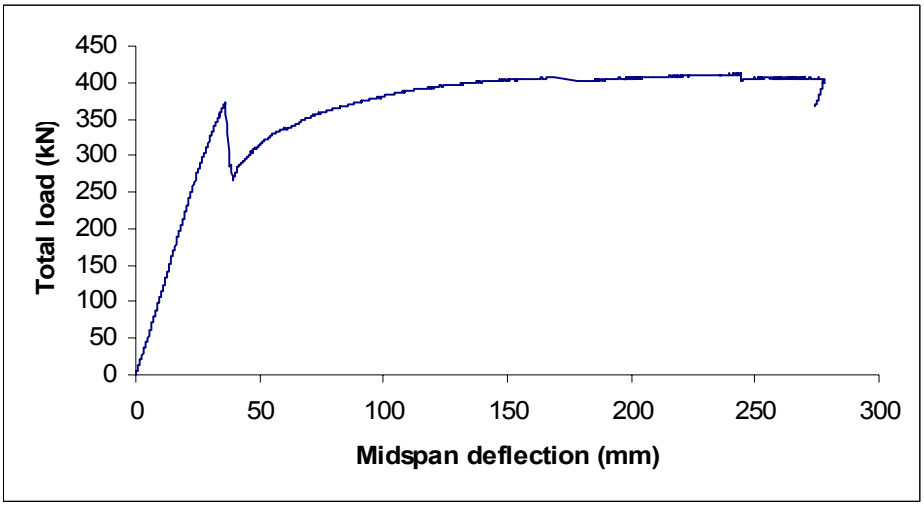

Figure B.1 load midspan deflection curve for beam R12P25-A105

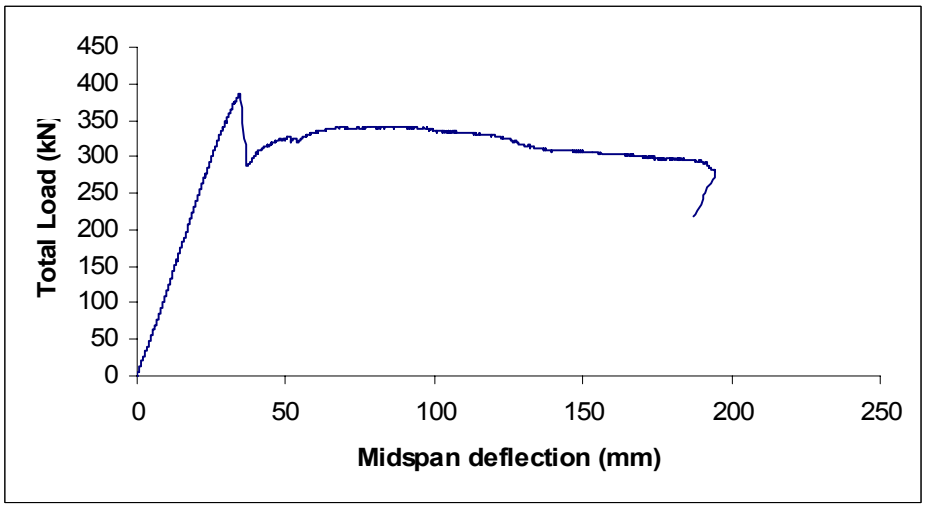

Figure B.2 load midspan deflection curve for beam R12P50-A105

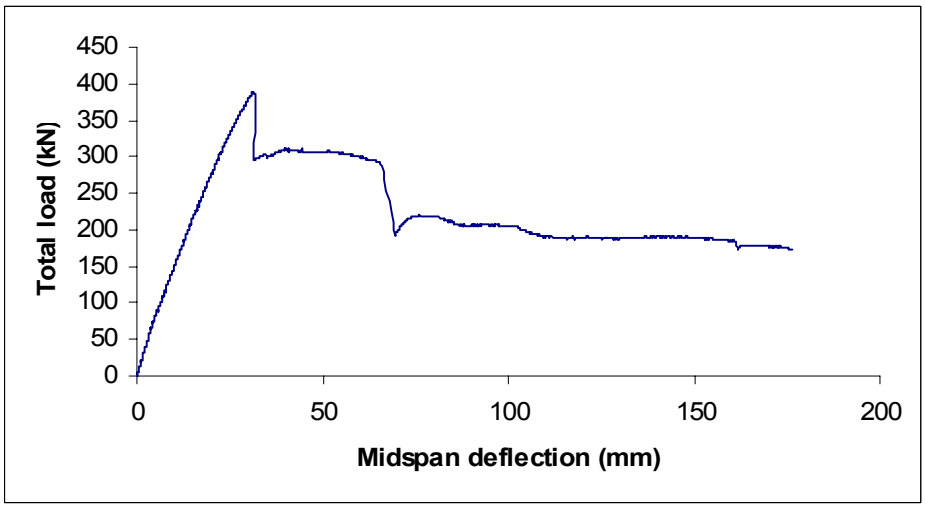

Figure B.3 load midspan deflection curve for beam R12P75-A105

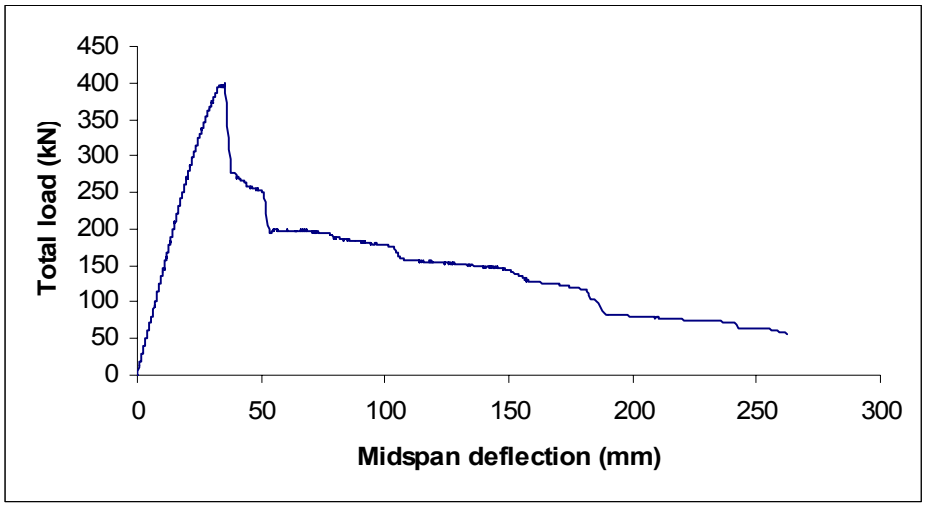

Figure B.4 load midspan deflection curve for beam R12P100-A105

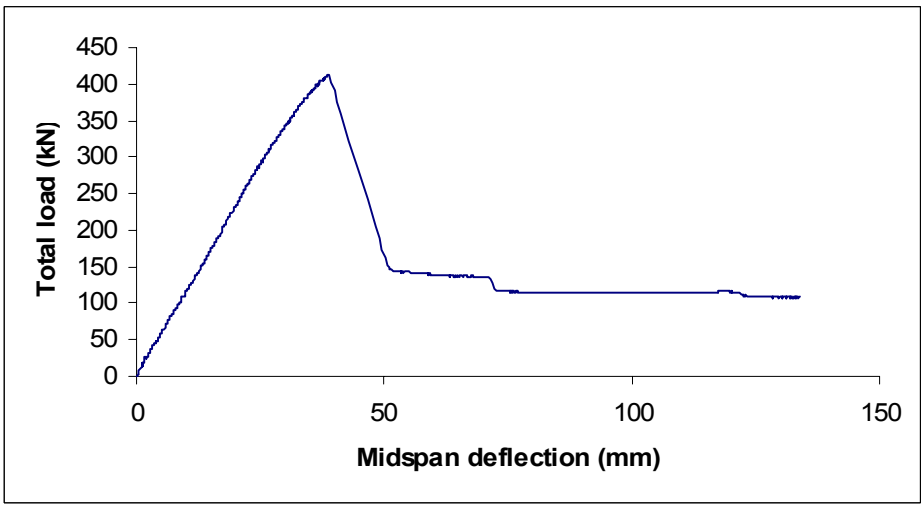

Figure B.5 load midspan deflection curve for beam R12P150-A105

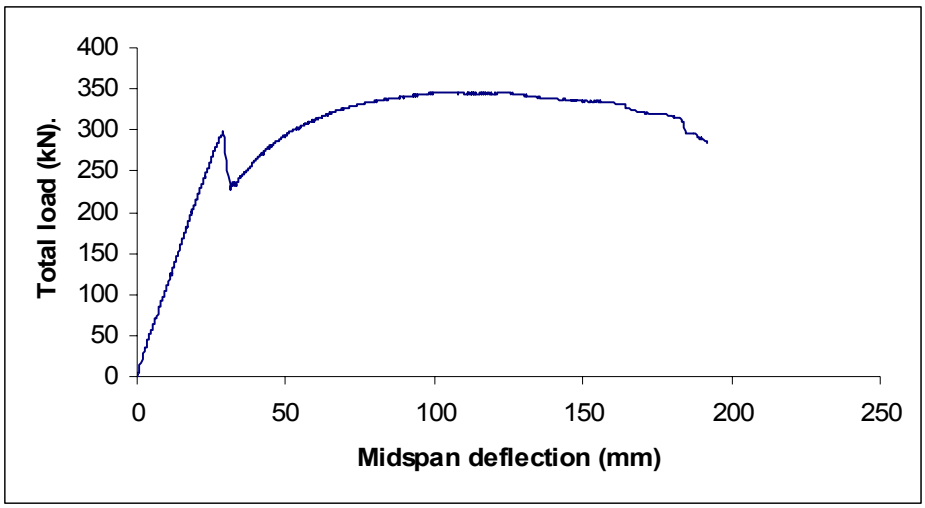

Figure B.6 load midspan deflection curve for beam N8P25-A80

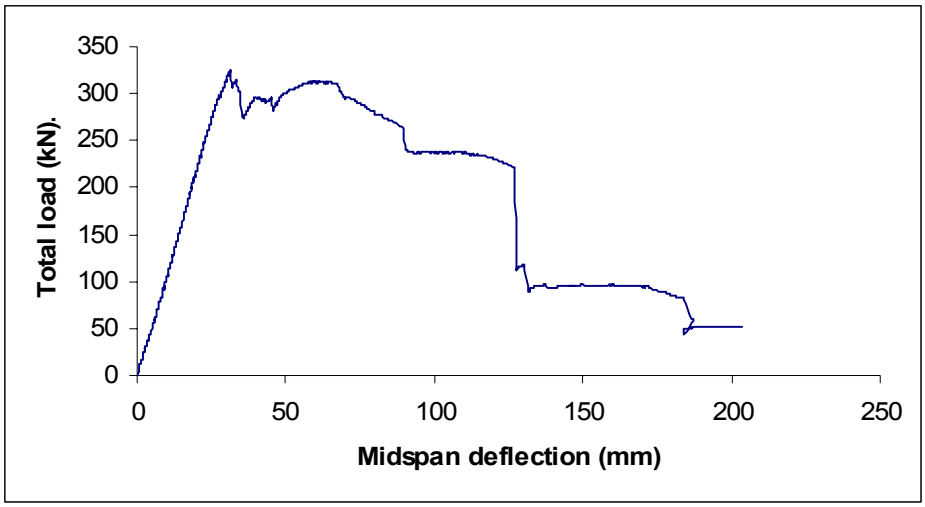

Figure B.7 load midspan deflection curve for beam N8P50-A80

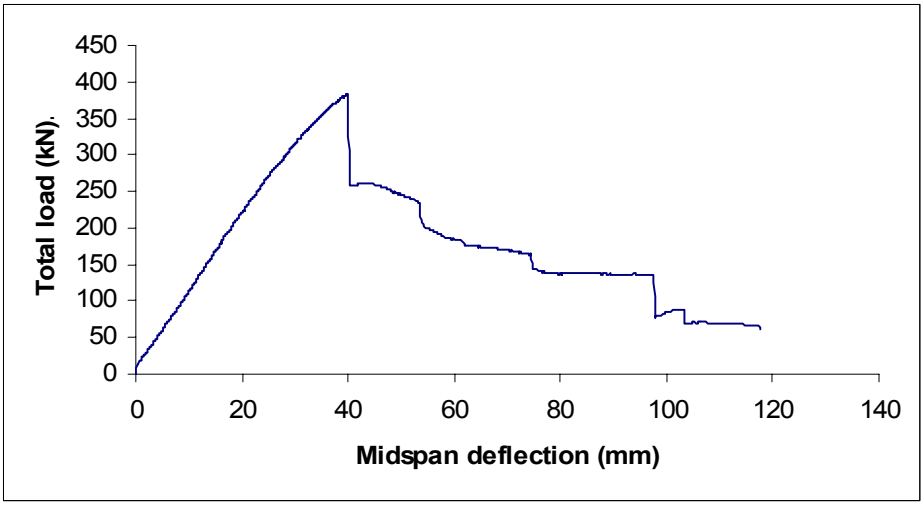

Figure B.8 load midspan deflection curve for beam N8P75-A80

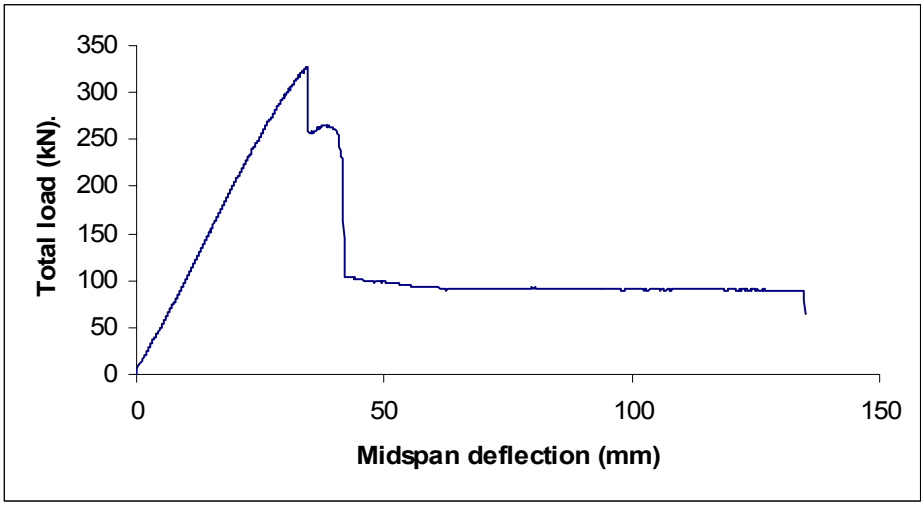

Figure B.9 load midspan deflection curve for beam N8P100-A80

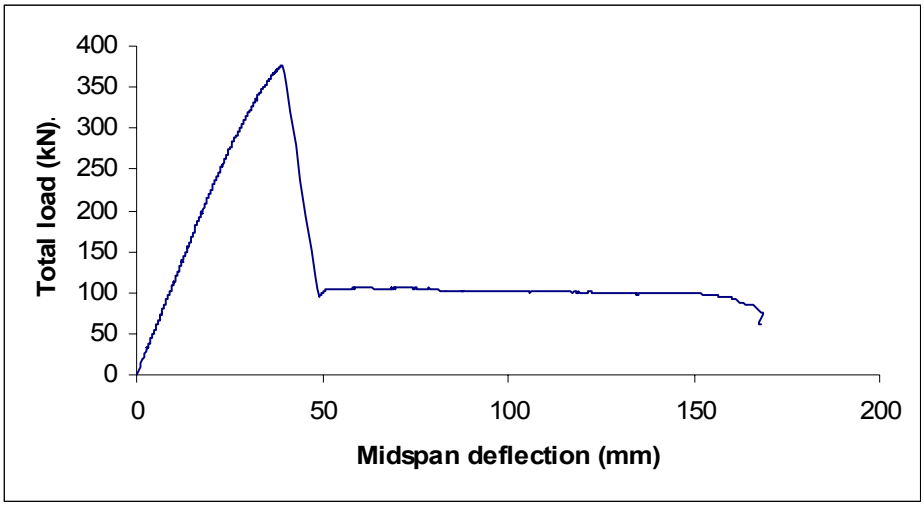

Figure B.10 load midspan deflection curve for beam N8P150-A80

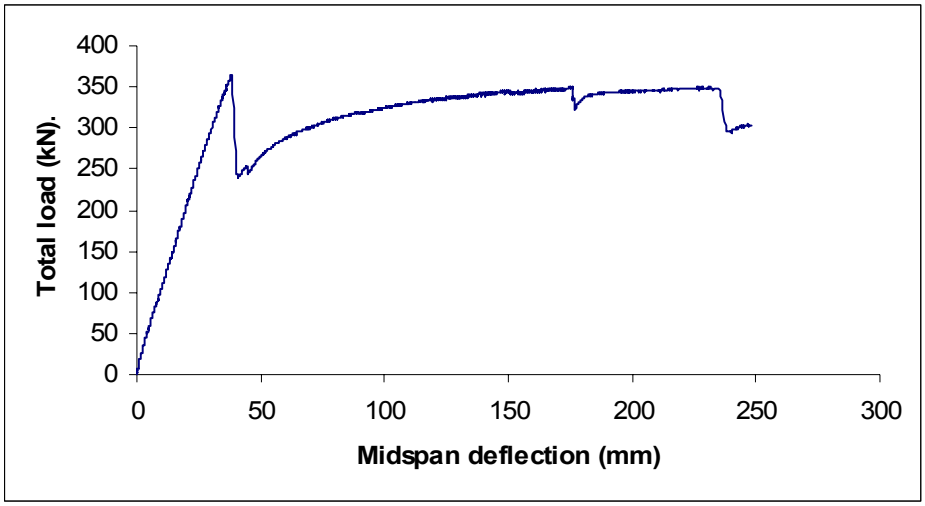

Figure B.11 load midspan deflection curve for beam R10P35-B72

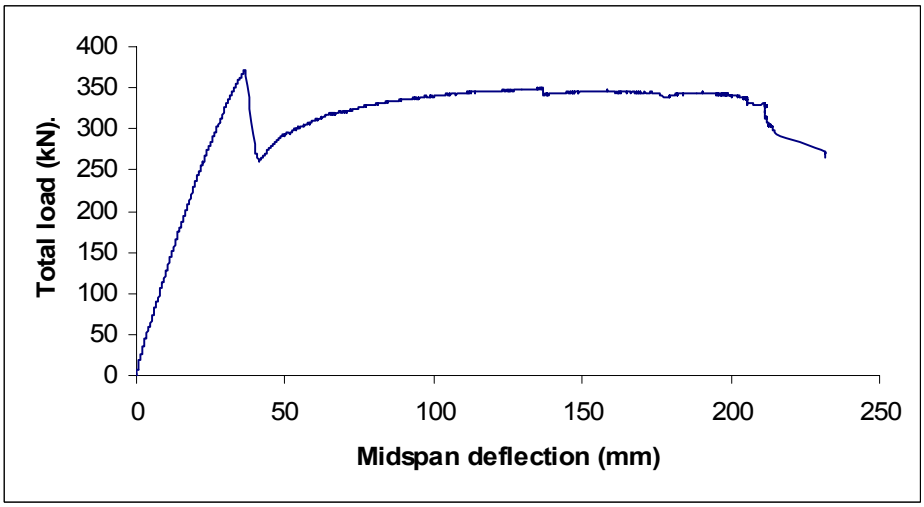

Figure B.12 load midspan deflection curve for beam R10P35-B83

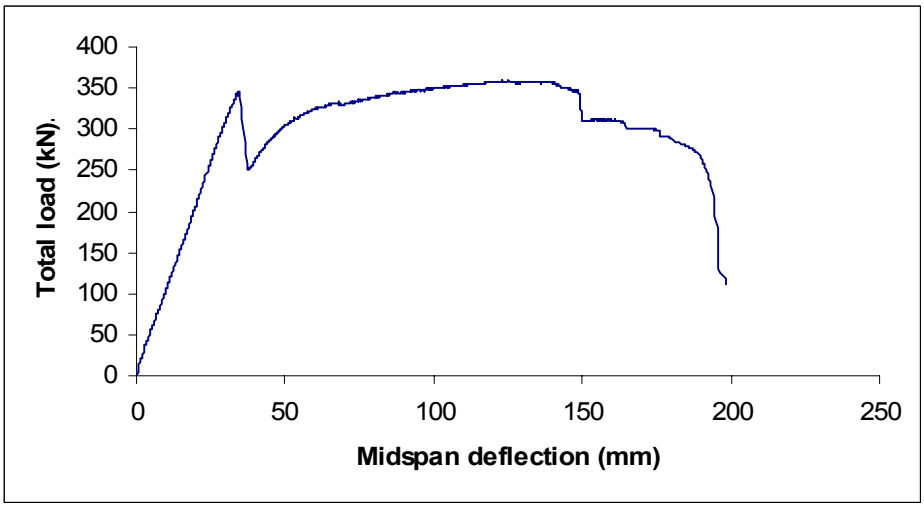

Figure B.13 load midspan deflection curve for beam R10P35-B95

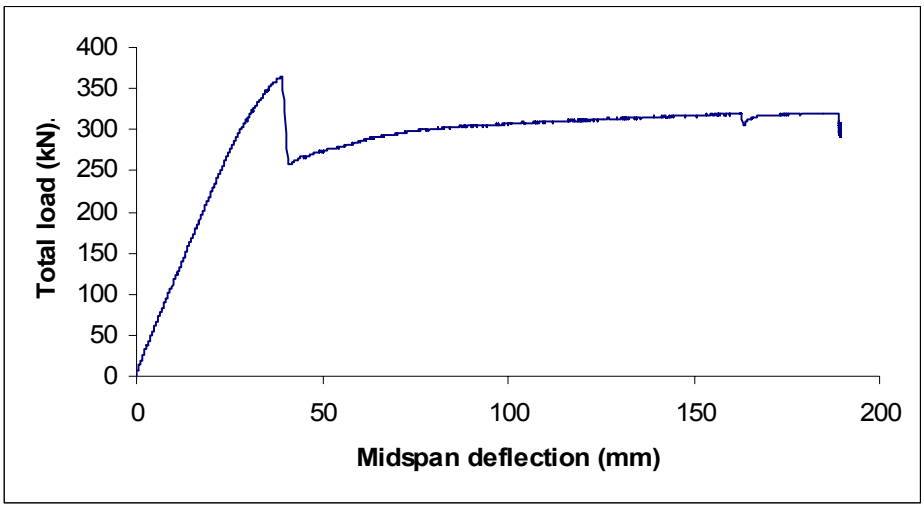

Figure B.14 load midspan deflection curve for beam R10P35-C95

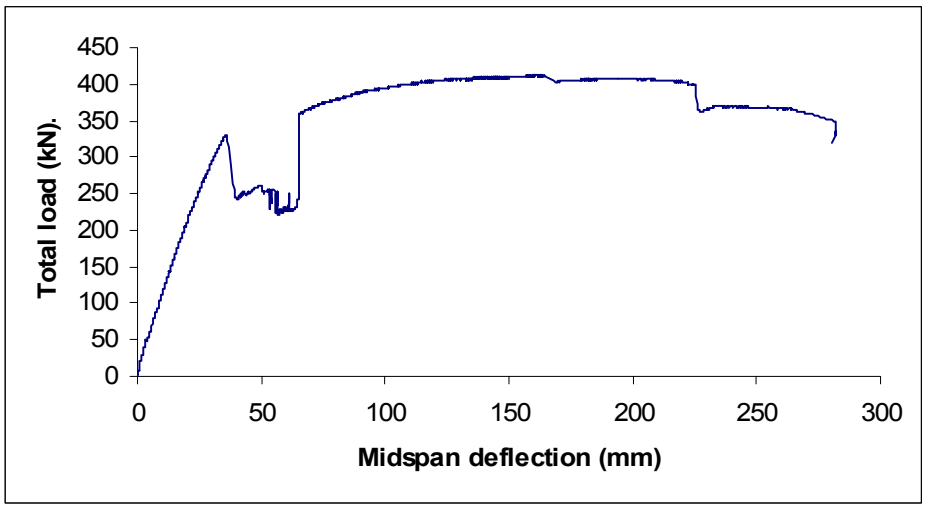

Figure B.15 load midspan deflection curve for beam R10P35-D95

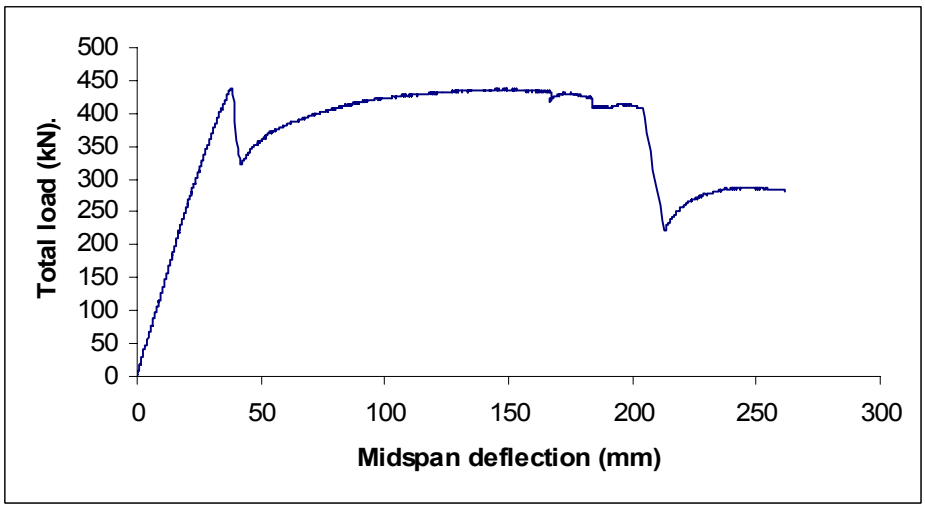

Figure B.16 load midspan deflection curve for beam N12P35-D85

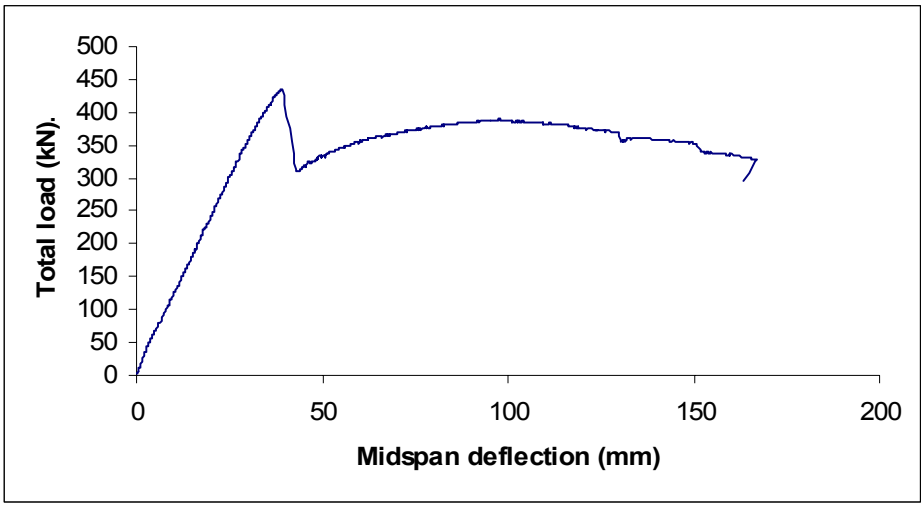

Figure B.17 load midspan deflection curve for beam R12P35-D85

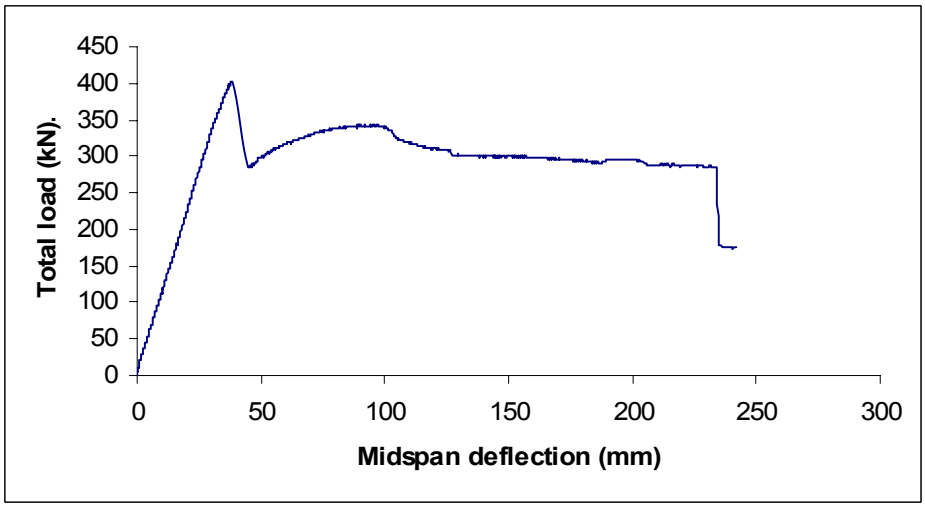

Figure B.18 load midspan deflection curve for beam R10P35-D85

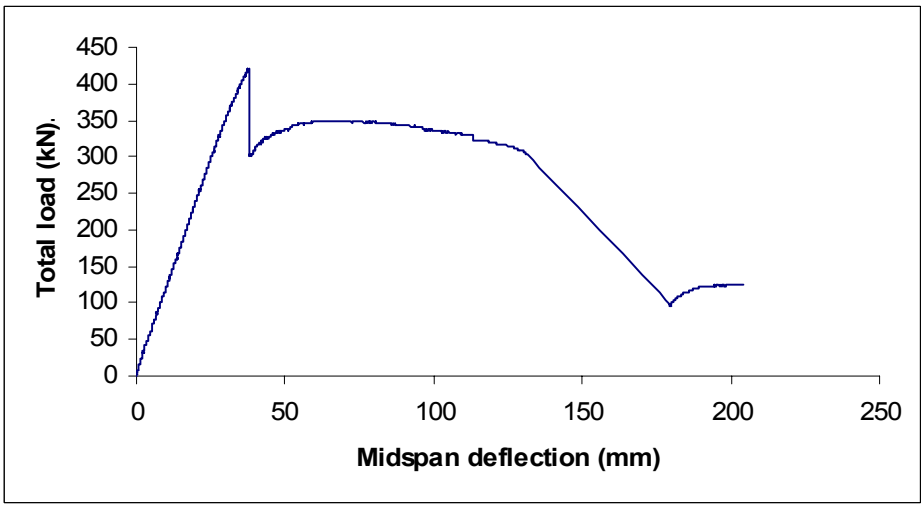

Figure B.19 load midspan deflection curve for beam R8P35-D85

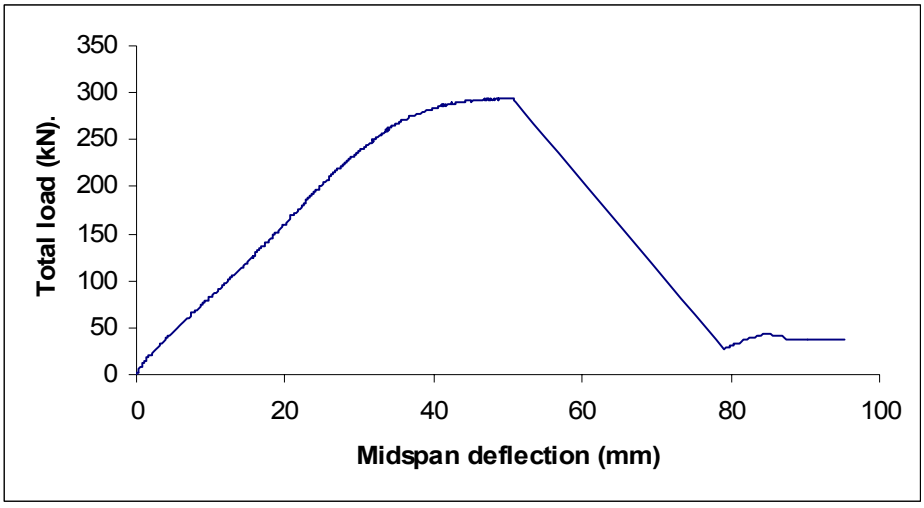

Figure B.20 load midspan deflection curve for beam 0P0-E85

Appendix C:

Strains at 0, 20 and 40 mm depth from top surface of the beams

Table C.1 Strains at 0, 20 and 40 mm depth from top surface of the beam R10P35-B95

Load (kN)	Measured strain at 40 mm depth	Calculated strain at 20 mm	Measured strain at concrete top surface	Calculated strain at concrete top surface
336.9	0.001121	0.002015916	0.002911	
338.7	0.001128	0.002027142	0.002926	
339.8	0.001131	0.002035179	0.002939	
341.3	0.001137	0.002045905	0.002955	
342.5	0.001142	0.002054348	0.002967	
341	0.00114	0.002050376	0.002961	
343.2	0.001147	0.002062791	0.002979	
344.2	0.001151	0.002070734	0.00299	
343.6	0.00115	0.002069639	0.002989	
344.7*	0.001154*	0.002076988*	0.003*	
250**	0.002636**	0.004786421**		0.006937**
249.8	0.002668	0.004844526		0.007021
251.2	0.002701	0.004904447		0.007108
251.6	0.002721	0.004940763		0.007161
251.5	0.002736	0.004968		0.0072
252.9	0.002757	0.005006132		0.007255
254.1	0.002779	0.005046079		0.007313
254.9	0.002797	0.005078763		0.007361
256.8	0.002823	0.005125974		0.007429
256.3	0.00283	0.005138684		0.007447
258.1	0.002856	0.005185895		0.007516

*Just before concrete spalling off

** Just after concrete spalling off

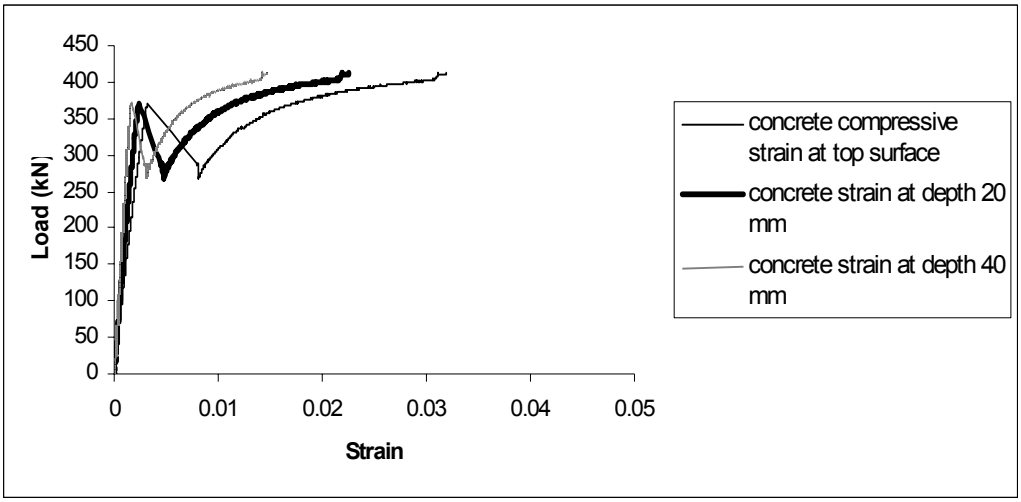

Figure C.1. Load versus concrete compressive strain at depth 0, 20 and 40 mm from top surface for beam R12P25-A105.

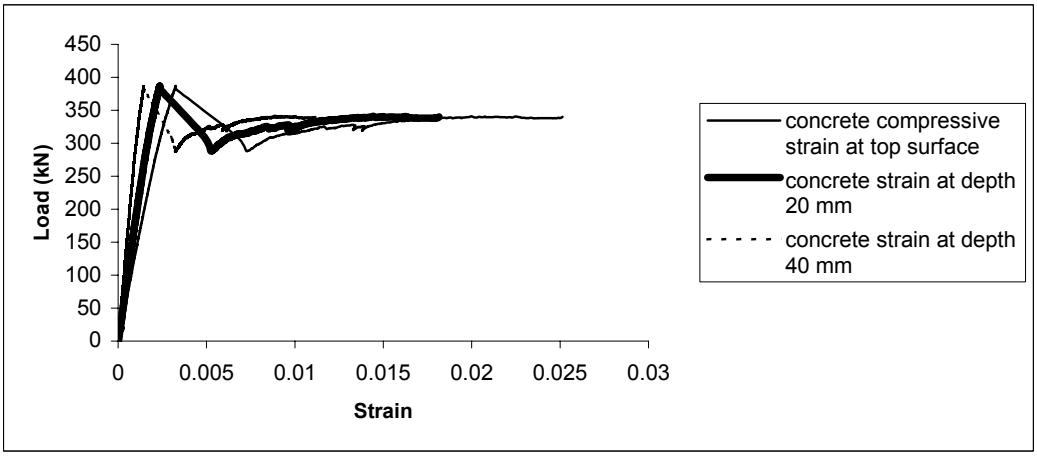

Figure C.2. Load versus concrete compressive strain at depth 0, 20 and 40 mm from top surface for the beam R12P50-A105.

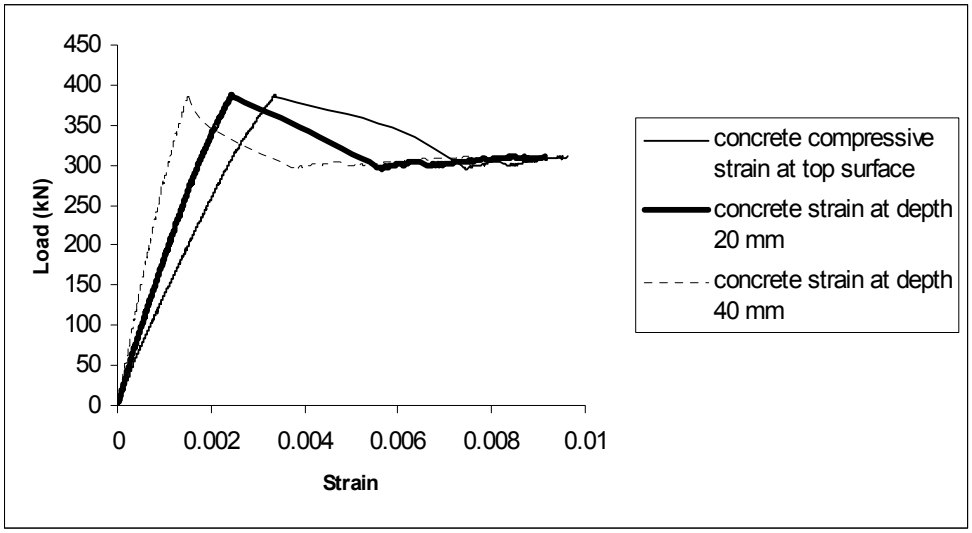

Figure C.3. Load versus concrete compressive strain at depth 0, 20 and 40 mm from top surface for the beam R12P75-A105.

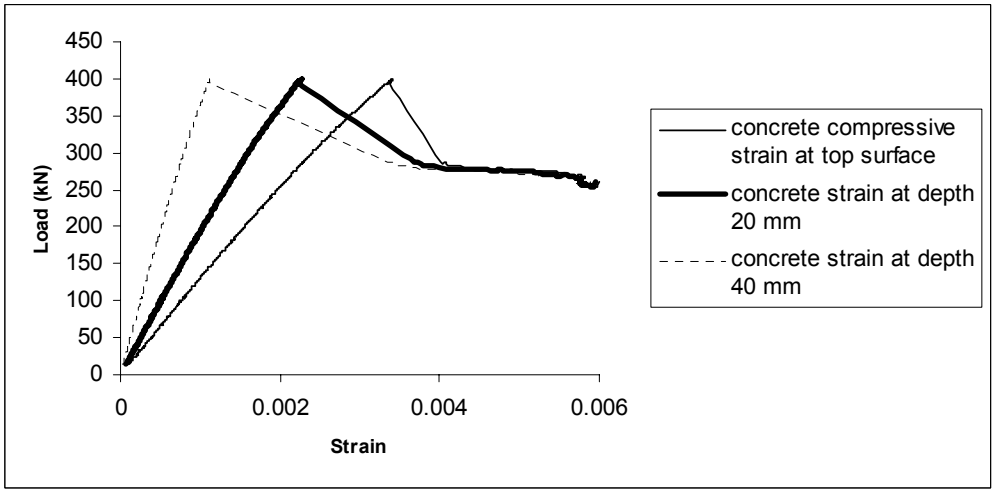

Figure C.4. Load versus concrete compressive strain at depth 0, 20 and 40 mm from top surface for the beam R12P100-A105.

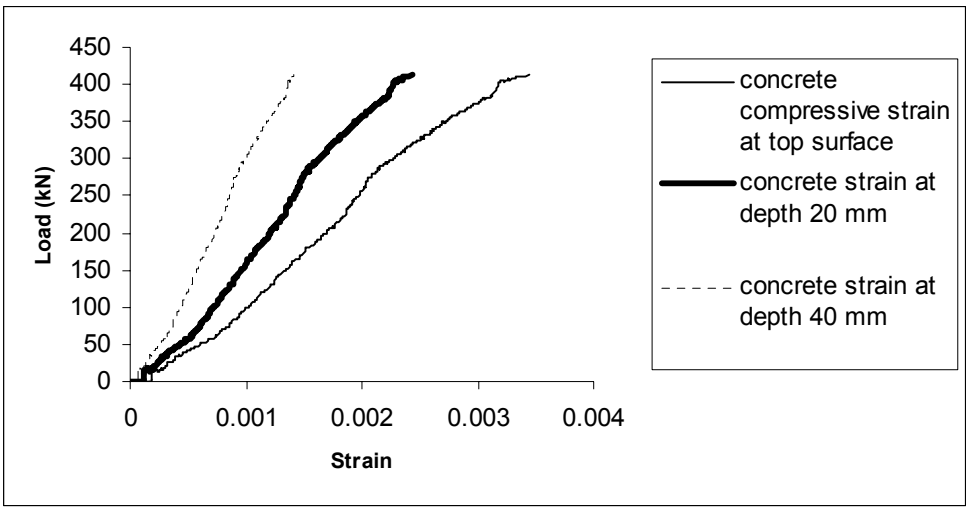

Figure C.5. Load versus concrete compressive strain at depth 0, 20 and 40 mm from top surface for the beam R12P160-A105.

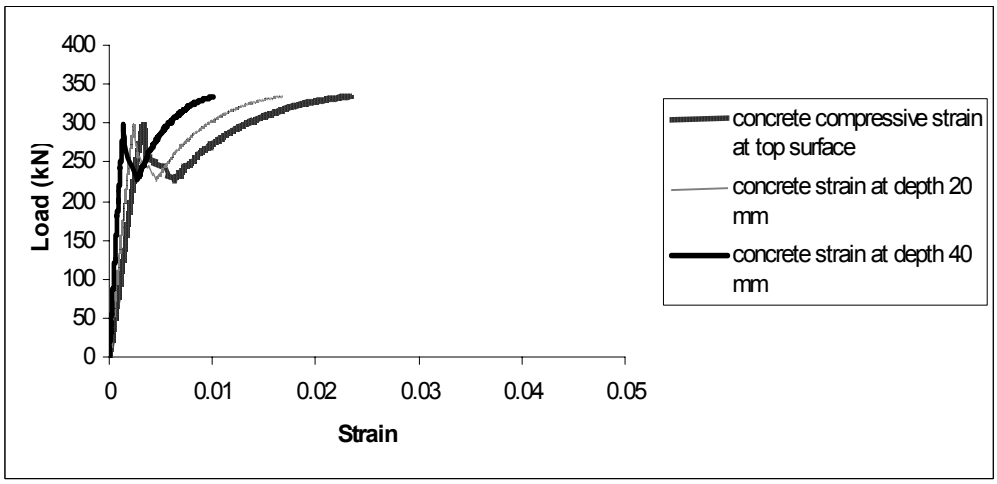

Figure C.6. Load versus concrete compressive strain at depth 0, 20 and 40 mm from top surface for the beam N8P25-A80.

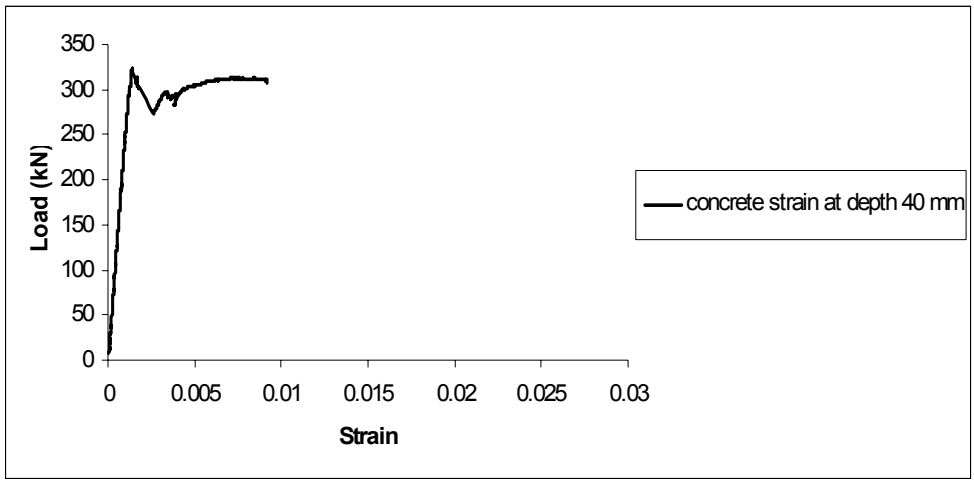

Figure C.7. Load versus concrete compressive strain at depth 40 mm from top surface for the beam N8P50-A80.

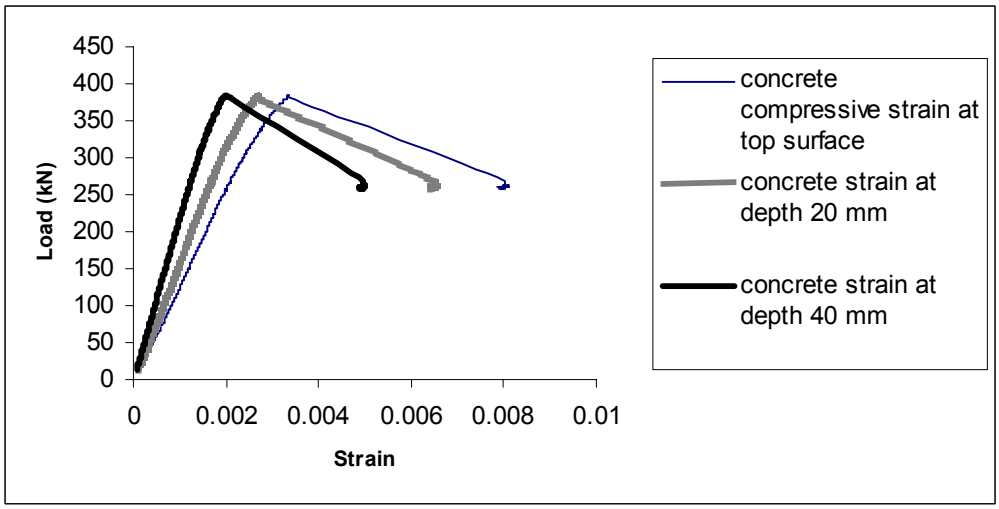

Figure C.8. Load versus concrete compressive strain at depth 0, 20 and 40 mm from top surface for the beam N8P75-A80.

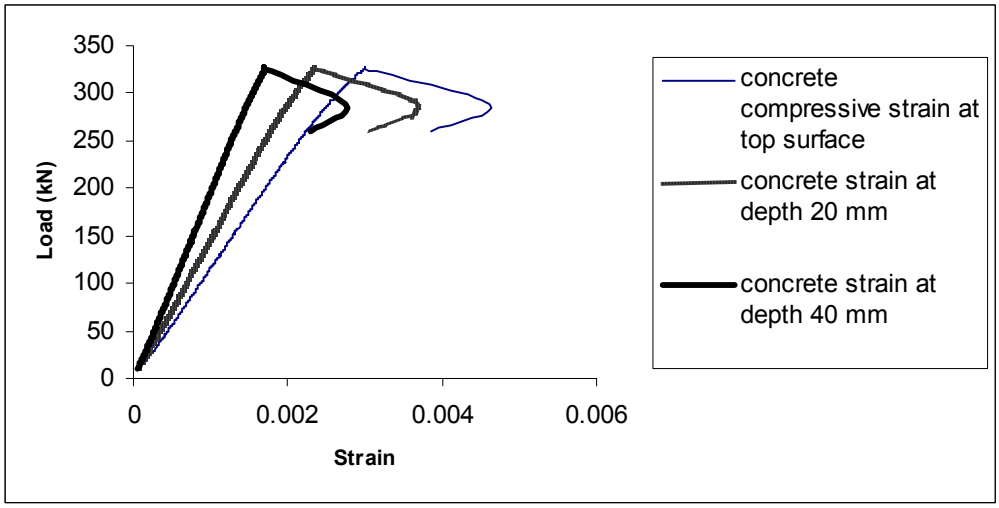

Figure C.9. Load versus concrete compressive strain at depth 0, 20 and 40 mm from top surface for the beam N8P100-A80.

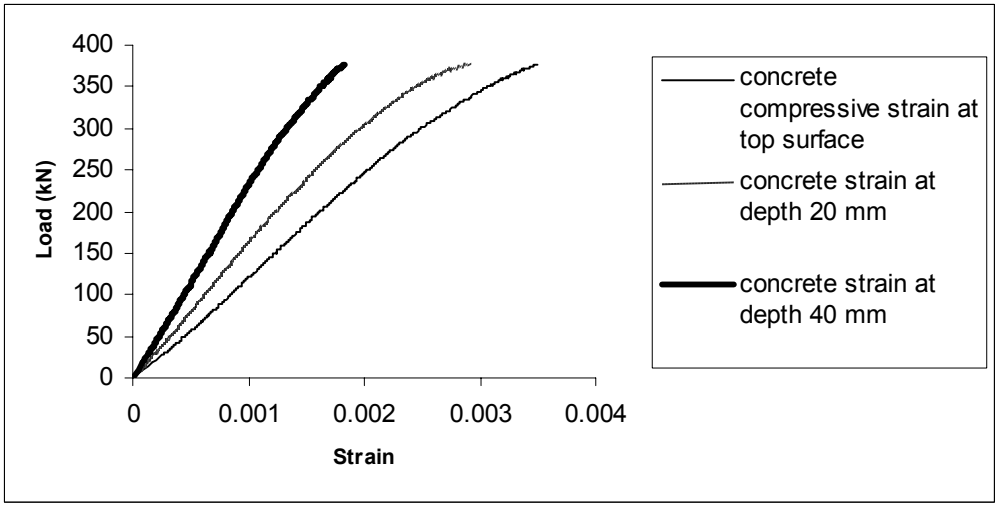

Figure C.10. Load versus concrete compressive strain at depth 0, 20 and 40 mm from top surface for the beam N8P160-A80.

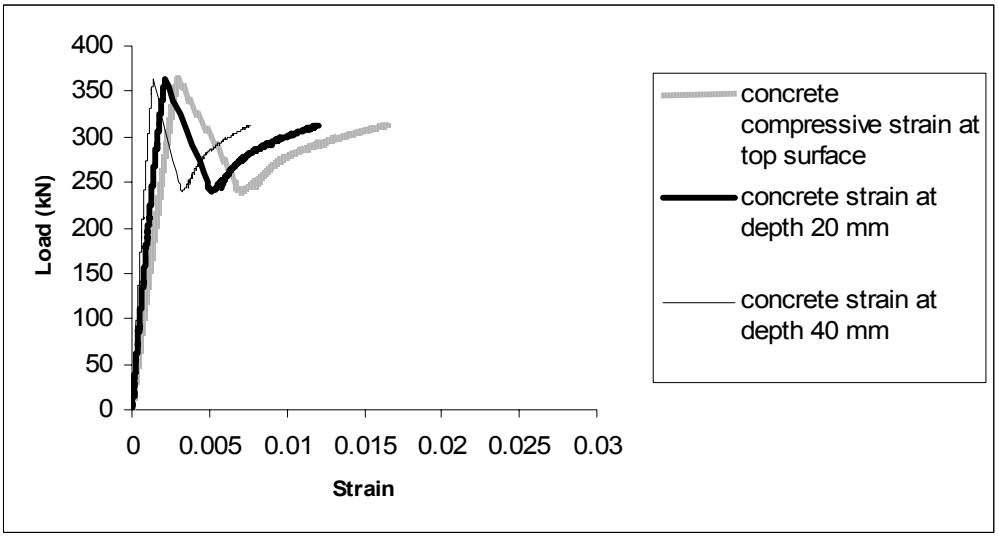

Figure C.11. Load versus concrete compressive strain at depth 0, 20 and 40 mm from top surface for beam R10P35-B72.

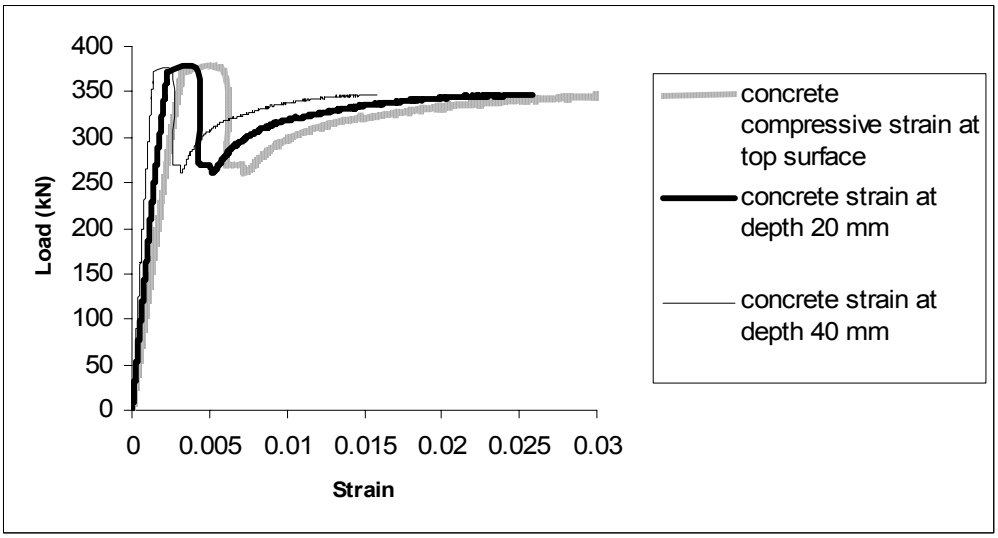

Figure C.12. Load versus concrete compressive strain at depth 0, 20 and 40 mm from top surface for beam R10P35-B83.

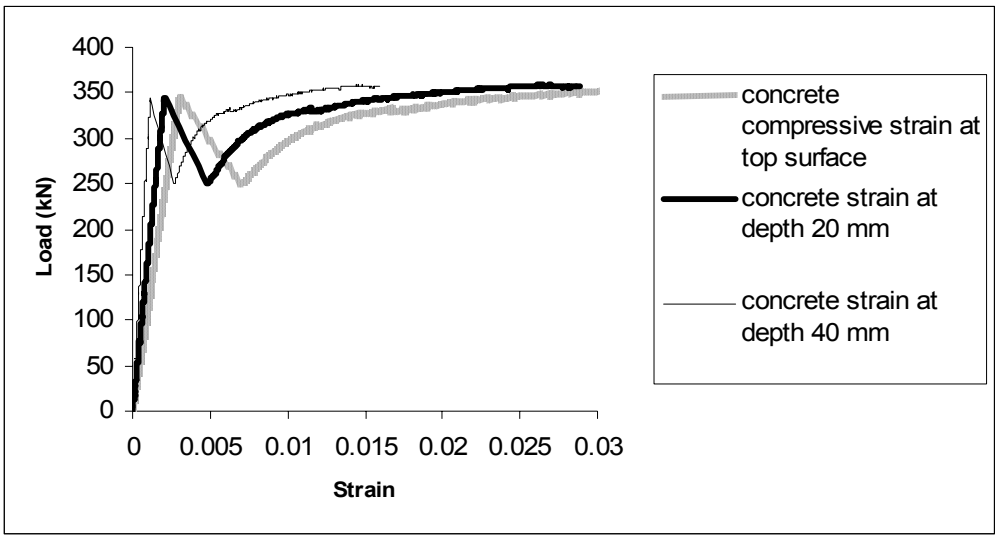

Figure C.13. Load versus concrete compressive strain at depth 0, 20 and 40 mm from top surface for beam R10P35-B95.

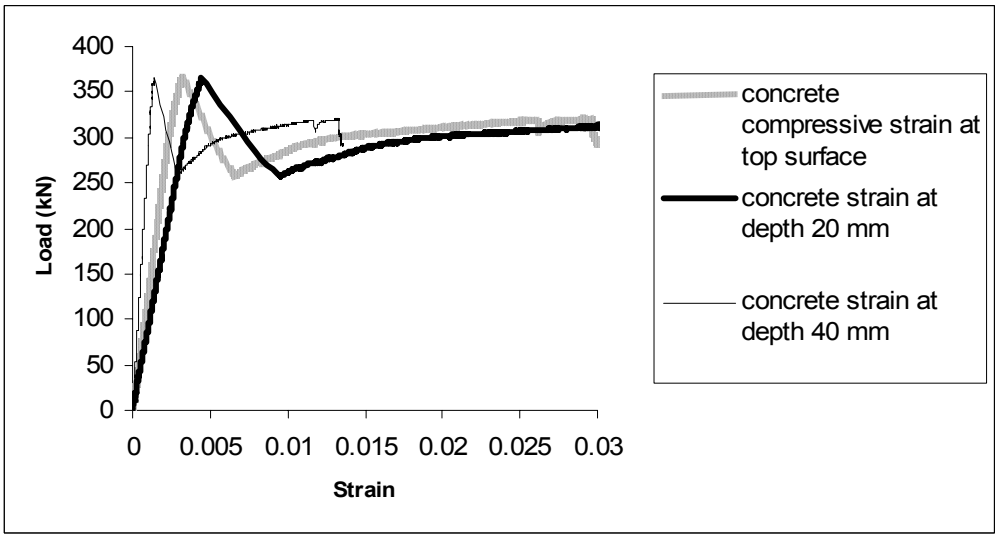

Figure C.14. Load versus concrete compressive strain at depth 0, 20 and 40 mm from top surface for beam R10P35-C95.

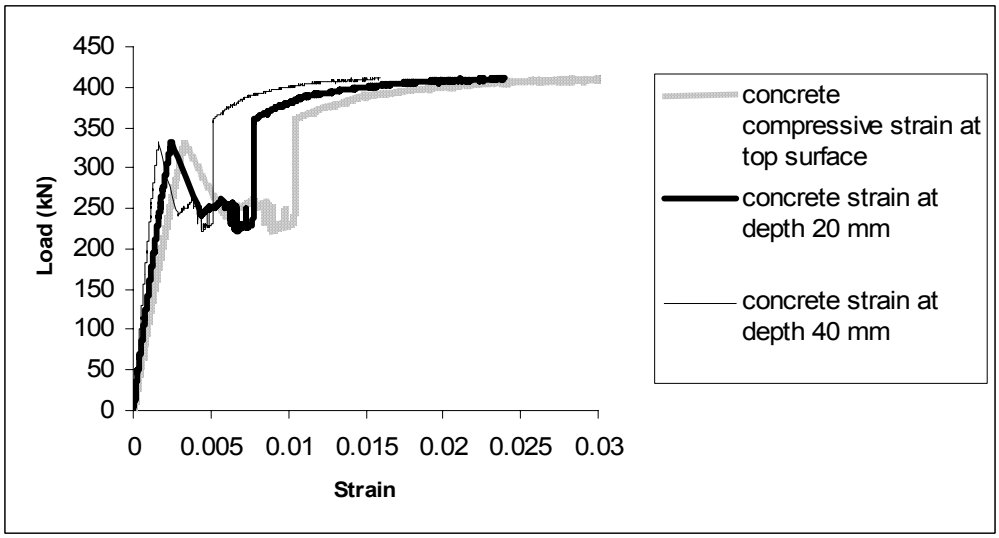

Figure C.15. Load versus concrete compressive strain at depth 0, 20 and 40 mm from top surface for beam R10P35-D95.

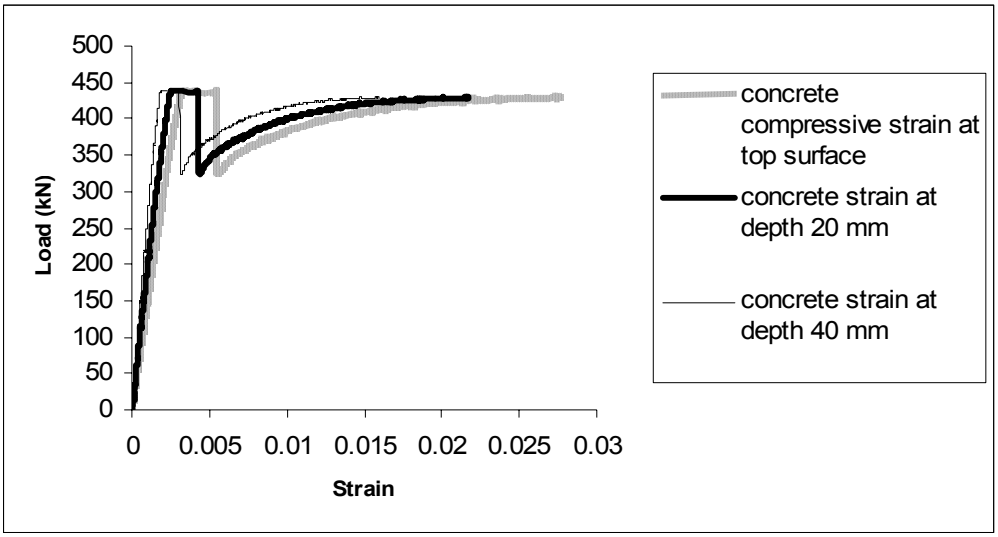

Figure C.16. Load versus concrete compressive strain at depth 0, 20 and 40 mm from top surface for beam N12P35-D85.

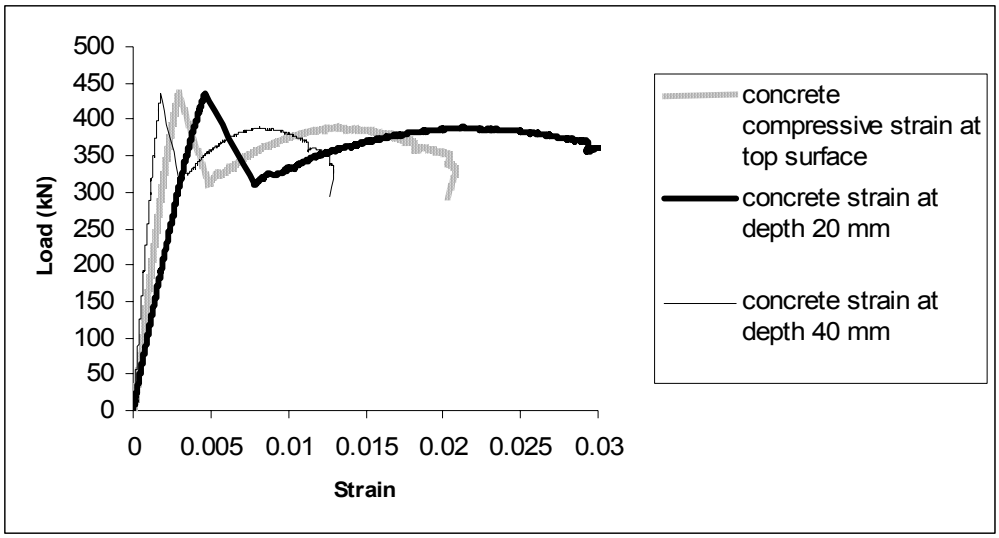

Figure C.17. Load versus concrete compressive strain at depth 0, 20 and 40 mm from top surface for beam R12P35-D85.

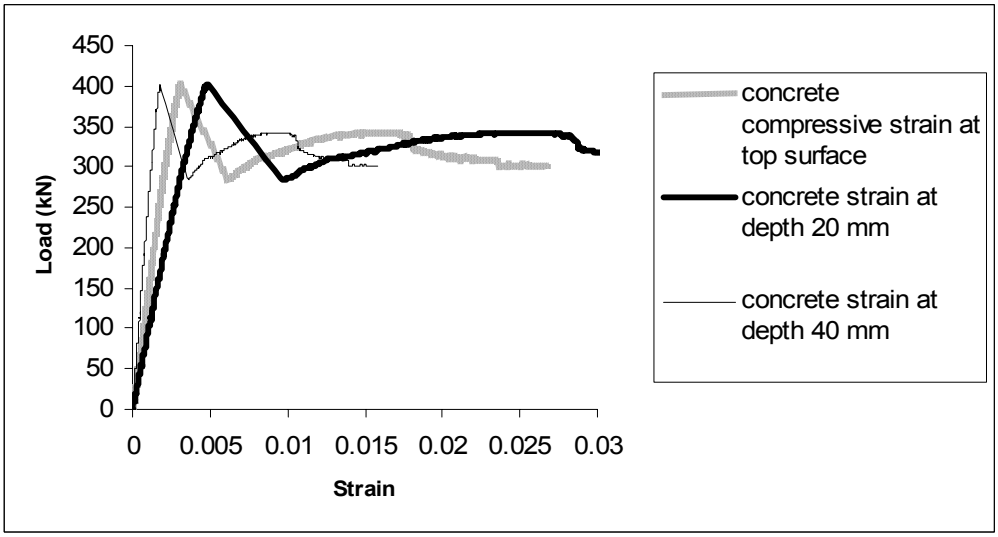

Figure C.18. Load versus concrete compressive strain at depth 0, 20 and 40 mm from top surface for beam R10P35-D85.

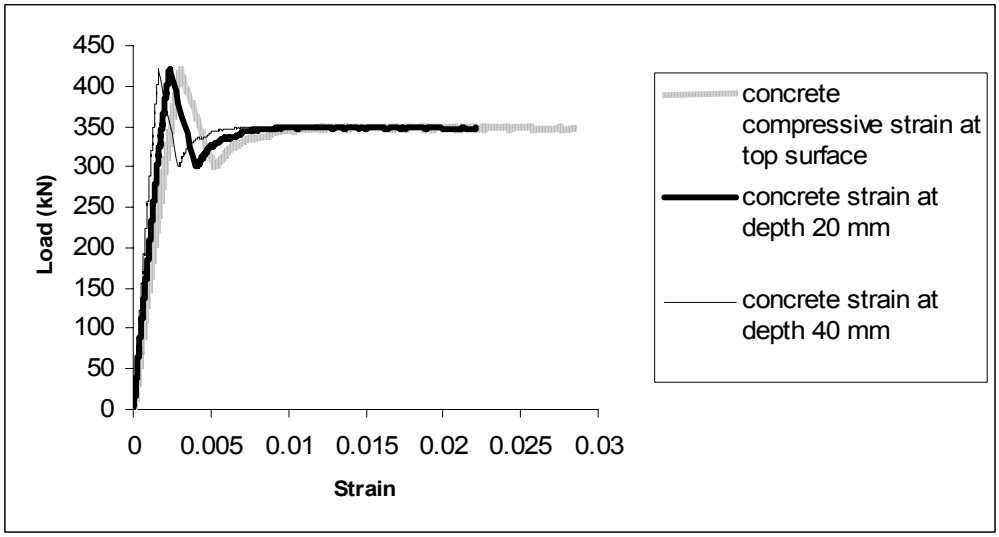

Figure C.19. Load versus concrete compressive strain at depth 0, 20 and 40 mm from top surface for beam R8P35-D85.

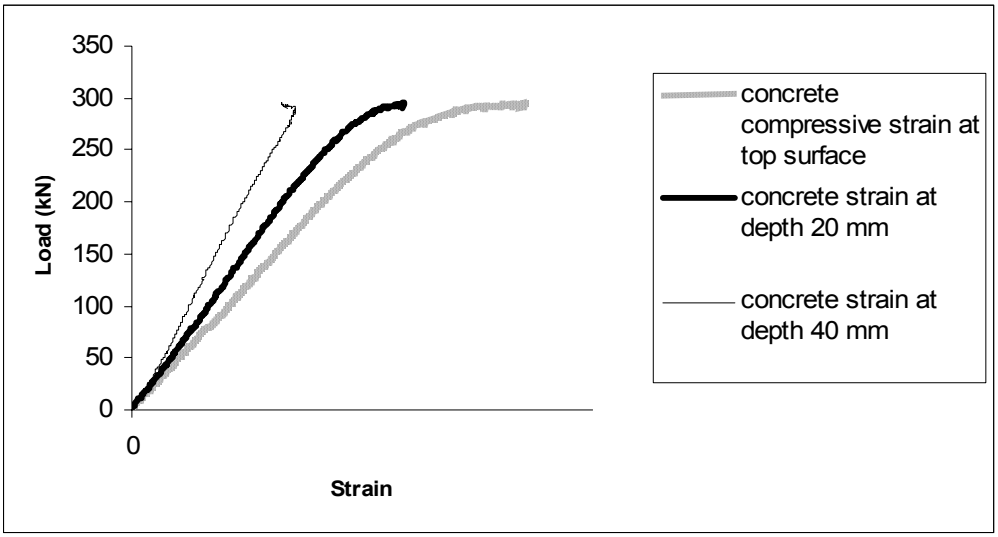

Figure C.20. Load versus concrete compressive strain at depth 0, 20 and 40 mm from top surface for beam 0P0-E85.

Appendix D:

Prediction moment capacity

D.1 Prediction moment capacity of an over-reinforced section using AS3600 (2001).

Prototype example: Beam R12P25-A105

Input data for concrete beam:

$f_c' = 105$ MPa

$f_y = 500$ MPa

$A_s = 3217$ mm^2

$b = 200$ mm

$d = 235$ mm

$$\gamma = 0.85 - 0.007(f_c' - 28)$$
$$0.65 \le \gamma \le 0.85$$

$$u = 0.6\frac{1}{\gamma}\frac{\varepsilon_u E_s}{f_c'}\frac{A_{st}}{b\ d}$$

$$u = 0.6\frac{1}{0.65}\frac{0.003\times 200\times 10^3}{105}\frac{3217}{200\times 235} = 0.361$$

$$K_u = \sqrt{u^2 + 2u} - u = 0.562$$

$K_u d = 132$ mm

$$Z_u = d(1 - 0.5\gamma K_u)$$

$$Z_u = 235(1 - 0.5 \times 0.65 \times 0.562) = 192 \text{ mm}$$

$$C = 0.85 f_c' b \gamma K_u d = \ 1532970 \text{ N}$$

The ultimate moment capacity $M_u = C \times Z_u = 294$ KN.m

According to AS 3600 (2001), the moment capacity, reduced by the capacity reduction factor ϕ. Table D.1 display the strength reduction factor (ϕ) for the 20 beams as recommended by AS 3600 (2001), in Clause 8.1.3 (c).

Then the calculated moment, $M_{cal} = 294 \times 0.61 = 176$ KN.m

The ratio of the experimental moment over the calculated moment

$$= \frac{246}{176} = 1.4$$

Where:

d = effective depth of a cross-section

b = width of a rectangular cross-section

f_c' = characteristic compressive cylinder strength of concrete at 28 days

K_u= neutral axis parameter

Z_u = lever arm

C = compressive force

Table D.1 – Calculating the strength reduction factor (ϕ)

SPECIMEN	M_{ud}, KN.m	M_u, KN.m	$0.8M_{ud}/M_u$	$\phi = 0.8M_{ud}/M_u \geq 0.6$
R12P25-A105	222.9	294.4	0.61	0.6
R12P50-A105	222.9	294.4	0.61	0.6
R12P75-A105	222.9	294.4	0.61	0.6
R12P100-A105	222.9	294.4	0.61	0.6
R12P150-A105	222.9	294.4	0.61	0.6
N8P25-A80	169.8	238.4	0.57	0.6
N8P50-A80	169.8	238.4	0.57	0.6
N8P75-A80	169.8	238.4	0.57	0.6
N8P100-A80	169.8	238.4	0.57	0.6
N8P150-A80	169.8	238.4	0.57	0.6
R10P35-B72	159.4	225.8	0.56	0.6
R10P35-B83	183.8	252.5	0.58	0.6
R10P35-B95	210.4	280.3	0.60	0.6
R10P35-C95	210.4	265.3	0.63	0.6
R10P35-D95	210.4	291.8	0.57	0.6
N12P35-D85	188.2	267.3	0.56	0.6
R12P35-D85	188.2	267.3	0.56	0.6
R10P35-D85	188.2	267.3	0.56	0.6
R8P35-D85	188.2	267.3	0.56	0.6
0P0-F85	196.1	233.3	0.67	0.7

M_{ud} is the reduced ultimate strength in bending
M_u is the ultimate strength in bending

D.2- Prediction moment capacity for over-reinforced helically confined HSC beams using AS3600 (2001).

Prototype example: Beam R12P50-A105

Input data for concrete beam:

$f_c^{'} = 105$ MPa

$f_y = 500$ MPa

$A_s = 3217$ mm^2

$b = 200$ mm

$d = 235$ mm

Input data for helical confinement

Helical diameter, $d_h = 12$ mm

Helical pitch = S = 50 mm

Concrete core diameter = D =150 mm

Yield strength of helical reinforcement = f_{yh} =310 MPa

First predict the enhanced concrete compressive strength using the new model

$$f_c = f_c^{'} + 4 f_2 \left(0.7 - \frac{S}{D} \right)$$

$$f_2 = 2 A_{sp} f_{sy} / DS$$

$$f_2 = \frac{2\times113.1\times310}{150\times50} = 9.35 \text{ MPa}$$

$$f_c = 105 + 4\times9.35\left(0.7 - \frac{50}{150}\right) = 118.71$$

$$K_s = \frac{f_c}{f_c'} = \frac{118.71}{105} = 1.13$$

Second predict the moment capacity using AS3600 (2001) with the following modification

1- Enhanced concrete compressive strength ($K_s f_c'$) is used instead of using concrete compressive strength (f_c').

2- $\alpha = 0.85\left(1 - \frac{k_s f_c'}{250}\right)$

3- $\gamma = 1.0$

$$\alpha = 0.85\left(1 - \frac{k_s f_c'}{250}\right) = 0.85\left(1 - \frac{1.13\times105}{250}\right) = 0.446$$

$$K_u = \frac{1}{\alpha\gamma}\frac{A_s}{b d_{co}}\frac{f_y}{K_s f_c'}$$

$$K_u = \left(\frac{1}{1\times 0.446}\right)\times\left(\frac{3217}{200\times 215}\right)\times\left(\frac{500}{1.13\times 105}\right) = 0.706$$

$$Z_u = d\times\left(1-0.5\times\gamma\times K_u\right)$$

$$Z_u = 215\times\left(1-0.5\times 1\times 0.706\right) = 139.1$$

$$M_{cal} = Z_u T = 223.76 \text{ kN.m}$$

Or, $M_{cal} = Z_u C$

$$C = \alpha K_s f_c' b \gamma K_u d$$

$$C = 0.446\times 1.13\times 105\times 200\times 1\times 0.706\times 215 = 1606.5 \text{ kN}$$

$$M_{cal} = Z_u C$$

$$M_{cal} = 0.139\times 1606.5 = 223.5 \text{ kN.m}$$

$$M_{\exp} = 229.8 \text{ kN.m}$$

$$E = \frac{M_{\exp} - M_{cal}}{M_{\exp}} = \frac{229.8 - 223.76}{229.8} = 2.6\%$$

To determine the steel strain

$$\varepsilon_y = \frac{f_y}{E_s} = \frac{500}{200000} = 0.0025$$

$$\varepsilon_s = \frac{(1 - K_u)}{K_u} \varepsilon_{con}$$

$$\varepsilon_{con} = 0.003 + \left(\frac{\rho_h f_{yh}}{50}\right)^2 \left(0.7 - \frac{S}{d_c}\right)$$

$$\rho_h = \frac{\pi d_h^{\,2}}{d_c S} = 0.06$$

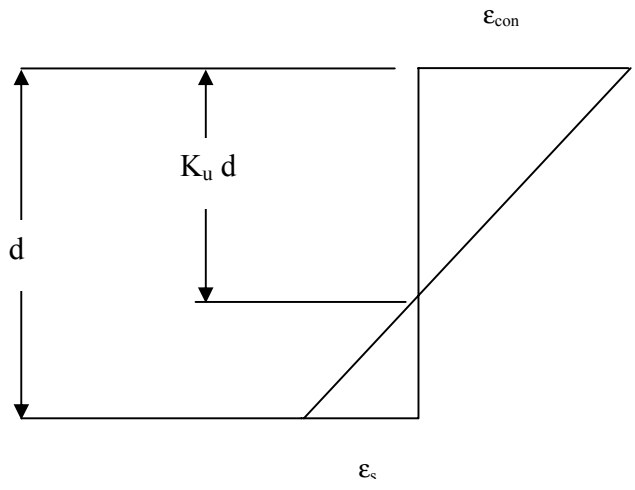

$$\varepsilon_{con} = 0.003 + \left(\frac{0.06 \times 310}{50}\right)^2 \left(0.7 - \frac{50}{150}\right) = 0.0537$$

$$\varepsilon_s = \frac{(1 - 0.706)}{0.706} \times 0.0537 = 0.0223 > \varepsilon_y$$

At maximum strength the steel strain is 9 times the yield strain, which means that the mode of failure is ductile.

Appendix E:

Statistical Modelling output

E-1 Fit y by x for 14 beams

Table E.1 Input data for regression analysis (Fit y by x)

Beam	μ_d	x1	x2	x3
R12P25-A105	7.7	0.354286	1.47	0.533333
R12P50-A105	4.3	0.177143	1.47	0.366667
R12P75-A105	1.3	0.118095	1.47	0.2
N8P25-A80	6.5	0.3375	1.94	0.533333
N8P50-A80	2.9	0.1675	1.94	0.366667
R10P35-B72	6.5	0.25	2.3	0.466667
R10P35-B83	5.8	0.216867	2	0.466667
R10P35-B95	5.3	0.189474	1.75	0.466667
R10P35-C95	4.8	0.189474	1.4	0.466667
R10P35-D95	7.8	0.189474	2.09	0.466667
N12P35-D85	5.3	0.505882	2.34	0.466667
R12P35-D85	3.8	0.313647	2.34	0.466667
R10P35-D85	2.7	0.211765	2.34	0.466667
R8P35-D85	2.7	0.183294	2.34	0.466667

y is μ_d

x1 is $\frac{\rho_h f_{yh}}{f_c'}$

x2 is $\frac{\rho}{\rho_{\max}}$

x3 is $0.7 - \frac{S}{D}$

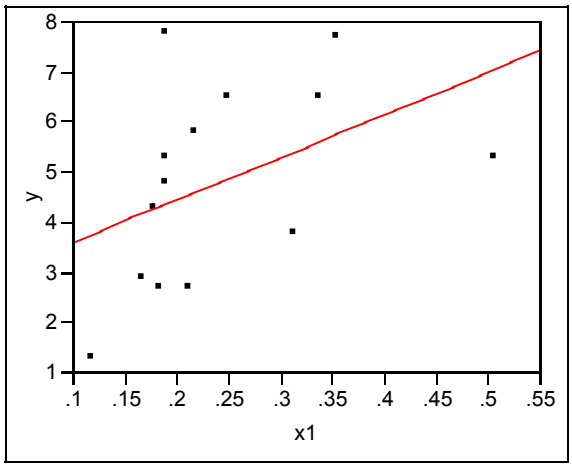

Linear Fit

y = 2.746829 + 8.502053 x1

Summary of Fit

RSquare	0.192673
RSquare Adj	0.125396
Root Mean Square Error	1.845367
Mean of Response	4.814286
Observations (or Sum Wgts)	14

Analysis of Variance

Source	DF	Sum of Squares	Mean Square	F Ratio
Model	1	9.752581	9.75258	2.8639
Error	12	40.864561	3.40538	Prob > F
C. Total	13	50.617143		0.1164

Parameter Estimates

Term	Estimate	Std Error	t Ratio	Prob>|t|
Intercept	2.746829	1.317481	2.08	0.0591
x1	8.502053	5.023967	1.69	0.1164

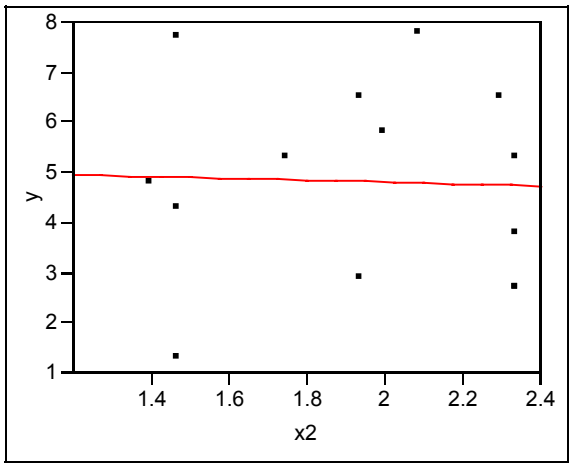

Linear Fit
y = 5.1801196 - 0.1883661 x2

Summary of Fit

RSquare	0.001252
RSquare Adj	-0.08198
Root Mean Square Error	2.052514
Mean of Response	4.814286
Observations (or Sum Wgts)	14

Analysis of Variance

Source	DF	Sum of Squares	Mean Square	F Ratio
Model	1	0.063372	0.06337	0.0150
Error	12	50.553771	4.21281	Prob > F
C. Total	13	50.617143		0.9044

Parameter Estimates

Term	Estimate	Std Error	t Ratio	Prob>|t|
Intercept	5.1801196	3.03281	1.71	0.1133
x2	-0.188366	1.535823	-0.12	0.9044

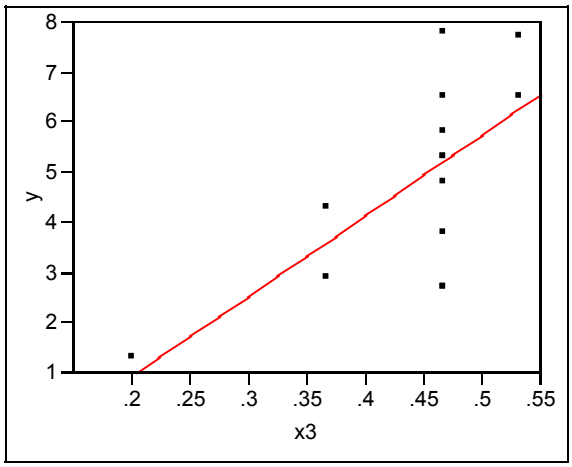

Linear Fit

y = -2.327931 + 16.127586 x3

Summary of Fit

RSquare	0.473073
RSquare Adj	0.429163
Root Mean Square Error	1.490848
Mean of Response	4.814286
Observations (or Sum Wgts)	14

Analysis of Variance

Source	DF	Sum of Squares	Mean Square	F Ratio
Model	1	23.945626	23.9456	10.7736
Error	12	26.671517	2.2226	Prob > F
C. Total	13	50.617143		0.0066

Parameter Estimates

Term	Estimate	Std Error	t Ratio	Prob>|t|
Intercept	-2.327931	2.212151	-1.05	0.3134
x3	16.127586	4.913484	3.28	0.0066

E-2 Fit Model for 14 beams

Whole Model
Actual by Predicted Plot

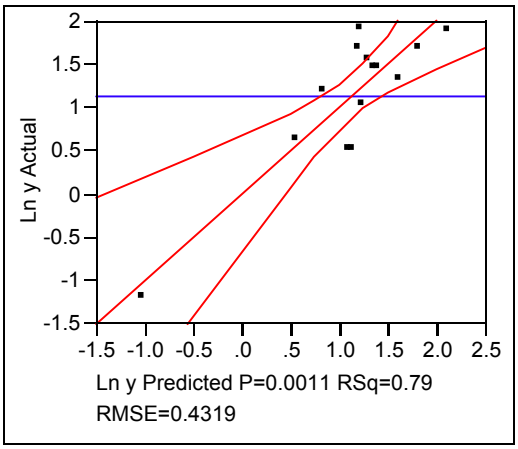

Summary of Fit

RSquare	0.786702
RSquare Adj	0.722713
Root Mean Square Error	0.431882
Mean of Response	1.126575
Observations (or Sum Wgts)	14

Analysis of Variance

Source	DF	Sum of Squares	Mean Square	F Ratio
Model	3	6.8794425	2.29315	12.2943
Error	10	1.8652173	0.18652	Prob > F
C. Total	13	8.7446598		0.0011

Parameter Estimates

Term	Estimate	Std Error	t Ratio	Prob>|t|
Intercept	4.5657999	0.816474	5.59	0.0002
Ln x1	0.2471829	0.430438	0.57	0.5785
Ln x2	-0.976182	0.658425	-1.48	0.1690
Ln x3	2.9140133	0.661969	4.40	0.0013

Effect Tests

Source	Nparm	DF	Sum of Squares	F Ratio	Prob > F
Ln x1	1	1	0.0615100	0.3298	0.5785
Ln x2	1	1	0.4099951	2.1981	0.1690
Ln x3	1	1	3.6144093	19.3780	0.0013

E-3 Fit Model for 8 beams

Whole Model
Actual by Predicted Plot

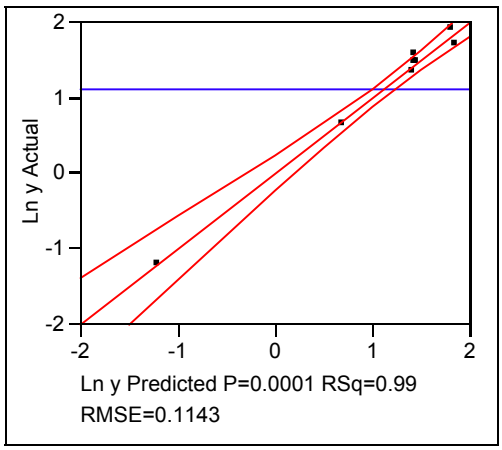

Summary of Fit

RSquare	0.992597
RSquare Adj	0.987044
Root Mean Square Error	0.114302
Mean of Response	1.108198
Observations (or Sum Wgts)	8

Analysis of Variance

Source	DF	Sum of Squares	Mean Square	F Ratio
Model	3	7.0065241	2.33551	178.7627
Error	4	0.0522594	0.01306	Prob > F
C. Total	7	7.0587835		0.0001

Parameter Estimates

Term	Estimate	Std Error	t Ratio	Prob>|t|
Intercept	3.7189426	0.272353	13.65	0.0002
Ln x1	-0.004498	0.147047	-0.03	0.9771
Ln x2	0.0994765	0.277771	0.36	0.7383
Ln x3	3.0915896	0.194093	15.93	<.0001

Effect Tests

Source	Nparm	DF	Sum of Squares	F Ratio	Prob > F
Ln x1	1	1	0.0000122	0.0009	0.9771
Ln x2	1	1	0.0016756	0.1283	0.7383
Ln x3	1	1	3.3147328	253.7138	<.0001